AD NUMBER

AD909922

NEW LIMITATION CHANGE

TO

Approved for public release, distribution unlimited

FROM

Distribution authorized to U.S. Gov't. agencies only; Administrative/Operational use; 15 April 1973. Other requests shall be referred to Air Force Rocket Propulsion Lab, Edwards AFB CA.

AUTHORITY

AFRPL ltr, 31 Jan 1974

AFRPL-TR-73-23

300-LB(f) MONOPROPELLANT HYDRAZINE THRUSTER LIFE EVALUATION

WALTER KIDDE & COMPANY, INC.

G. M. Hall
T. P. Layendecker

April 1973

AFRPL-TR-73-23

AIR FORCE ROCKET PROPULSION LABORATORY
DIRECTOR OF SCIENCE AND TECHNOLOGY
AIR FORCE SYSTEMS COMMAND
EDWARDS, CALIFORNIA

NOTICE

When Government drawings, specifications, or other data are used for any purpose other than in connection with a definitely related Government procurement operation, the United States Government thereby incurs no responsibility nor any obligation whatsoever; and the fact that the Government may have formulated, furnished, or in any way supplied the said drawings, specifications, or other data, is not to be regarded by implication or otherwise as in any manner licensing the holder or any other person or corporation, or conveying any rights or permission to manufacture, use, or sell any patented invention that may in any way be related thereto.

Copies of this report should not be returned unless return is required by security considerations, contractual obligations, or notice on a specific document.

REPRODUCTION QUALITY NOTICE

This document is the best quality available. The copy furnished to DTIC contained pages that may have the following quality problems:

- Pages smaller or larger than normal.
- Pages with background color or light colored printing.
- Pages with small type or poor printing; and or
- Pages with continuous tone material or color photographs.

Due to various output media available these conditions may or may not cause poor legibility in the microfiche or hardcopy output you receive.

☐ If this block is checked, the copy furnished to DTIC contained pages with color printing, that when reproduced in Black and White, may change detail of the original copy.

300 LB(f) MONOPROPELLANT HYDRAZINE THRUSTER LIFE EVALUATION

G. M. Hall
T. P. Layendecker

FOREWORD

The program reported herein was sponsored by the United States Air Force Rocket Propulsion Laboratory under Air Force Systems Number 62302F, AFRPL Project No. 3058 and Air Force Contract Number FO 4611-72-C-0027 with program surveillance under Mr. Paul Erickson (LKDA) AFRPL Project Officer. The work was accomplished by Walter Kidde & Company, Inc., 675 Main St., Belleville, New Jersey 07109 during the period November 1, 1971 through April 30, 1972. The subject report, initially identified as Kidde Report No. 4928-FTR-1 was submitted for approval March 1973.

This technical report has been reviewed and is approved.

Paul Erickson (LKDA)
Project Officer

ABSTRACT

There was a primary need to demonstrate the extended life capability of a nominal 300-lb (f) monopropellant hydrazine thruster beyond qualification limits. In addition, there were secondary needs to attain end of life performance characteristics; first to verify a catalyst bed pressure drop buildup theory of performance degradation, and second to test a causal theory for the occurrence of "washout" performance degradation. The program documented herein takes three steps toward the fulfillment of these needs by conducting life tests on three thrust chambers, two which already had specified mission life accumulated and one which was refurbished to the "as new" condition. All three units tested demonstrated extended life capability, but each provided performance characteristics which reflected the particular type of duty cycle conducted. The unit which produced high catalyst bed pressure drop also produced higher than usual in-run manifold temperature. The other two units produced low catalyst bed pressure drop buildup and consequently attained a longer unencumbered life characteristic. Based upon these results, it is concluded that extended life capability is demonstrated and the secondary need to verify catalyst bed pressure drop buildup theory was accomplished. However, "washout" performance characteristics were never accomplished preventing the accumulation of convincing data to support the causal theory. Recommendations based upon these findings include investigation and elimination of variability in sensitive build parameters, life testing to verify elimination of variability as well as obtain end of life data, and the determination of safe in-run and shutdown manifold temperature on high catalyst bed pressure drop units.

TABLE OF CONTENTS

LIST OF ILLUSTRATIONS

LIST OF ILLUSTRATIONS (CONT)

LIST OF ILLUSTRATION (CONT)

LIST OF TABLES

SECTION I

INTRODUCTION

1. MOTIVATIONAL REVIEW

In 1967 Walter Kidde and Company, Inc. was awarded an Air Force subcontract to develop the first large hydrazine thruster, a nominal 300-lb thrust design for an orbiting vehicle propulsion system. The fruits of this contract are presented in Figure 1. The program has progressed through development, qualification and delivery of two blocks of flight units, the latter block including an Engineering Evaluation Unit (EEU) and a Production Reliability Assessment Test (PRAT) unit. These latter pieces of test hardware were subjected to full mission life tests to anticipated worst case duty cycles at extreme corners of the operating regime. Both units successfully completed mission testing with useful life remaining. In this condition, they both had considerable value for life evaluation tests.

In the same time period, a state-of-the-art problem called "washout" was encountered in testing monopropellant hydrazine thrust chambers. Washout is the in-run escape of undecomposed propellant from the thrust chamber which results in a drop in thrust and specific impulse. Factors which influence washout have been isolated and empirical influence coefficients have been established which allow the prediction of critical performance parameters within the range of available data. Purely analytical prediction of these same parameters is not practical due to the complexity of modeling the flow dynamics of the decomposition-dissociation reaction and the influence of temporary and permanent catalyst degradation on this reaction.

More recently, a relationship between injector flow characteristics and washout characteristics has been established which resulted in controlled injector distribution characteristics. In particular, average injector flow out the end of the distribution tubes penetrating the catalyst bed was controlled to a 49 - 50% of total flow range where previously this parameter was uncontrolled and ranged up to 55% of the total flow. Linear extrapolation of the higher flow range data indicated that units containing 49 - 50% of the total flow out the end of the distribution tube would possess significantly better washout resistance. However, the apparent sensitivity of washout to a relatively small change in end flow made this prediction difficult to accept, creating a need for verification testing.

Control of average distribution tube end flow per ship-set of tubes was initiated on the EEU and PRAT units giving them unique credentials for verification of washout resistance with controlled end flow. Endurance testing these particular units to the point of washout would provide the data needed to verify life predictions for 49 - 50% average end flow design as well as provide a method to test the hypothesis for cause of washout by offering opportunities to demonstrate recovery from washout conditions. With these primary objectives in mind, a program was formulated which would best use the hardware available.

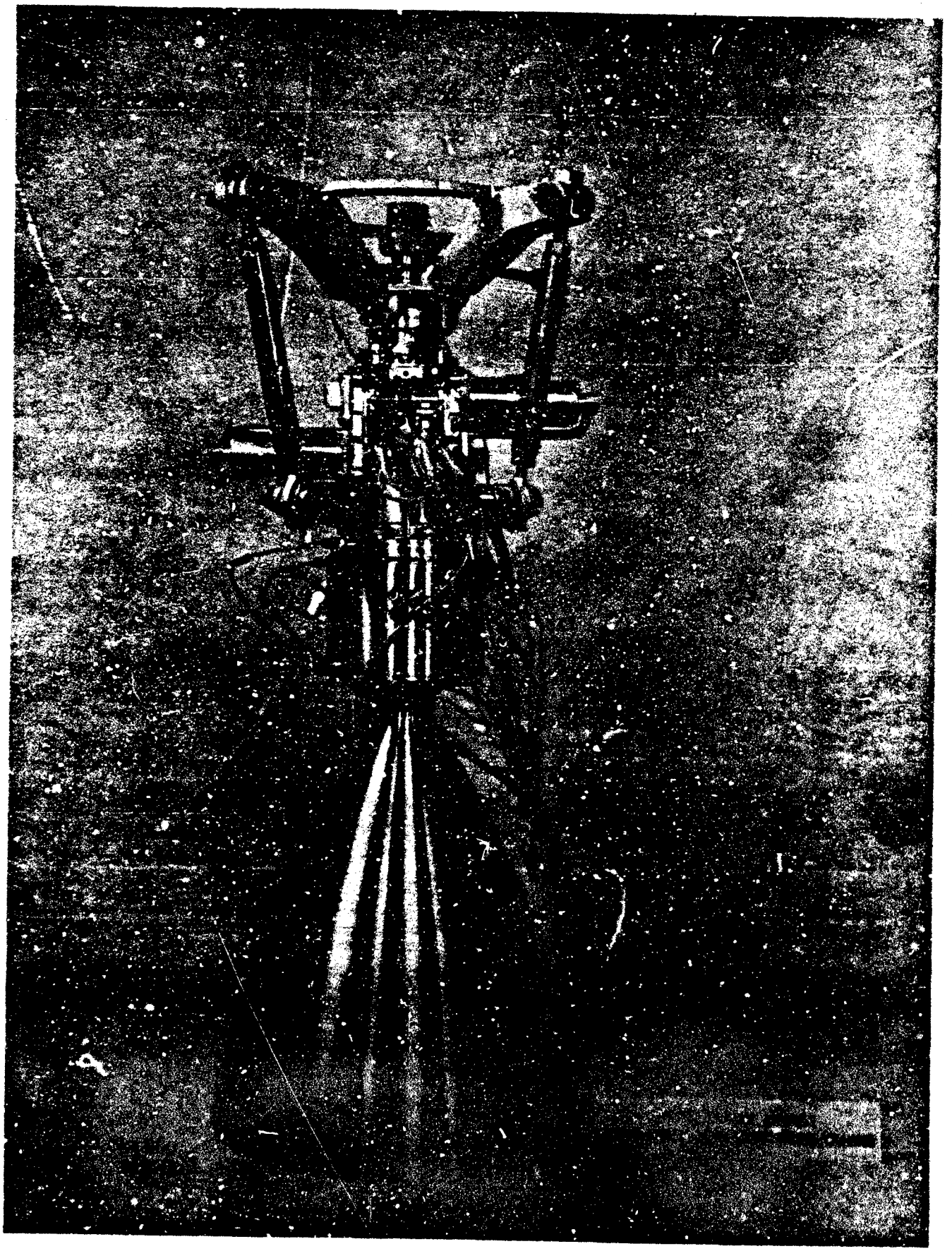

The program conceived included life testing of both available units as well as refurbishment of one, the EEU, to obtain a third test unit which could be life tested to a more severe duty cycle thereby demonstrating the ability of the engine to meet future mission needs. The actual tests conducted and the results obtained are presented herein supported by analysis of findings, conclusions and recommendations. Data concerning the thrust chamber assembly design, the test facility requirements and procedures, the hardware build data and prior performance are presented in the Appendix.

2. DESIGN REVIEW

The thrust chamber assembly shown in Figure 1 contains three major subassemblies, a thrust mount, containing a cavitating venturi, the quad-valve and the thrust chamber. In addition there are valve and manifold heaters, pressure transducers and thermocouples to complete the unit.

The cavitating venturi is the first element in the flow path. It provides flow characteristics which are independent of downstream pressure drop changes as long as it is operating within its range of cavitation. As a consequence, the influence of increasing catalyst bed pressure drop is removed from the propellant pressure-thrust characteristic.

The venturi is located within the thrust mount bellows assembly, which also contains individual concentric bellows for sealing redundancy. These bellows in conjunction with a gimbal ring provide the thrust chamber assembly with a mounting alignment capability which can be adjusted and locked with alignment links.

Propellant leaving the venturi enters the quad-valve through a tapered cone filter before dividing into two flow paths. Each path contains two valve elements providing series redundancy against leakage. The combined unit provides series-parallel redundancy against single valve failure to open or close. Valve position is indicated by switches permitting diagnosis of failure to open or close. A more comprehensive discussion of the valve design is included in the Appendix.

The thrust chamber design is the most significant aspect of the TCA since it is the life limiting element. It contains the catalyst which spontaneously decomposes hydrazine to produce thrust. Degradation of this catalyst, chemical and physical, is the prime limitation on satisfactory performance and subsequently life.

The thrust chamber contains a single inlet tube, a manifold to divide the inlet flow into 37 paths and 37 distribution tube assemblies to inject the propellant into the catalyst bed. Flow in each of the 37 paths enters the distribution tube through an orifice tube in the manifold face. Each distribution tube is surrounded with a cylinder or 20-24 mesh catalyst contained in a cylindrical screen with end plugs. This subassembly is called a partition assembly.

The 37 partition assemblies are contained within a shell assembly consisting of the manifold and a cylindrical shell. The volume between partitions within the shell assembly is filled with 8-12 mesh catalyst. This catalyst is contained within the shell assembly with screens, a screen retainer plate and a support plate, the latter designed to transmit the pressure loading from the catalyst bed to the shell assembly. The support plate is locked into the shell assembly by the nozzle which is welded into the shell assembly.

A detailed description of the thrust chamber with drawings, sketches and photographs is presented in the Appendix. This information includes construction materials, instrumentation, and build parameters. Nominal nozzle throat diameter is 1.542 inch and the nozzle area ratio is 88.

3. REQUIREMENTS REVIEW

Primary design parameters for the thrust chamber assembly are presented in the Design Parameters list, Table I, below. Steady state thrust requirements are stipulated at several levels because the specification requires the unit to operate over a decaying inlet pressure range. Transient thrust peak at start is limited to 520 lbsf over most of the thrust range, but may peak to 1000 lbsf at the high end of the range. Similarly, thrust oscillation of ± 23 lbsf is permitted over most of the thrust range, with peaks to 45 lbsf permitted at the high end of the thrust range.

The specific impulse minimums indicated apply to worst case conditions of minimum thrust level, minimum propellant temperature and end of life conditions. Steady state conditions by specification definition, begin after 5000 lb-sec. total impulse have been delivered. Average specific impulse measured during the transient period, up to 500 lb-sec delivered total impulse, shall not be less than 175 lb-sec/lb.

The operating range data presented covers the basic design range of 100 to 280 psia propellant pressure as well as the limits demonstrated during this program. The typical data presented for all propellant pressure levels is taken from performance data obtained with the EEUR during this program.

TABLE I

DESIGN PARAMETERS

Specification Requirements

Thrust

Minimum 138.5 lbf at 100 psia propellant pressure
Minimum 167 lbf at 148 psia propellant pressure
Minimum 235.4 lbf at 286 psia propellant pressure
Maximum 280 lbf at 300 psia propellant pressure

Total Impulse

Cumulative	760,000 lbf-sec
Single firing (maximum)	165,000 lbf-sec

Specific Impulse

Steady state (minimum)	228.3 lbf-sec/lbm
Transient (average over first 5000 ib-sec)	220.0 lbf-sec/lbm

Firings

Total	109
Ambient hardware temp. starts	51
Hot starts	58

Operating Range

Propellant Feed Pressure (psia)	Typical (1) Thrust (lbf)	Typical (1) Flow Rate (lb/sec)	Typical (1) PCH (psia)
76(2)	101.4	.452	32
85(3)	114.6	.511	36
100	138.2	.602	43
148	174.4	.728	54
286	243.0	1.027	75
310	253.2	1.070	77.5
330(4)	261.5	1.110	80
397.3(5)	286.9	1.210	87.8

Notes:
(1) Typical data from EEUR performance, Section V
(2) Minimum demonstrated in this program
(3) Required minimum safe operating limit
(4) Required maximum safe operating limit
(5) Maximum demonstrated in this program

4. PERFORMANCE REVIEW

The specification requires that minimum thrust requirements for selected propellant pressure and temperature requirements be maintained over the duration of use. In addition, it limits the maximum thrust level and requires that the engine operate within specified transient thrust overshoot and steady state thrust oscillation. The particular minimum and maximum thrust limits are presented on Figure 2 which also contains all the test data for the units tested during this program as well as prior test results on the EEU and PRAT units.

The data on Figure 2 shows that all units tested (EEU, PRAT and EEUR) were within specification requirements over the normal operating range with minor exceptions; most notably the PRAT unit which was tested to a duty cycle known to produce high catalyst bed ΔP buildup and resultant reduced propellant flow. The two outlying points were the last two runs in the prior mission. In all other cases, borderline points were in some respect overparameter tests with respect to requirements.

Data below 100 psia and above 286 psia are outside the normal operating range and need not meet the requirements. Actually, the sharp change in characteristic at the low end of the range is caused by decavitation of the venturi at the low flow limit with associated change in propellant flow characteristic.

The transient thrust requirement permits a starting peak between 520 and 1000 lbf and steady state thrust oscillations between ± 23 and ± 45 lbf depending upon propellant pressure. These limits are well above characteristics demonstrated by all units tested. Figure 3 presents a typical test trace for an acceptance test at the beginning of engine life, and a trace from the last test conducted. These traces show no overshoot and insignificant thrust oscillations over an operating span of 2,295,000 lbf-sec.

Useful thrust chamber life is determined by the peculiar requirements of a given application; i.e., it may be over when thrust produced at a specified propellant pressure falls outside narrow tolerance limits or it may be over when the unit no longer produces any thrust upon command. Between these extremes in producing thrust, the life can be measured in terms of chamber pressure transient overshoot, chamber pressure roughness, total impulse, specific impulse, system pressure drop or number of firings. Consequently, life is a matter of definition, and tends to be defined by users in terms of their needs and suppliers in terms of their particular unit characteristics.

By most standards, the end of life was not attained on any of the engines tested. Starting overshoot was not significant on even the last runs of any of the units tested. Roughness was insignificant over the total test span on each unit. Total impulse accumulated was impressive relative to requirements and specific impulse was high relative to theoretical maximum right down to the last firings. Total impulse capability in excess of 2,000,000 lbf-sec was demonstrated during this program as indicated in Table II.

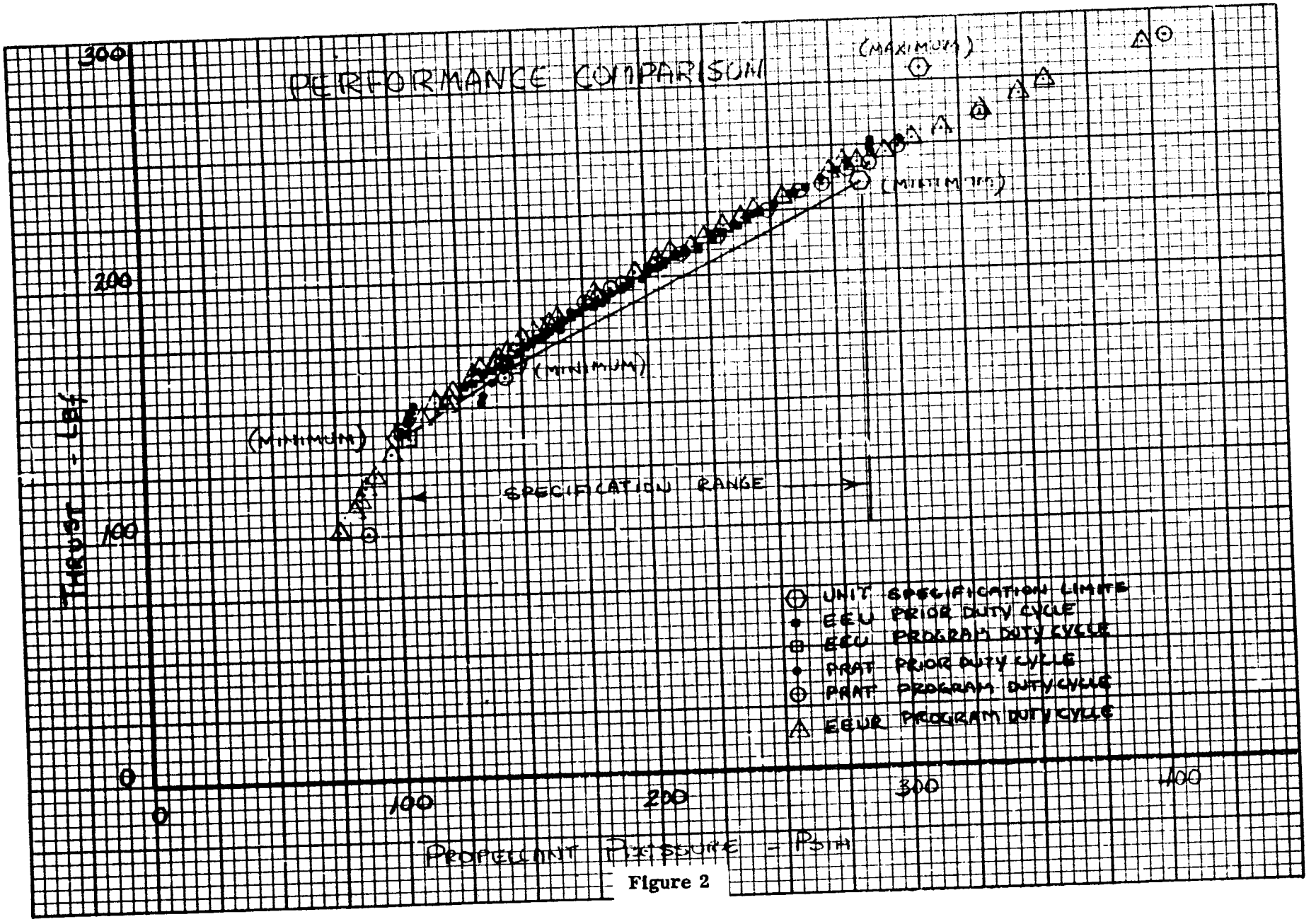
PERFORMANCE COMPARISON
(MAXIMUM)
(MINIMUM)
(MINIMUM)
(MINIMUM)
SPECIFICATION RANGE
UNIT SPECIFICATION LIMITS
ECU PRIOR DUTY CYCLE
ECU PROGRAM DUTY CYCLE
PRAT PRIOR DUTY CYCLE
PRAT PROGRAM DUTY CYCLE
EEUR PROGRAM DUTY CYCLE
300
200
100
0
0
100
200
300
400
PROPELLANT PRESSURE = PSIA

Figure 2

RUN 2018 ENGINEERING EVALUATION UNIT ACCEPTANCE TEST

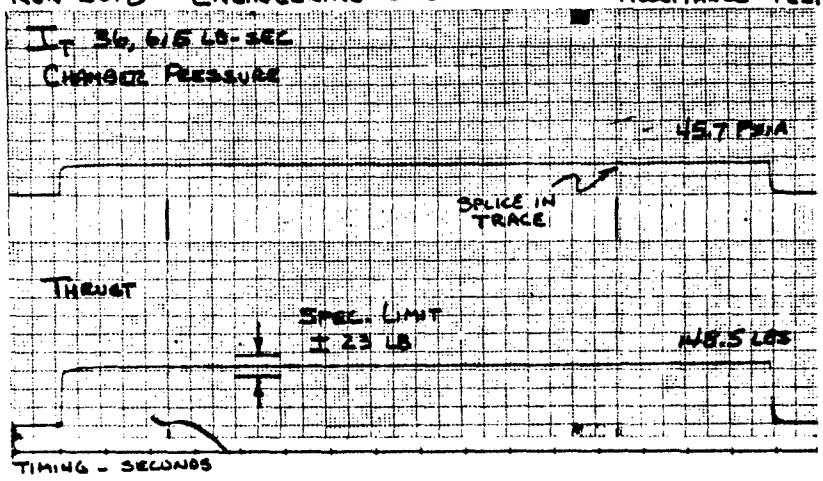

RUN 3299 ENGINEERING EVALUATION UNIT - LAST 5000 SEC. FIRING

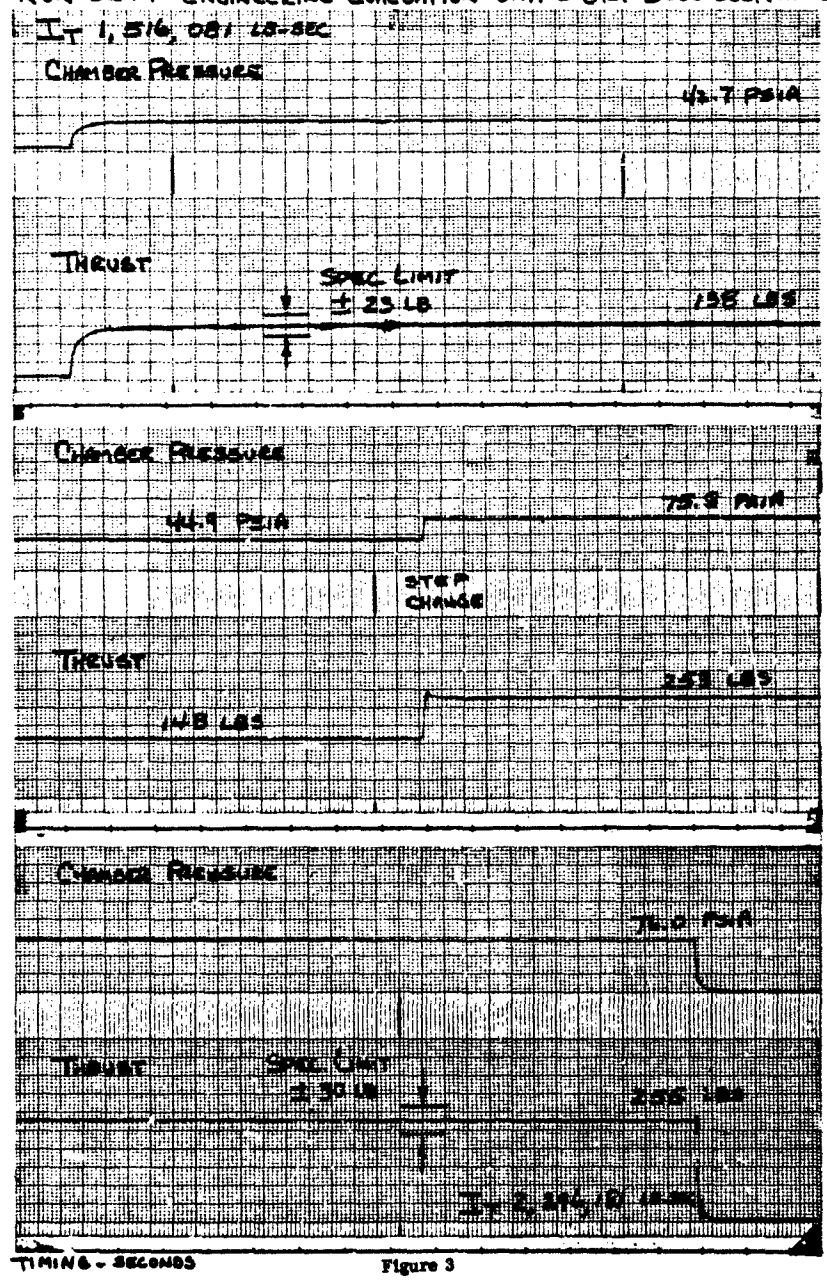

Figure 3

TABLE II

IMPULSE CHART

Requirement	Demonstrated		
	EEU	PRAT	EEUR
Single Burn 165,000 lbf-sec	780,000	178,600	362,700
Total Impulse 760,000 lbf-sec	2,295,000	1,093,449	1,552,341

This is almost three times the life requirement. Single burn capability of 780,000 lbf-sec was also demonstrated in this program, a figure several times the specification requirement. Since all of these tests were concluded according to plan rather than for cause, the total impulse limit has yet to be established.

The propellant injection technique used in the Kidde engine promotes high specific impulse over the flow range, a characteristic attributed to the fact that the percentage of flow out the end of the distribution tubes increases with decreasing flow rate. This results in deeper average propellant injection into the catalyst bed at lower flow conditions, and consequently smaller distance for decomposes gases to travel through the remaining catalyst bed. Dissociation of ammonia (an endothermic reaction) is thereby reduced allowing the higher energy working fluid to reach the nozzle plenum. The specific impulse characteristic is shown on Figure 4 for all testing on EEU, PRAT and EEUR. Over the normal operating range, the specific impulse is always in excess of 230 lbf-sec/lbm during the test duration.

The number of ambient temperature firings and the sequence of these firings has a demonstrated influence on the thrust chamber life characteristics. Specifically, back to back ambient temperature starts cause more rapid degradation of the catalyst bed pressure drop, a potential life limiting parameter. Alternate hot and cold starts have a restraining effect on the buildup in catalyst bed pressure drop tending to prolong life characteristics. Details of the theory behind these influences are presented in subsequent sections.

The total firing capability of the subject units is presented in Table III for each of the units tested, along with specified start requirements.

WALTER KIDDE & CO
BELLEVILLE, N.J.

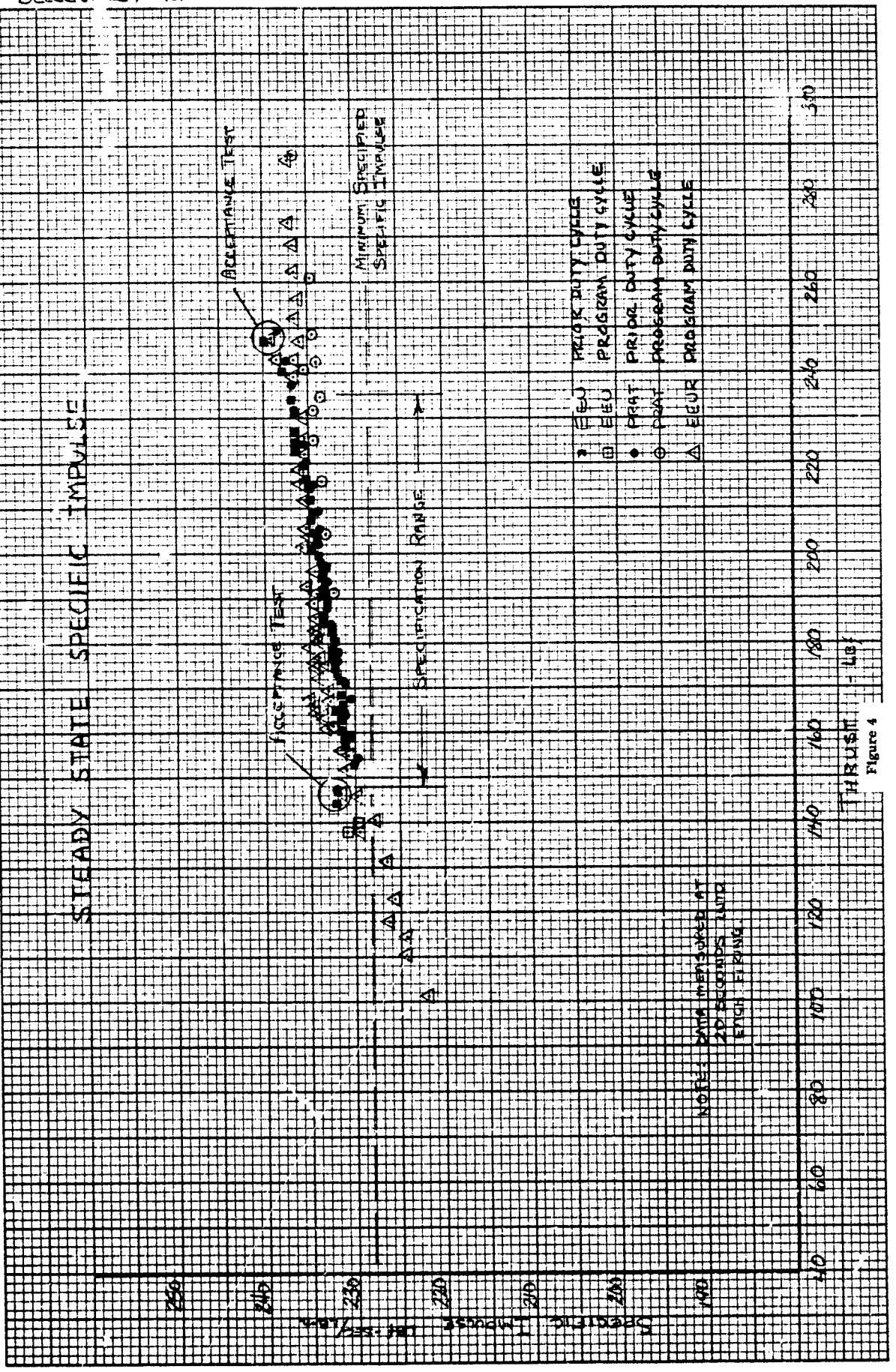

Figure 4

TABLE III

TOTAL FIRINGS

Requirement	Demonstrated		
	EEU	PRAT	EEUR
51 Ambient Starts	51	43	67
58 Hot Starts	52	32	66
109 Total Starts	103	75	133

The EEU and EEUR were subjected to pair firing missions and easily equaled or exceeded specification requirements. The PRAT unit was subjected to a single ambient start firing mission which caused pressure drop buildup and subsequent venturi decavitation, an undesirable event but not necessarily an end of life factor. The peak pressure drop buildup was attained during program testing, indicating that the unit could still be subjected to further testing. In other words, the data in Table III is a result accumulated at the end of tests planned and and not a limit where any failure occurred.

5. MEASUREMENT ACCURACY REVIEW

The data acquisition system used for this program is shown in block diagram form on Figure 5. The output signal from the sensing elements are conditioned, amplified, converted and displayed as indicated. The measurement errors associated with the sensing element and each of the signal conditioning steps, as well as calibration errors and zero shift errors on chamber pressure and thrust have been evaluated to produce the Performance Data Variability Summary presented on Table IV. This summary gives variability over the full range of TCA operation and includes measured test parameters and computed performance parameters.

The transducer zero shift profile relative to the time into each firing has not been established. The size of the shift is measured, for thrust and chamber pressure, at the end of each firing and a linear shift with time is assumed for purposes of correcting data integrated over the whole firing. The last data slice (thrust and chamber pressure) of each firing is corrected using the zero shift existing at the end of each run. Accuracies stated for thrust and chamber pressure in Table IV are based upon corrected final data slices. All data printout during a single firing includes any inaccuracy resulting from a zero shift. However, the zero shift is small for short runs and can be assumed even smaller at the 20 second point into each firing where most of the plotted data is taken. Consequently, the effect of ignoring zero shift does not significantly influence any comparisons, correlations or conclusions drawn from the data plotted.

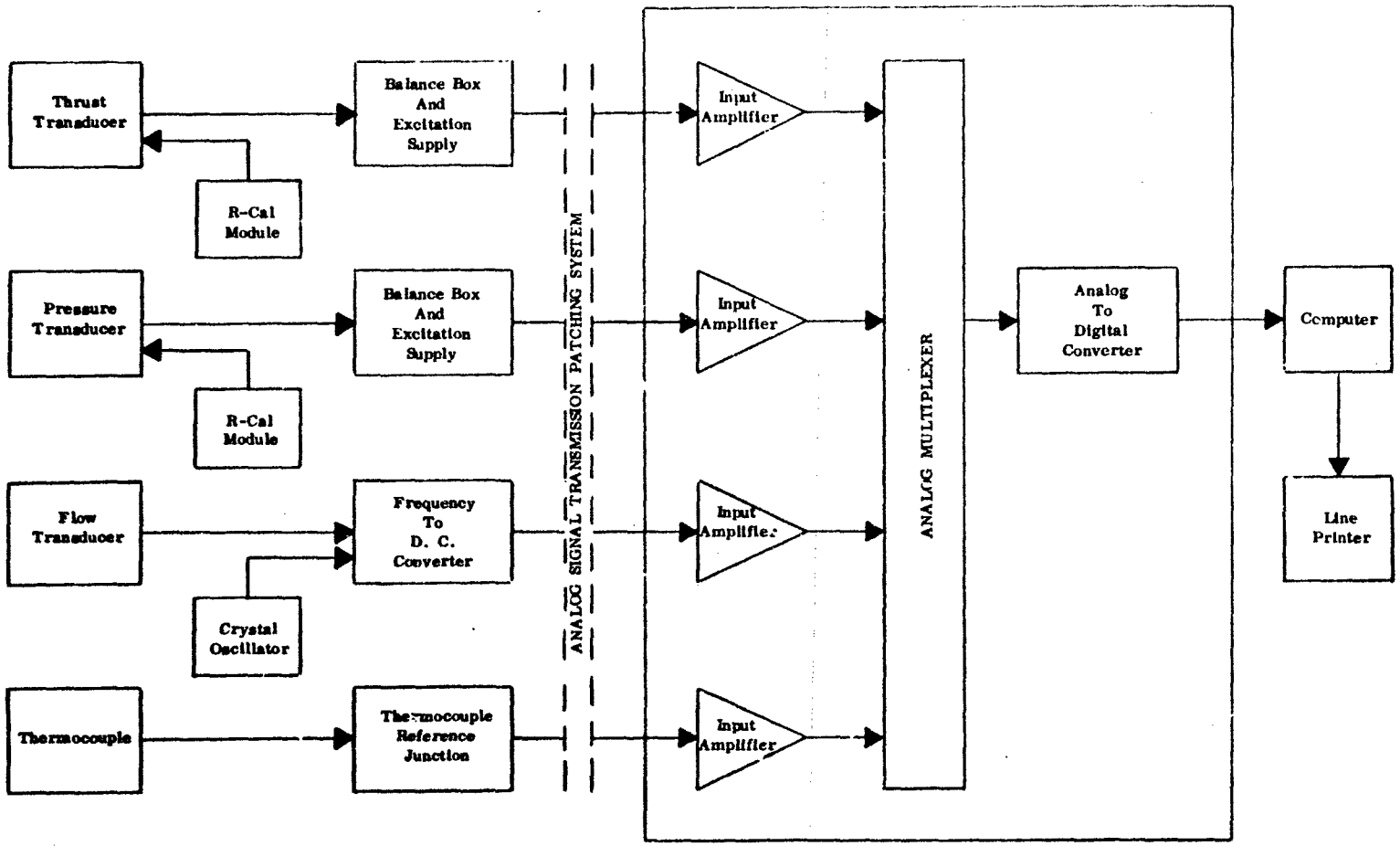

TEST DATA ACQUISITION SYSTEM BLOCK DIAGRAM

FIGURE 5

TABLE IV

PERFORMANCE DATA VARIABILITY[1] SUMMARY

MEASURED PARAMETER VARIABILITY[2]							CALCULATED PARAMETER VARIABILITY			
Propellant[3] Pressure (PFI) PSIA	Propellant Temperature (TFC) °F	Propellant Flow (WFC) Lb/Sec	Catalyst Bed Pressure Drop (DP3) PSI	Chamber Pressure (PCH) PSIA	Chamber[4] Temperature (TCH) °F	Thrust (F) LBF	Specific Impulse (ISP) Sec	Total Impulse LBF Sec	Characteristics Velocity C*	Thrust Coefficient C_F
76.0 ± 1.97%	± 1.52%	.458 ± .59%	25.6 ± .823%	32.1 ± 1.51%	± .79%	101.4 $^{+1.0}_{-0.0}$ %	+1.16 % −.590 %	+1.39 % − .96 %	± 1.62%	+1.81 % −1.5 %
126.4 ± 1.19%	± 1.52%	.689 ± .49%	29.9 ± .691%	49.9 ± 1.16%	± .79%	160.9 $^{+0.72}_{-0.0}$ %	+.871 % −.490 %	+1.14 % − .88 %	± 1.26%	+1.37 % −1.16 %
159.5 ± .955%	± 1.52%	.771 ± .45%	32.9 ± .626%	55.5 ± 1.04%	± .79%	180.6 $^{+0.64}_{-0.0}$ %	+.783 % −.450 %	+1.05 % − .83 %	± 1.14%	+1.22 % −1.04 %
200.9 ± .750%	± 1.52%	.893 ± .41%	35.9 ± .594%	62.9 ± .917%	± .79%	202.4 $^{+0.60}_{-0.0}$ %	+.727 % −.410 %	+.95 % −.74 %	± 1.01%	+1.10 − .917%
256.6 ± .577%	± 1.52%	.978 ± .37%	38.6 ± .551%	70.9 ± .789%	± .79%	230.3 $^{+0.46}_{-0.0}$ %	+.573 % −.370 %	+.81 % −.66 %	± .872%	+.914 % −.789 %
297.3 ± .366%	± 1.52%	1.210 ± .33%	44.8 ± .502%	87.8 ± .669%	± .79%	286.9 $^{+0.46}_{-0.0}$ %	+.565 % −.330 %	+.79 % −.62 %	± .746%	+.813 % −.669 %
434.6 ± .345%	± 1.52%	1.267 ± .32%	46.5 ± .488%	92.0 ± .617%	± .79%	302 $^{+0.46}_{-0.0}$ %	+.561 % −.320 %	+.76 % −.60 %	± .693%	+.770 % −.617 %

(1) Variabilities cover end to end measurements and are stated as percent of reading.

(2) Includes influence of zero shift where applicable.

(3) Absolute values for propellant pressure and all other measured parameters are typical values over the operating range.

(4) Temperature measurement variability is independent of operating thrust level.

SECTION II

ENGINEERING EVALUATION UNIT (EEU) WASHOUT AND REPRESSURIZATION TEST

1. INTRODUCTION

The Engineering Evaluation Unit was initially built to evaluate the influence of a pair firing duty cycle on life characteristics. Concern about the influence of pair firings developed as a result of prototype testing, where premature specific impulse degradation was encountered and associated with pair firings. This type duty cycle had not previously been accomplished on a flight configuration thrust chamber.

Premature performance degradation, termed washout, had previously been encountered and was initially related to test conditions including propellant temperature, total impulse accumulated and the number of ambient temperature starts accumulated. Subsequently, correlation was established between injector (distribution tube) flow characteristics (percentage end flow) and washout tendency which indicated that an average end flow in the 49-50% range would improve washout resistance. This led to a decision to build the EEU incorporating predicted washout resistant distributor flow characteristics and to conduct a pair firing duty cycle which would accumulate a large total impulse and a large number of ambient temperature starts. The average flow characteristics used were obtained from analysis of prior unit performance which contained distribution tube flow characteristics above and below the optimum percentage.

The critical components in the fabrication of the thrust chamber are the manifold and the distribution tubes. These form the injection system. All manifolds and distribution tubes are subjected to component testing against established limits as a basis for acceptance or rejection. From this stock of acceptable components, an EEU manifold and a ship-set of (37) distribution tubes was selected, the latter set to a 49-50% average percentage end flow. Summary test data for the manifold and the 37 distribution tubes selected is presented in Appendix III.

Prior to testing conducted under this program, the EEU was subjected to a standard acceptance test and a pair firing mission as described in Appendix III. This testing accumulated 4166 seconds of propellant flow time and 738,281 lb-sec of total impulse. There was no indication of any washout tendency during this testing. Data plots showing specific impulse and thrust as a function of propellant pressure, catalyst bed pressure drop as a function of accumulated impulse, and manifold temperature as a function of accumulated impulse is presented in Appendix III. Catalyst bed pressure drop buildup was low in relation to prior unit characteristics through mission testing confirming the prior observation that pair firings tend to reduce buildup in catalyst bed pressure drop. However, the concern that washout would

accompany the lower ΔP buildup characteristics was not supported, leaving the quantitative question of washout threshold location with respect to ΔP characteristics. This question, along with the opportunity presented to obtain test data on a unit in the latter stage of life, formed the basis for the proposal to test the EEU to washout.

2. WASHOUT AND REPRESSURIZATION TEST

Two 5000-second firings at low thrust level were conducted on the EEU to evaluate washout resistance. Both runs were completed without encountering washout. At the 4800-second point in each run, a repressurization to high thrust level was accomplished to evaluate the influence on specific impulse. In both instances specific impulse increased to peak level and remained there for the duration of the run.

The first 5000-second firing was conducted using 70°F propellant and the second firing was conducted using 53 - 55°F propellant temperature. Both runs were made with 100 psi propellant pressure and hardware in the 70 - 90°F range. Propellant pressure was maintained until the repressurization point when it was increased to 290 psia and held there for the remainder of each run. Figure 3 presents sections of the oscillograph traces from the second 5000-second firing which shows the start, the repressurization and the shutdown characteristics. Also included is the startup and shutdown characteristic of the EEU unit at approximately the same thrust level during the acceptance test on that unit. These traces compare characteristics over a span of 2.3 million pound-seconds total impulse.

Signs of washout were most evident during the second 5000-second burn as several downward excursions of specific impulse occurred toward the end of the run. However, none of these excursions exceeded the selected washout limit definition of -10 points of specific impulse below the peak attained during the firing. Peak specific impulse on the first run was 247+ lb-sec/lb. and minimum I_{sp} just before repressurization was 243 lb-sec/lb. Peak specific impulse on the second run was 245 lb-sec/lb. and minimum I_{sp} just before repressurization was 235+ lb-sec/lb. Specific impulse after repressurization was 247 lb-sec/lb. on the first firing and 244 lb-sec/lb. on the second firing.

The change in catalyst bed pressure drop is presented in Figure 6 which shows upstream catalyst bed pressure in comparison with chamber pressure in the nozzle plenum. The ΔP decreased from 30 psi near the start to about 10 psi before it leveled out with respect to chamber pressure. Since the catalyst retainer assembly pressure drop is in the order of 8 to 9 psia as a minimum before significant buildup has occurred at the screen, the apparent steady state ΔP across the catalyst bed was less than 2 psia, a level previously associated with washout conditions.

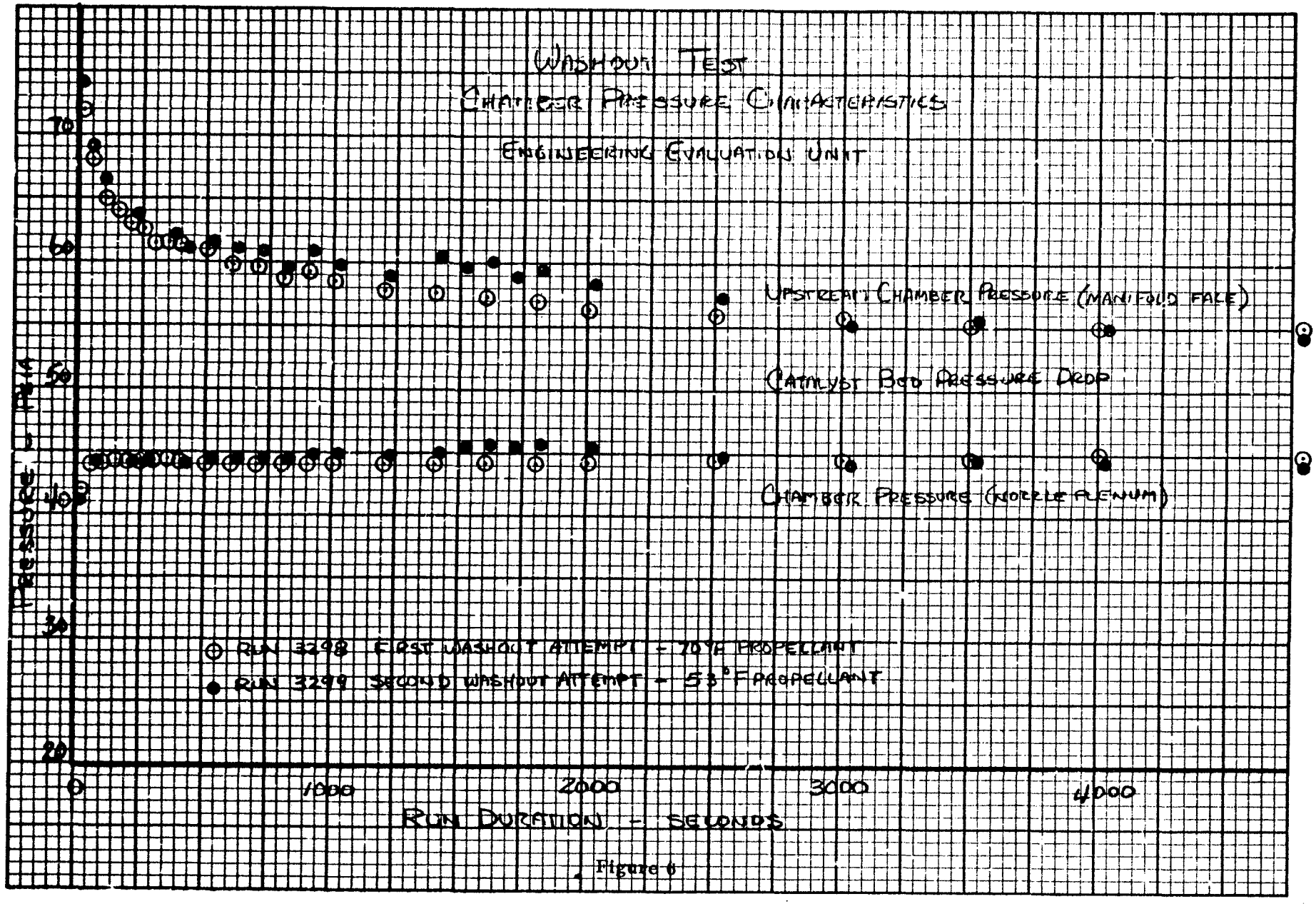
WASHOUT TEST
CHAMBER PRESSURE CHARACTERISTICS
ENGINEERING EVALUATION UNIT
UPSTREAM CHAMBER PRESSURE (MANIFOLD FACE)
CATALYST BED PRESSURE DROP
CHAMBER PRESSURE (NOZZLE PLENUM)
RUN 3298 FIRST WASHOUT ATTEMPT - 70°F PROPELLANT
RUN 3299 SECOND WASHOUT ATTEMPT - 53°F PROPELLANT
Pressure - psia
70
60
50
40
30
20
0
1000
2000
3000
4000
RUN DURATION - SECONDS

Figure 6

Figure 7 presents the catalyst bed pressure drop history normalized to eliminate the influence of the continuously changing flow profile of a decaying pressure propellant supply. The two points labeled "washout tests" are the runs mode during this program.

The two 5000-second runs accumulated 1,557,900 lb-sec. total impulse, 777,800 lb-sec. on the first firing and 780,100 lb-sec. on the second firing. Total propellant consumed was 3200 pounds on the first firing and 3250 pounds on the second firing producing 243.6 lb-sec/lb. and 240.2 lb-sec/lb respective average specific impulse during each firing.

WALTER KIDDE & CO
BELLEVILLE, N.J.

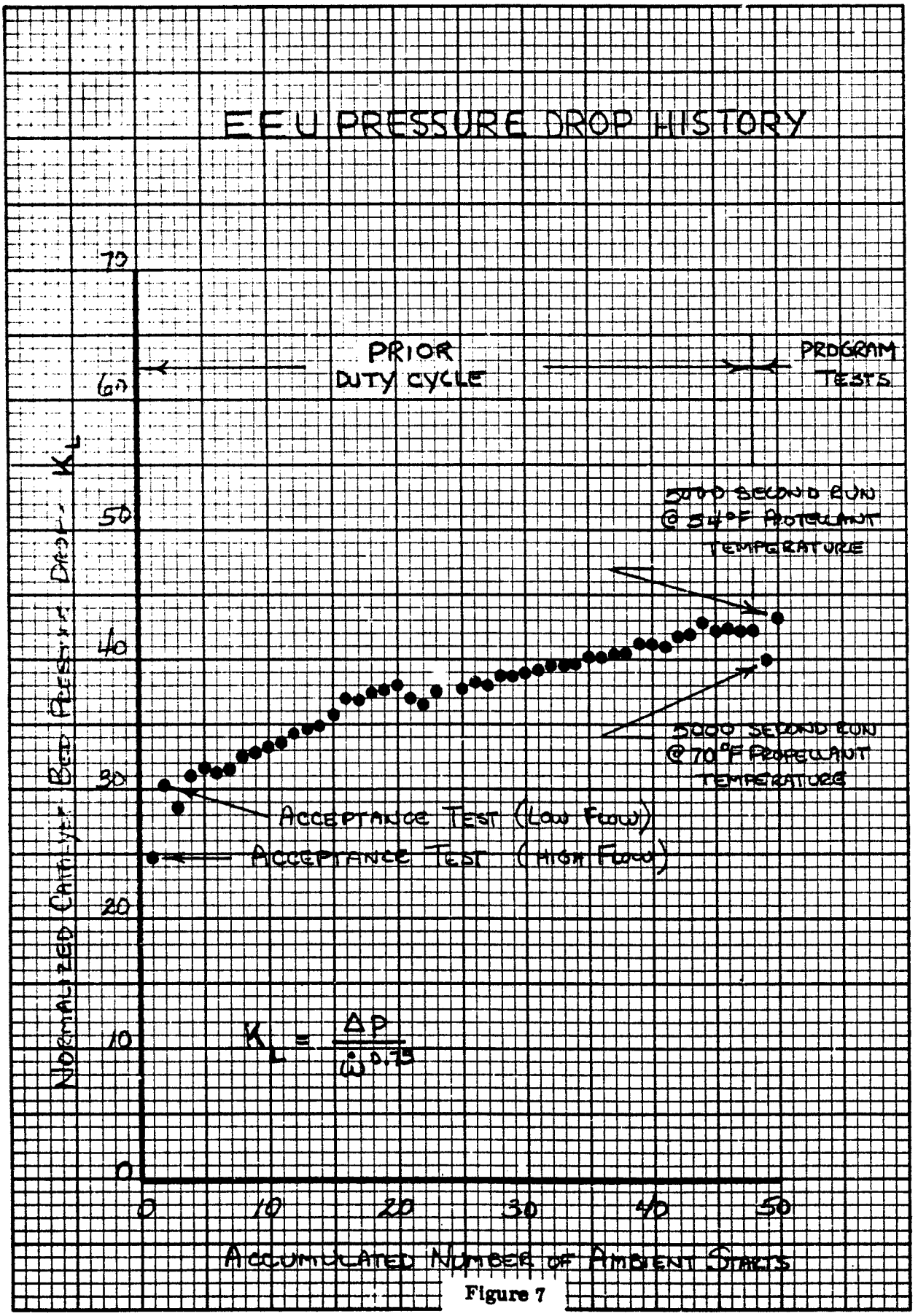

Figure 7

SECTION III

ENGINEERING EVALUATION UNIT (EEU) DISASSEMBLY

The EEU thrust chamber was subjected to a critical disassembly to determine internal component condition. The findings were normal with respect to previous disassembly experience, though it was noted that the coarse catalyst retainer screens and retainer plate were less deformed than most prior units disassembled. Total catalyst lost was comparable with prior data, but fine catalyst lost from partitions was less than prior units.

Prior to disassembly, the overall thrust chamber was x-rayed to examine general internal condition. Some evidence of partition distortion was evident and this is normal.

Disassembly of the thrust chamber was accomplished using an abrasive wheel to slit the nozzle to shell girth weld. During this procedure, the engine is oriented nozzle down in a milling machine and rotated slowly by the abrasive wheel in the milling head. Once the weld is broken, the thrust chamber is re-oriented to the nozzle up position in a holding fixture and the nozzle is easily removed. Figure 8 presents a view looking into the opened thrust chamber, with the support plate, retainer plate and retainer screens in view.

The support plate and retainer plate are withdrawn using a pulling device in the center threaded hole, leaving the retainer screws shown on Figure 9. Distortion of partitions is indicated by the lack of parallelism between the partition pins protruding through the screens. Distortion of partitions usually causes the partition locator pins to jam in the support plate and lift the partitions out of the catalyst as the support plate is withdrawn. This tendency is overcome by pushing the retainer screens down as the plate is withdrawn, a procedure which is only partially effective and does place a strain on the screens and partitions. Figure 10 shows the result after the retainer screens have been removed. In several partitions, these strains have caused the partition screens to break, releasing their contents to some degree. Otherwise, the coarse catalyst appearance was normal, and did not show any signs of sintering.

The main catalyst bed was removed first in sections. Section A included the last 1/2-inch at the downstream end of the catalyst bed. Section B is the next 1/2-inch in the upstream direction. Section C and D were respectively the top and bottom

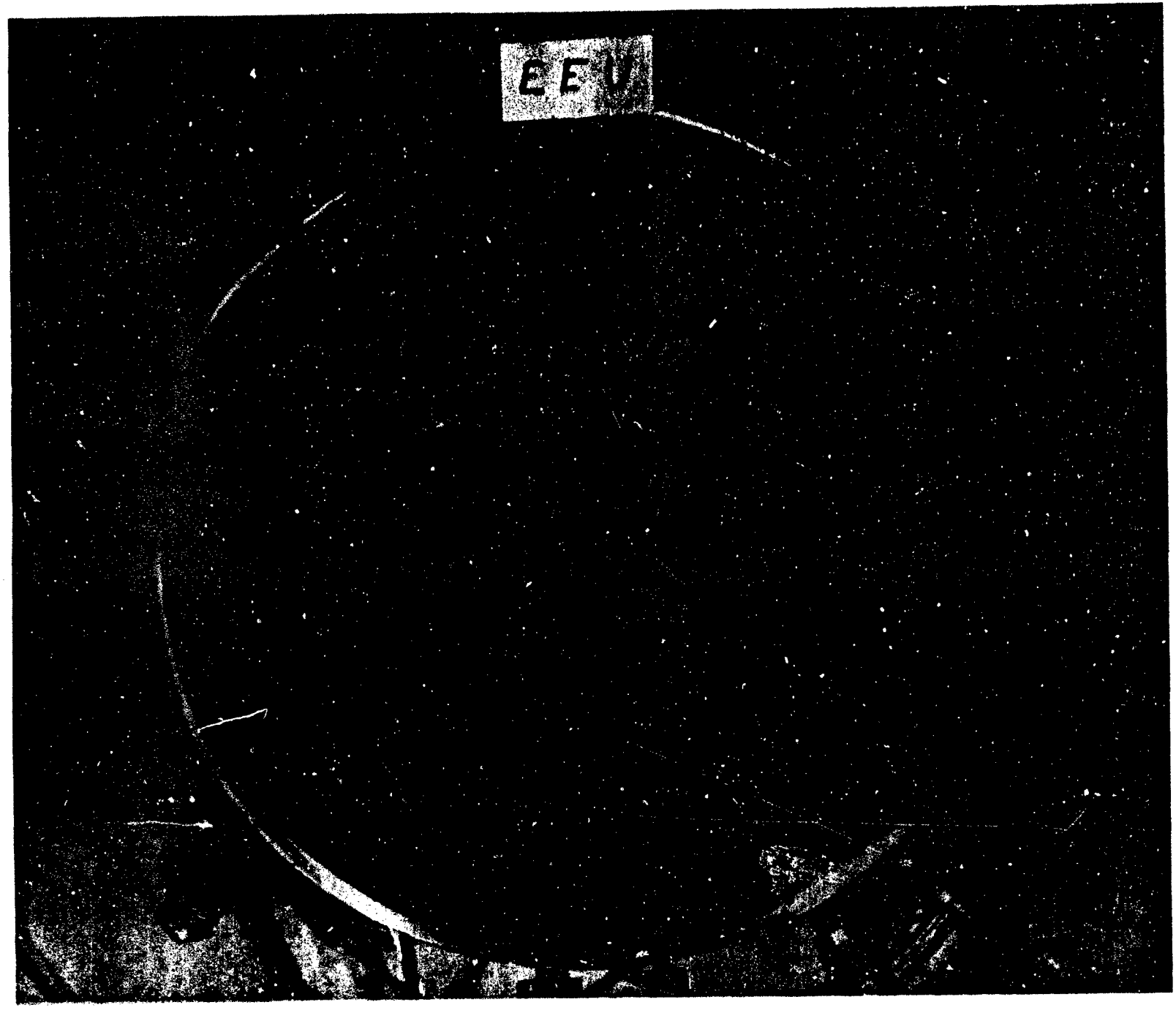
E E M

Figure 9

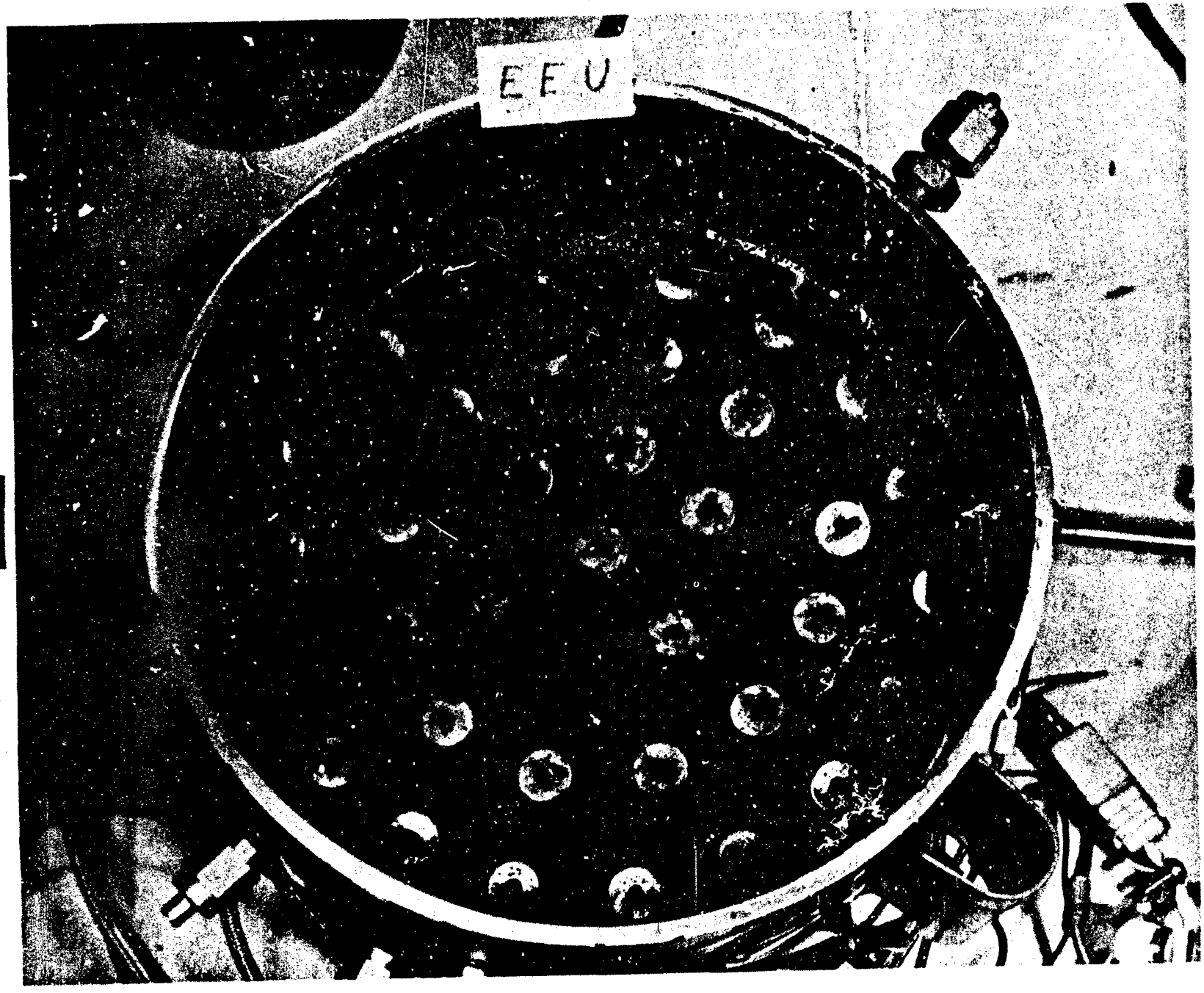
EEU

half of the remaining catalyst with respect to the test position of the engine. The catalyst from each of these sections was weighed and sifted separately to establish post test particle size ranges. Partitions removed from the thrust chamber were weighed to establish catalyst lost, x-rayed to determine internal condition and disassembled to obtained contained catalyst. Figure 11 shows x-rays of partitions from positions 21 to 27 which are typical of post test partition condition. Catalyst from disassembled partitions was combined and sifted to establish post test particle size range.

The results of coarse and fine catalyst analysis is presented on Tables V and VI, which also include the similar data from previously disassembled units, and an indication of the duty cycle imposed upon each unit.

The total fine catalyst removed from the partitions was 183.9 gms., allowing the determination of 9.2 gms of catalyst lost from the partitions. The loss per partition varied from .2 to .6 gms over the 37 partitions contained and the overall catalyst lost was 4.8% of that initially loaded in the partitions. In order to escape from the partitions, particles must pass through the 40 mesh size opening of the cylindrical partition screen.

Sieving the fine catalyst determined that 153.8 gms was still within the nominal installed size range, and 30.1 gms was under the nominal specified size range. Of the 30.1 gms under size, 7.9 gms was under 30 mesh and 5.7 gms was under 40 mesh. When compared to particle size range of a sample of new catalyst, which shows 91.7% in the nominal specified rance of 20-24 mesh, 8.2% smaller than 24 mesh but larger than 30 mesh, .04% smaller than 30 mesh but larger than 40 mesh and .04% smaller than 40 mesh, the degree of catalyst particle size breakdowns can be established. This procedure is approximate since the new catalyst sample is a representative sample only and not an actual sample of the catalyst packed in the EEU.

Based upon the percentages for new catalyst stated above, 177 gms of catalyst larger than 24 mesh was installed in the EEU. Post test analysis shows 153.8 gms remaining, indicating a breakup of 23.2 gms or 13.1% of that installed. Similarly, 1.5 gms of catalyst under 30 mesh was installed. Post test analysis shows 13.6 gms remaining, indicating a gain in particles under 30 mesh of 12.1 gms. Since the catalyst lost had to be under 30 mesh, the total fines under 30 mesh formed was 21.4 gms or 11.1% of the total new partition catalyst installed. The same technique is also used to establish that 14.2 gms of fines under 40 mesh size is formed which represents 7.3% of the total new partition catalyst installed.

The total coarse catalyst removed from the main catalyst bed was 905.1 gms, allowing the determination of a total post test catalyst weight of 1080 gms (coarse plus fine remaining). Total catalyst lost from the engine is then the difference between the total packed (1151.4 gms) and that which remained after test or 62.4 gms. Knowing 9.2 gms was lost from the partition catalyst, the loss from the

WK 876062 05 F

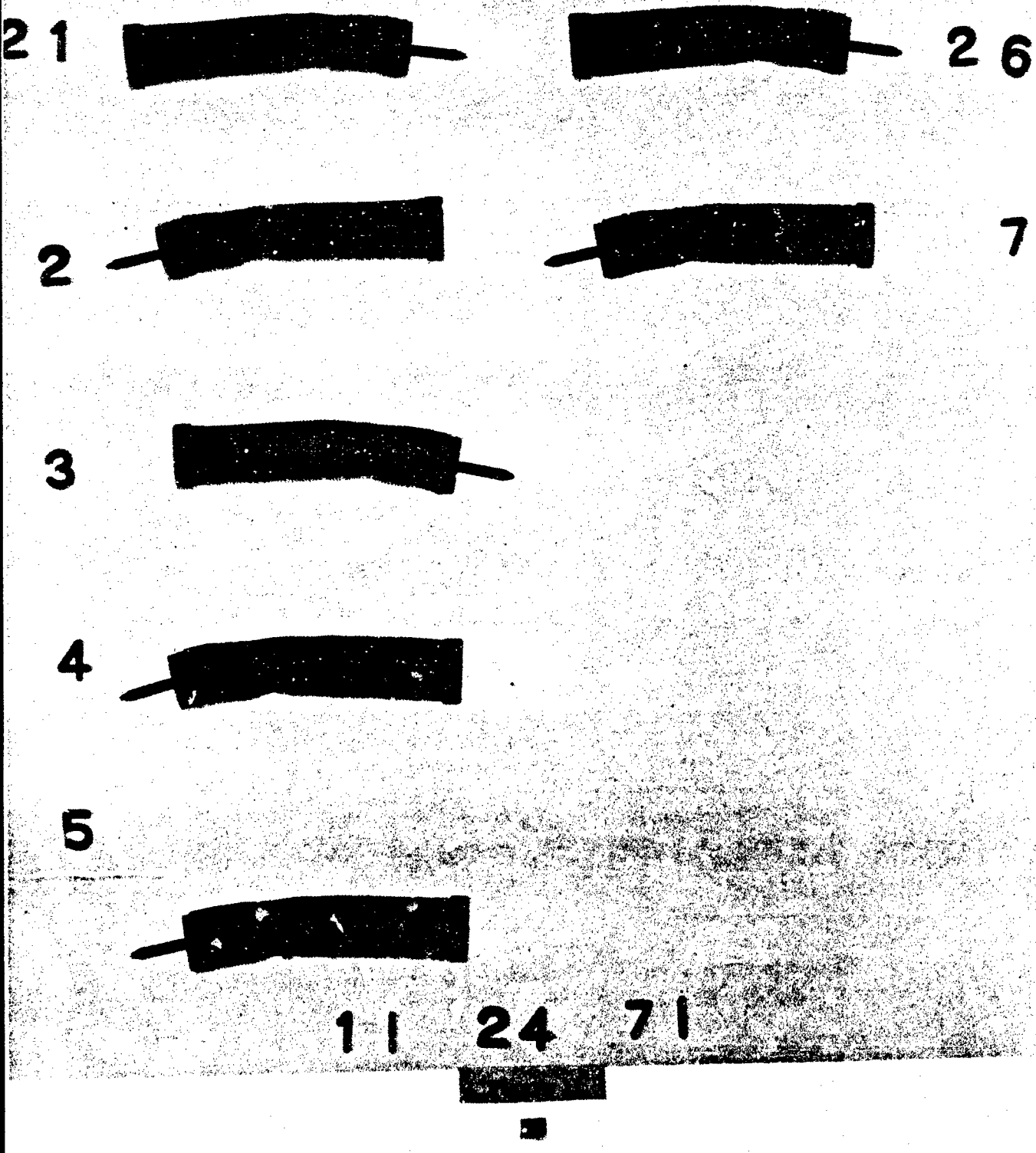

TABLE V - COARSE CATALYST BED DISASSEMBLY DATA COMPARISON

	ENGINEERING EVALUATION UNIT EEU	DEVELOPMENT UNIT X-3R	DEVELOPMENT UNIT X-3R2	QUALIFICATION UNIT QA-1	QUALIFICATION UNIT QA-2	RELIABILITY UNIT R-001	DEVELOPMENT UNIT (1/8 x 1/8 CATALYST) Y-3
1. FINE CATALYST INSTALLED - GMS	193.2	204.6	193.5	200.4	202.3	201.9	339.3
2. COARSE CATALYST INSTALLED - GMS	958.2	949.0	999.9	986.6	972.4	979.6	821.5
3. TOTAL CATALYST INSTALLED - GMS	1151.4	1153.6	1193.4	1187.0	1174.7	1191.5	1160.8
4. TOTAL POST TEST COARSE CATALYST	905.1	886.5	944.2	941.2	925.6	928.3	739.0
5. TOTAL FINE CATALYST LOST FROM PARTITIONS	9.3	22.2	32.2	13.7	14.2	16.7	17.5
6. TOTAL CATALYST WEIGHT AFTER TEST	1089.0	1068.9	1105.5	1127.9	1113.7	1113.5	1060.8
7. TOTAL CATALYST LOST FROM ENGINE	62.4	84.7	87.9	59.1	61.0	78.0	100.0
8. TOTAL COARSE CATALYST LOST	53.1	62.5	55.7	45.4	46.8	51.3	82.5
9. PERCENT OF TOTAL CATALYST LOST	5.4%	7.4%	7.4%	5.0%	5.2%	6.6%	8.6%
10. PERCENT OF COARSE CATALYST LOST	5.5%	6.6%	5.5%	4.6%	4.9%	5.2%	10.0%
11. TOTAL FINES IN COARSE SMALLER THAN 16 MESH	34.2	55.0	73.1	56.3	55.1	61.2	38.6
12. TOTAL COARSE AFTER TEST LARGER THAN 16 MESH	870.1	831.6	871.2	884.9	870.5	863.5	700.5
13. TOTAL COARSE BROKEN SMALLER THAN 16 MESH	88.1	117.4	128.7	101.7	101.9	116.1	121.0
14. PERCENT OF COARSE BROKEN SMALLER THAN 16 MESH	9.2%	12.4%	12.8%	10.3%	10.5%	11.8%	14.7%
15. TOTAL FINES IN COARSE SMALLER THAN 40 MESH	7.0	12.4	22.2	14.1	11.7	17.7	20.3
16. TOTAL FINES SMALLER THAN 40 MESH LOST FROM THE BED OR FOUND IN THE COARSE CATALYST	69.4	97.1	109.1	73.2	72.7	95.7	120.3
17. TOTAL FINES SMALLER THAN 40 MESH FOUND IN COARSE CATALYST	60.1	74.9	76.9	59.5	58.5	79	102.8
18. PERCENT OF COARSE CATALYST DEGRADATION TO FINES SMALLER THAN 40 MESH	6.3%	7.9%	7.7%	6.0%	6.0%	8.1%	12.8%
PROPELLANT TEMPERATURE °F	70	50	70	70	100	70	50
PERCENT AREA 4 FLOW AT LOW FLOW	49.8	53.4	54.6	50.4	49.4	50.6	-
TOTAL IMPULSE ACCUMULATED LB-SEC	2,295,000	1,109,983	2,433,447	760,167	784,255	867,035	1,247,557
NUMBER OF STARTS AMBIENT/HOT	51/52	61/64	33/20	29/13	21/13	37/106	24/15
TOTAL RUN TIME - SECONDS	14166	6743	14,502	4374	4248	4777	7612
TOTAL PROPELLANT CONSUMED LBS	9622	4820	10,270	3258	3294	3769	5537

TABLE VI - PARTITION CATALYST DISASSEMBLY DATA COMPARISON

	ENGINEERING EVALUATION UNIT EEU	DEVELOPMENT UNIT X-3R	DEVELOPMENT UNIT X-3R2	QUALIFICATION UNIT QA-1	QUALIFICATION UNIT QA-2	RELIABILITY UNIT R-001	DEVELOPMENT UNIT (1/8 x 1/8 CATALYST) Y-3
1. TOTAL CATALYST INSTALLED IN PARTITIONS	193.2	204.6	193.5	200.4	202.3	201.9	339.3
2. TOTAL CATALYST REMOVED FROM PARTITIONS	183.9	182.4	161.5	186.7	188.1	185.2	321.8
3. TOTAL CATALYST LOST FROM PARTITIONS	9.3	22.2	32.2	13.7	14.2	16.7	17.5
4. PERCENT OF PARTITION CATALYST LOST	4.8%	10.8%	16.6%	6.8%	7.0%	8.3%	5.2%
5. TOTAL NEW CATALYST RETAINED - 24 MESH SCREEN	177	187	177	183.7	185.0	-	311
6. TOTAL USED CATALYST RETAINED - 24 MESH SCREEN	153.8	135.2	109.4	149.7	160.5	-	268.4
7. TOTAL BREAKUP OF 20-24 MESH PARTICLES	23.2	51.8	67.6	34.0	24.5	-	42.6
8. PERCENT OF 20-24 MESH PARTICLE BREAKUP	13.1%	25.3%	38.2	17%	13.1%	-	13.7%
9. TOTAL NEW CATALYST INSTALLED UNDER 30 MESH	1.5	1.7	1.6	1.6	1.6	-	2.7
10. TOTAL USED CATALYST UNDER 30 MESH FOUND	13.6	16.8	15.3	16.6	16.9	-	17.7
11. NET GAIN IN PARTICLES UNDER 30 MESH	12.1	15.1	13.7	15.0	15.3	-	14.8
12. TOTAL FINES UNDER 30 MESH FORMED	21.4	37.3	45.9	28.7	29.5	-	32.3
13. PERCENT OF FINES UNDER 30 MESH FORMED	11.1%	18.2%	23.7%	14.3%	14.6%	-	9.5%
14. TOTAL NEW CATALYST INSTALLED UNDER 40 MESH	.8	.8	.8	.8	.8	-	1.4
15. TOTAL USED CATALYST UNDER 40 MESH FOUND	5.7	6.0	11.6	7.6	8.4	-	8.8
16. NET GAIN IN PARTICLES UNDER 40 MESH	4.9	5.2	10.8	6.8	7.6	-	7.1
17. TOTAL FINES UNDER 40 MESH FORMED	14.2	27.4	43.0	20.5	21.8	-	24.6
18. PERCENT OF FINES UNDER 40 MESH FORMED	7.3%	13.4%	22.2%	10%	10.8%	-	7.25%
PROPELLANT TEMPERATURE °F	70	50	70	70	100	70	50
PERCENT AREA 4 FLOW AT LOW FLOW	49.8	53.4	54.6	50.4	49.4	50.6	-
TOTAL IMPULSE ACCUMULATED LB-SEC	2,295,000	1,109,983	2,433,447	760,167	784,255	867,035	1,297,557
NUMBER OF STARTS AMBIENT/HOT	51/52	61/64	33/20	29/13	21/13	34/106	24/15
TOTAL RUN TIME SECONDS	14466	6743	14502	4374	4284	4777	7612
TOTAL PROPELLANT CONSUMED - LBS	9622	4820	10270	3258	3294	3769	5537

main bed of 53.1 gms is calculated. This figure is 5.5% of the installed coarse catalyst, and the total catalyst loss is 5.4% of the total catalyst initially installed in the engine.

Sieving of the coarse catalyst determined that 34.2 gms or 9.2% of that installed had broken down to particles smaller than will be retained on a 16 mesh screen. Of this quantity, 7 gms was found to pass through a 40 mesh screen and could have escaped from the engine. If this is added to the 53.1 gms of coarse catalyst which was lost, a total of 60.1 gms of coarse catalyst which degraded to fines smaller than 40 mesh particle size equivalent can be calculated. This is 6.3% of the total coarse catalyst (8 - 12 mesh) initially packed in the engine.

Twenty distribution tubes removed from the EEU thrust chamber were subjected to a post test flow calibration as part of the disassembly task. The procedure used was identical to that used to calibrate new distribution tubes as described in Appendix I. The data obtained is presented in Table VII, which also includes the acceptance flow calibration data for the same distribution tubes. If the averages given near the bottom of the table, are compared on a "new" versus "used" basis, a trend of reduced area 4 flow is evident. Total end flow stays nearly constant, indicating that a flow shift from area 4 to area 3 has taken place. This change is explained by the slight bending of distribution tubes over the life of the unit. A shift of this nature would support an increased resistance to washout performance characteristics since more upstream average injection of propellant into the catalyst bed would occur.

Partition screens removed from the EEU thrust chamber were subjected to metallographic analysis for effects of exposure to high temperature nitrogen and ammonia. The results confirmed a deep penetration of the Hastelloy C screen wire material and conversion of the alloy material to brittle nitrides. The degree of embrittlement is indicated on Figure 12, which shows the specimen analyzed, a sample of the specimen mounted and two photomicrographs of specimen sectors at 50 times and 500 times magnification. The nitride case is evident in these pictures.

A transverse section of the downstream end of the partition was selected for a specimen and mounted in Bakelite. After polishing, Marbles etch was applied to the specimen. A dark etching layer accompanied by a light etching outer fringe was revealed in the specimen wire. This structure is composed of nitrides of chromium, molybdenum, iron, tungsten and vanadium. All five are known to form stable nitrides. Micro-hardness readings confirm the high hardness of this layer which is typical of nitrided surfaces.

Additional micro-hardness readings taken at the center of the wire cross-section revealed higher than "as fabricated" hardness indicating diffusion of nitrogen and the formation of nitrides which are not easily discernible in the microstructure. Examination of the photomicrographs show the visible nitride layer to be .0028 to .004 inches thick which represents the major cross-section of the .010 inch diameter wire.

TABLE VII

DISTRIBUTION TUBE FLOW ANALYSIS ENGINEERING EVALUATION UNIT DISASSEMBLY
NEW VS USED TUBES - PERCENT OF TOTAL FLOW

S/N	Average Area 4 Flow		Average End Flow		Average Body Flow		Manifold Loc.	Average Area 4 Flow		Average End Flow		Average Body Flow	
	High Flow	High Flow	High Flow	High Flow	High Flow	High Flow		Low Flow	Low Flow	Low Flow	Low Flow	Low Flow	Low Flow
	New	Used	New	Used	New	Used		New	Used	New	Used	New	Used
1147	43.7	33.6	61.0	63.9	39.0	36.1	1	51.1	52.4	64.0	70.9	36.0	29.1
1149	45.8	44.8	58.8	59.3	41.2	40.7	3	49.1	51.4	64.2	63.6	35.8	36.4
1150	45.4	43.1	58.0	59.7	42.0	40.3	4	45.6	47.7	64.7	62.1	35.3	37.9
1151	43.2	42.2	59.5	59.0	40.5	41.0	5	46.8	51.2	66.5	64.4	33.5	35.6
1153	44.9	44.1	58.5	57.7	41.5	42.3	7	48.7	51.2	62.8	63.2	37.2	36.8
1154	44.8	43.1	58.6	57.3	41.4	42.7	8	48.5	51.3	62.6	63.0	37.4	37.0
1155	43.3	38.1	60.3	58.0	39.7	42.0	9	49.9	40.7	65.3	61.4	34.7	38.6
1150	40.4	37.4	59.0	59.0	41.0	41.0	10	49.4	41.6	64.0	63.8	36.0	36.2
1157	42.7	35.5	56.4	59.9	43.6	40.1	11	48.0	48.6	64.0	64.8	36.0	35.2
1172	42.9	33.8	59.3	58.5	40.7	41.5	22	46.6	37.5	61.6	62.2	38.4	37.8
1173	40.0	36.2	60.2	60.5	39.8	39.5	23	45.2	48.3	66.8	69.9	33.2	30.1
1175	40.1	38.3	59.3	57.4	40.7	42.6	24	47.3	40.1	65.0	61.5	35.0	38.5
1176	41.5	33.3	57.5	57.4	42.5	42.6	25	53.0	42.2	66.2	64.5	33.8	35.5
1188	40.5	36.0	64.0	62.3	36.0	37.7	28	57.0	54.6	67.0	67.0	33.0	33.0
1189	43.0	38.7	62.0	62.0	38.0	38.0	29	45.0	45.7	65.5	64.0	34.5	36.0
1190	42.5	37.9	56.5	63.9	43.5	36.1	30	54.5	44.0	62.0	61.7	38.0	38.3
1192	42.0	45.9	60.0	59.6	40.0	40.4	31	52.5	52.8	63.0	65.3	37.0	34.7
1193	49.5	42.8	60.5	63.9	39.5	36.1	32	52.5	54.3	65.5	73.2	34.5	26.8
Ave	43.1	39.0	59.4	59.9	40.6	40.1		49.4	47.5	64.4	64.8	35.6	35.2
DISTRIBUTION TUBES FLOWED BUT NOT USED IN ABOVE AVERAGE													
1159	46.6	46.0	59.2	86.4	40.8	13.6	12	50.6	60.3	62.3	80.1	37.7	19.9
1171	43.4	41.8	60.7	83.9	39.3	16.1	21	57.0	58.4	65.8	73.4	34.2	26.6

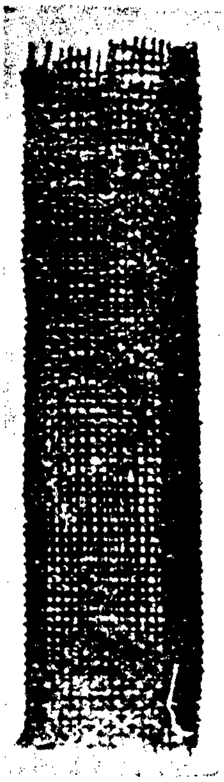

PARTITION SCREEN
2X SIZE

CROSS-SECTION
2X SIZE

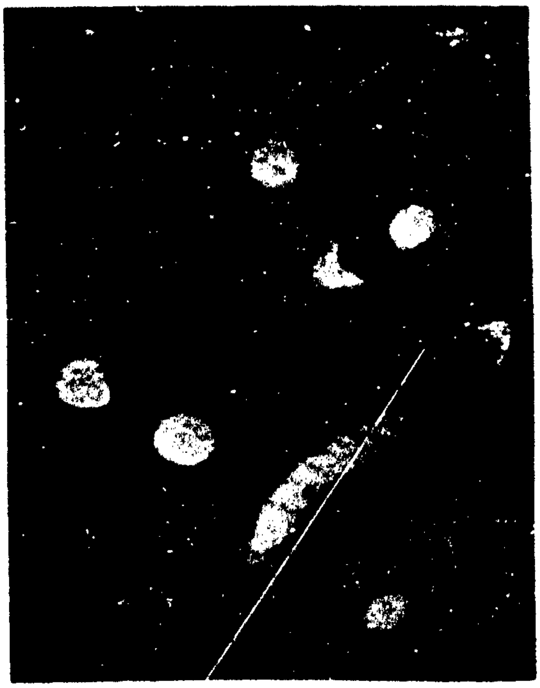

[illegible]

[redacted]

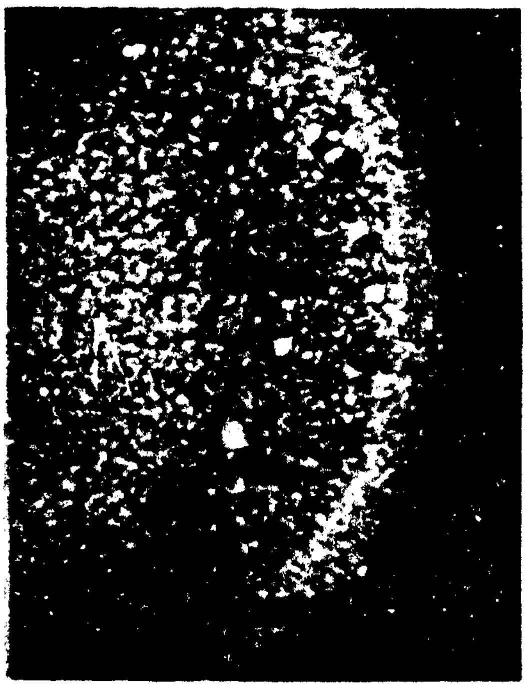

WIRE SECTION
[illegible]X SIZE

SECTION IV

PRODUCTION RELIABILITY ASSESSMENT TEST (PRAT) UNIT CATALYST BED PRESSURE DROP BUILDUP EVALUATION

1. INTRODUCTION

The Production Reliability Assessment Test TCA was initially built to demonstrate the reproducibility of production units for the second lot of flight articles. It was the second unit build (EEU was first) with controlled average distribution tube end flow in the range of 49-50% of the total flow at low thrust conditions. Summary test data for the manifold and the 37 distribution tubes selected for this unit is presented in Appendix IV.

Prior to testing conducted under this program the PRAT was subjected to a standard acceptance test and a single firing mission (all ambient temperature starts) as described in Appendix IV. This testing accumulated 4001 seconds of propellant flow time and 731,013 lb-sec of total impulse. Data plots showing specific impulse and thrust as a function of propellant pressure; catalyst bed pressure drop as a function of accumulated impulse; and manifold temperature as a function of accumulated impulse is presented in Appendix IV.

Catalyst bed pressure drop buildup was high in relation to prior unit characteristics through mission testing, confirming the prior observation that single ambient temperature start firings tend to increase buildup in catalyst bed pressure drop.

Near the end of mission life, the $\triangle P$ buildup exceeded the compensation capability of the cavitating venturi at which point decavitation occurred and flow rate became a function of the downstream pressure drops.

The pressure drop buildup continued throughout the mission which led to speculation about the subsequent effect of higher $\triangle P$ buildup for longer mission requirements. High $\triangle P$ could ultimately create excessive stress loading of internal parts, cause overheating of the manifold and have an amplifying effect on performance degradation. However, should the $\triangle P$ characteristic level off, these potential problems may never arise. Consequently, it was proposed to continue the single firing sequence and establish the $\triangle P$ buildup characteristic for several more firings or until a peak was established.

2. CATALYST BED PRESSURE DROP BUILDUP EVALUATION

Twelve 22,000 lb-sec. firings using 100°F propellant were conducted on the PRAT unit to verify that the normalized catalyst bed pressure drop characteristic would peak out as anticipated. Subsequently, five pair firings consisting of a 9300 lb-sec firing and a 1200 lb-sec firing with 45 minutes off-time were accomplished, and this was followed by 20 hot pulses of 6.9 second duration with 53.1 seconds off-time. Both sequences were conducted to evaluate their influence on established catalyst bed pressure drop characteristics, and both proved to have no significant influence as established by a repeat 22,000 lb-sec firing. Finally, a low-low thrust run was undertaken (8.1 psia propellant pressure) to evaluate stability characteristics under the influence of high catalyst bed pressure drop and high total impulse effects. Results verified stability equivalent to acceptance test performance. Figure 13 presents oscillograph traces for several test measurements taken during the final PRAT firing.

On the first PRAT firing, one of the manifold metal temperature measurements adjacent to the catalyst bed exceeded the in-run limit of 850°F causing an automatic computer shutdown of the unit. This phenomenon was not unique having occurred on other high catalyst bed ΔP units, near the end of mission testing where propellant pressure is normally low. However, prior operation of this unit at the same 100°F propellant temperature and firing impulse, but at low inlet pressure had not resulted in a manifold temperature shutdown, suggesting that the condition may be more severe with higher inlet pressure. Propellant pressure for the PRAT test was initially 290 psia while propellant pressure near the end of normal mission testing is 125 psia. Consequently, a decision was made to increase inlet pressure to the maximum level anticipated (400 psia) and continue the single ambient start 22,000 lb-sec firings along a new decay curve.

Four additional high manifold temperature shutdowns occurred after repressurization in an every-other firing pattern starting at the 400 psia propellant pressure level. However, below 280 psia propellant pressure, manifold temperature no longer reached 850°F and there were no further automatic shutdowns.

Performance obtained is presented on Figures 14 and 15 which also contain prior test results on this unit for comparative purposes. Figure 14 is a composite plot showing catalyst bed pressure drop and propellant flow as functions of accumulated impulse over the full life of the PRAT unit. All of the prior firings are presented in the range up to 750,000 lb-sec. Subsequently, current program firings are presented showing repressurization, the decaying flow and the catalyst bed pressure drop characteristics. On these plots, catalyst bed pressure drop

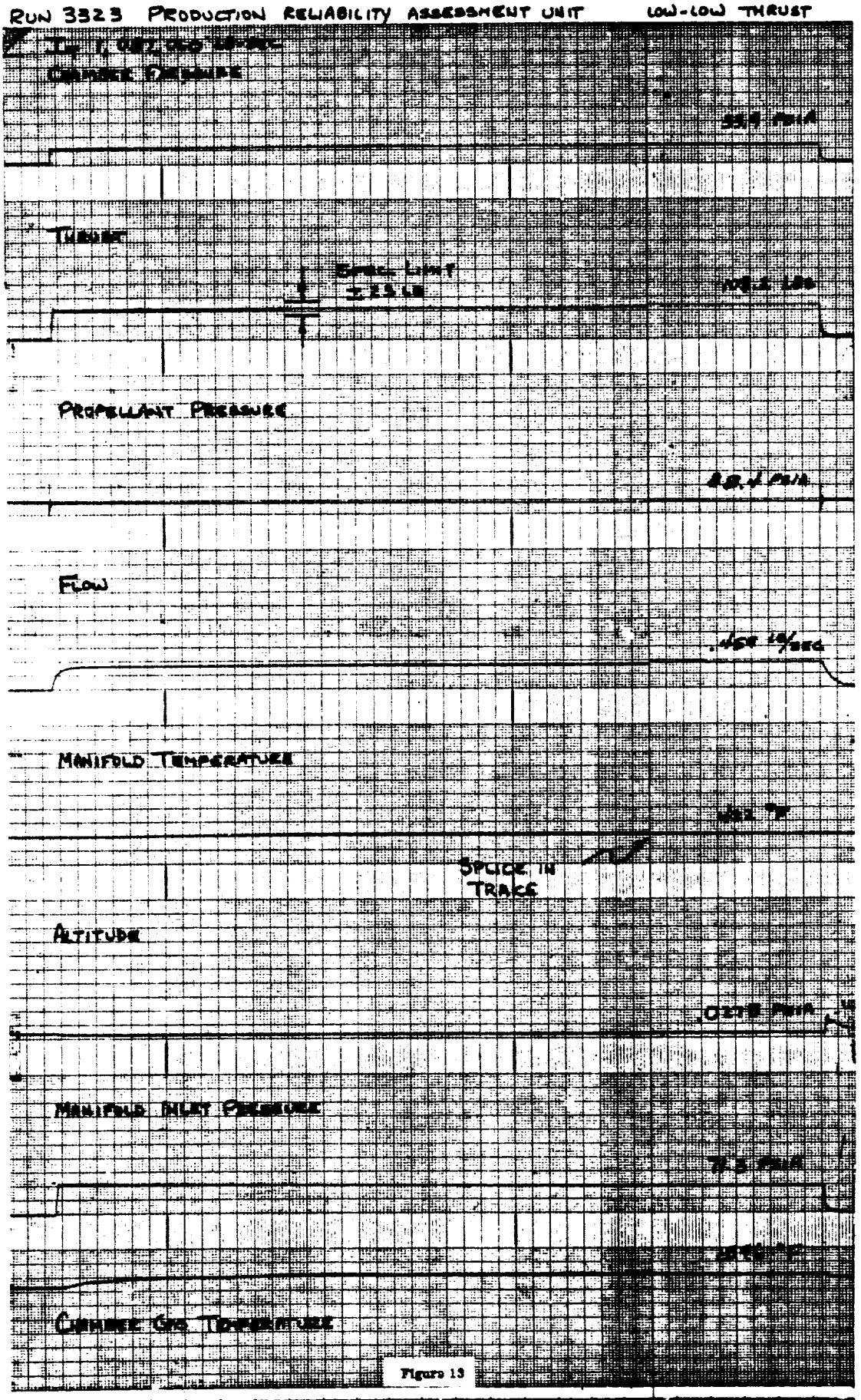

Figure 13

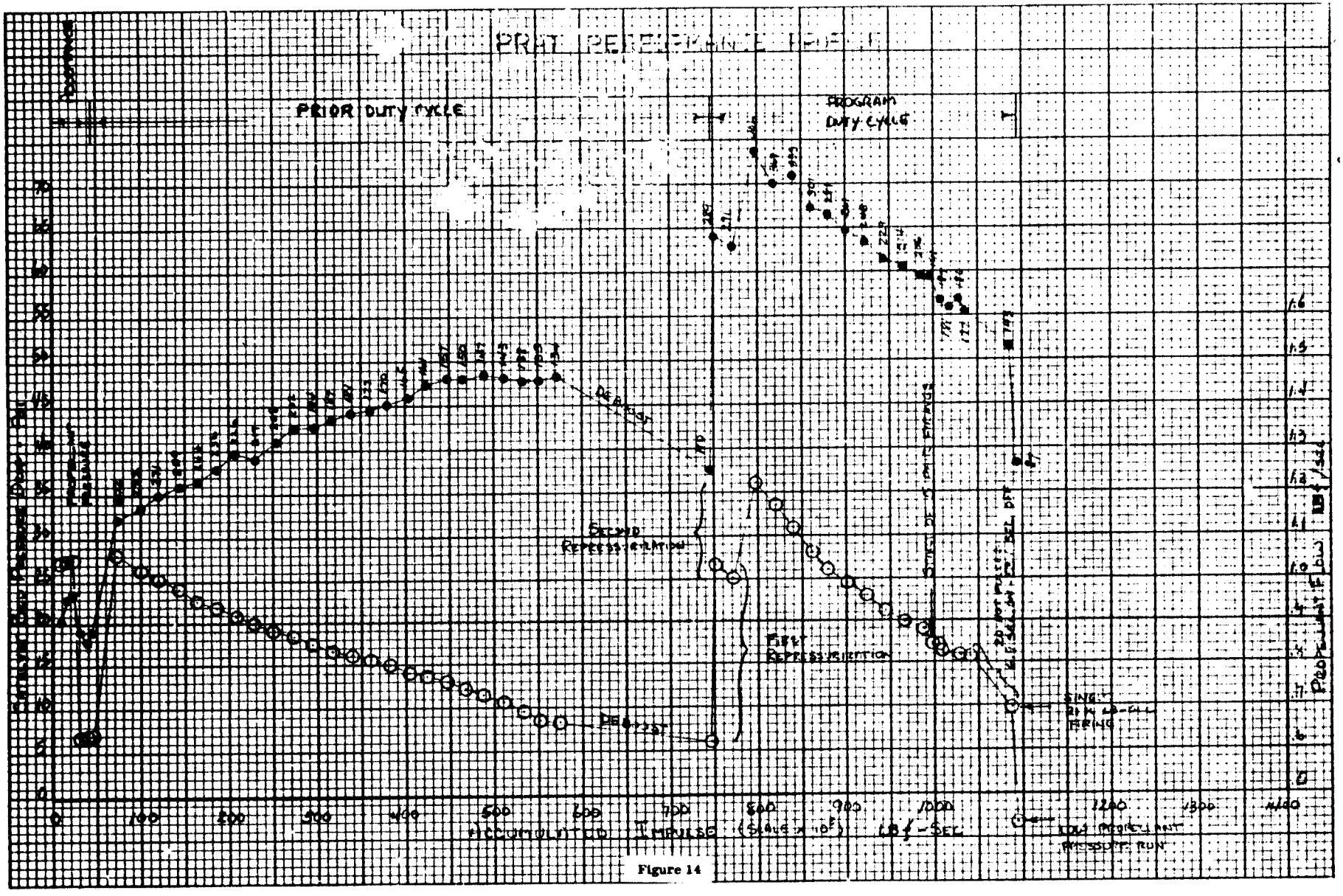

Figure 14

increases in early life and appears to decrease in later life, while in reality, the normalized pressure drop increases rapidly in early life and peaks out in later life. Figure 15 presents the catalyst bed pressure drop history, normalized to eliminate the influence of the continuously changing flow profile of a decaying pressure propellant supply. Normalizing methods are discussed in Appendix VI.

Figure 16 is also a composite plot showing manifold temperature TO2 and upstream catalyst bed temperature TO3 over the full life of the PRAT unit. TO2 is not the same temperature which produced the high manifold temperature shutdown conditions. This data shows a rising trend consistent with normalized catalyst bed pressure drop, including a leveling off characteristic in later life.

The 43 firings conducted on the PRAT unit including 18 ambient temperature starts, accumulated 362,436 lb-sec total impulse. Total propellant consumed was 1555.7 lbs producing an average specific impulse of 233 lb-sec/lb. over the current test program.

Figure 15

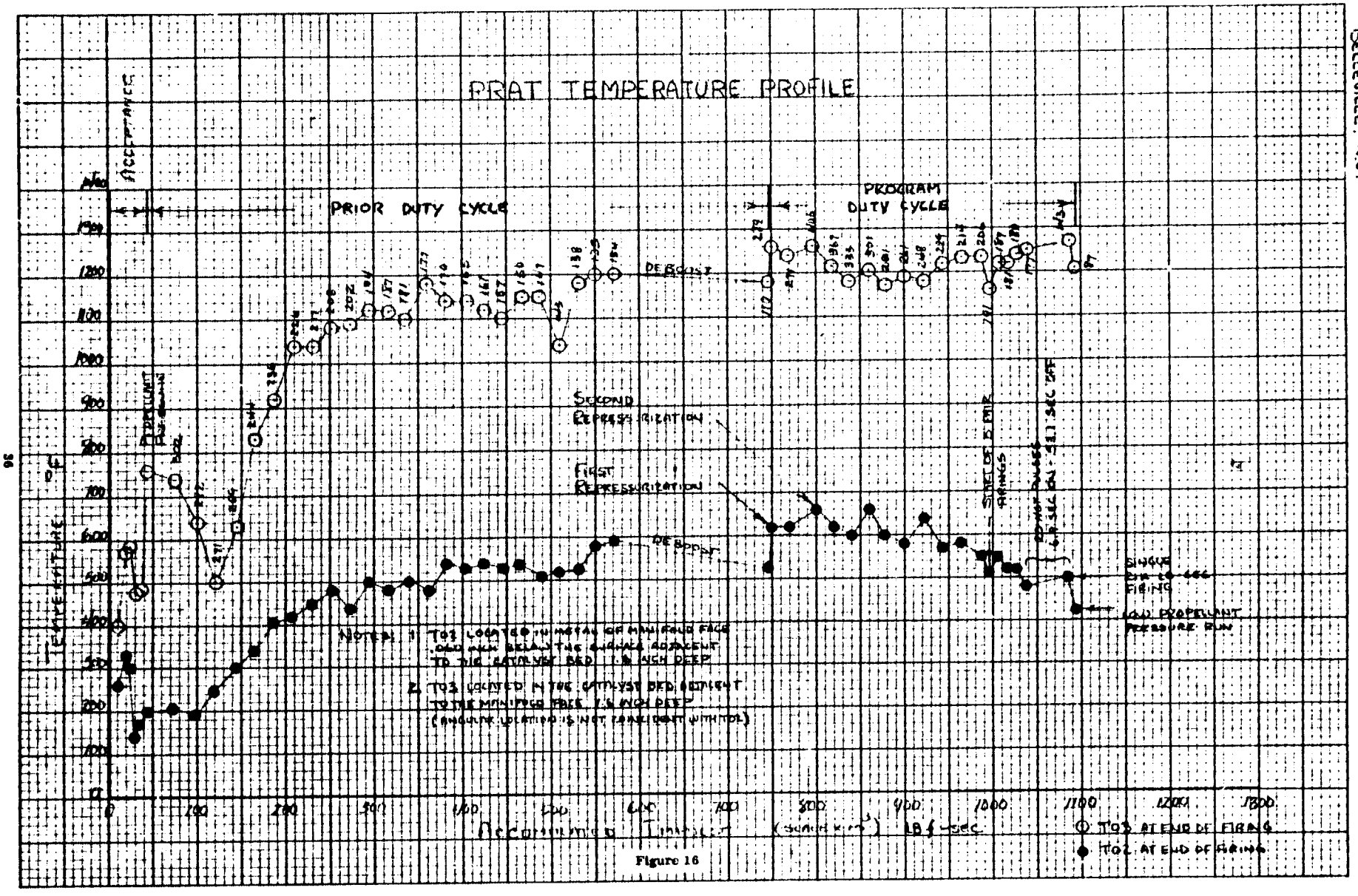

Figure 16

WALTER KIDDE AND CO
BELLEVILLE, N.J.

SECTION V

ENGINEERING EVALUATION UNIT REBUILD (EEUR)

Rebuild of a thrust chamber to "as new" condition requires replacement of partition assemblies, catalyst, thermocouples, retainer screens and the retainer plate. It also requires verification of manifold reusability. Therefore, prior to reassembly of the thrust chamber, the used manifold was subjected to a total flow test to assure that no manifold blockage existed as a result of prior usage or the disassembly procedure. This check produced a flow of 47.055 lbs of water in 90.89 seconds using an inlet pressure of 14 psig. This compares with a prior flow check of 47.096 lbs of water in 90.57 seconds at the same inlet pressure. Based upon this result, it was assumed that no blockage exists and that the individual element flow remained as initially measured.

Each distribution tube used in the EEUR was subjected to a flow test inspection as a basis for acceptance. Four flow tests were conducted on each distribution tube; two at the high end of the flow range and two at the low end of the flow range. Inlet pressure was set to obtain the required flow and the back pressure was adjusted to simulate the thrust chamber operating pressure. The distribution tube was fixtured to collect flow from each of four areas as discussed in Appendix I , and the data from areas 3 and 4 were compared with established limits.

A set of distribution tubes was selected from the stock of acceptable tubes which resulted in a ship-set average area 4 flow at low flow conditions of 49% of the total flow. The units selected are listed by serial number in Table VIII, which includes the average (of two readings taken) high flow and low flow percentages for area 4, end flow (area 3 plus area 4) and body flow (area 1 plus area 2) measurements.

The characteristics of the selected set of distribution tubes for the EEUR are compared with the ship-sets for several prior units, including the original EEU build in Table IX. The units are listed in chronological order since the implementation of controls on ship-set average flow. The area 4 flow and the total end flow are presented along with the range of measurements which make up the average. It is seen that the EEUR is basically in the range of all compared units, but is on the high side of average area 4 flow and total end flow at high flow conditions.

Selected distribution tubes were assembled into partitions and ultimately installed into the thrust chamber at final assembly. These EEUR assembly steps are identical to those described in Appendix I.

TABLE VIII

DISTRIBUTION TUBE FLOW ANALYSIS ENGINEERING EVALUATION UNIT REBUILD
PERCENT OF TOTAL FLOW

S/N	Average Area 4 Flow		Average End Flow		Average Body Flow		S/N	Average Area 4 Flow		Average End Flow		Average Body Flow	
	High Flow	Low Flow	High Flow	Low Flow	High Flow	Low Flow		High Flow	Low Flow	High Flow	Low Flow	High Flow	Low Flow
1557	46.4	49.1	57.4	63.3	42.6	36.7	1607	44.4	55.7	61.3	67.4	38.7	32.6
1559	44.1	47.1	59.9	62.2	40.1	37.8	1611	44.6	48.2	63.6	69.1	36.4	30.9
1560	44.8	52.0	58.7	63.1	41.3	36.9	1612	44.9	47.5	61.9	69.1	38.1	30.9
1581	48.3	53.5	60.8	67.0	39.2	33.0	1613	47.6	52.2	64.5	70.7	35.5	29.3
1582	47.1	50.6	62.8	65.7	37.2	34.3	1614	40.5	47.3	62.1	69.0	37.9	31.0
1585	42.2	45.8	61.5	65.5	38.5	34.5	1615	47.6	53.2	64.5	70.2	35.5	29.8
1588	50.5	50.7	64.0	66.6	36.0	33.4	1617	41.1	45.5	62.9	68.1	37.1	31.9
1589	46.0	49.4	61.3	67.2	38.7	32.8	1618	45.7	47.3	64.1	65.6	35.9	34.4
1592	45.4	45.9	59.3	62.6	40.7	37.4	1619	47.3	50.1	58.7	62.5	41.3	37.5
1593	41.1	45.4	63.3	65.2	36.7	34.8	1620	41.6	49.7	62.5	61.9	37.5	38.1
1594	44.3	46.9	60.2	64.1	39.8	35.9	1621	44.2	47.0	61.7	67.0	38.3	33.0
1596	48.1	49.8	61.8	63.6	38.2	36.4	1622	41.6	46.2	63.9	70.1	36.1	29.9
1597	48.4	49.4	61.5	65.3	38.5	34.7	1623	49.0	52.7	62.0	64.0	38.0	36.0
1598	43.5	46.5	61.9	66.4	38.1	33.6	1624	46.6	49.3	61.5	63.3	38.5	36.7
1599	44.3	51.7	58.7	64.0	41.3	36.0	1625	42.6	47.8	63.4	69.6	36.6	30.4
1600	47.9	49.8	60.2	63.1	39.8	36.9	1626	49.7	52.4	62.2	67.6	37.8	32.4
1601	47.4	50.5	63.1	62.5	36.9	37.5	1628	39.3	47.2	62.3	66.6	37.7	33.4
1602	45.0	47.7	59.9	62.3	40.1	37.7							
1244	45.9	48.1	60.1	61.7	39.9	38.3	Ave	45.3	49.1	61.7	64.1	38.3	36.9
1606	47.0	48.5	61.6	66.5	38.4	33.5							

COMPARATIVE DISTRIBUTION TUBE FLOW DATA

Unit	Area 4 High Flow	Area 4 High Flow Range	Area 4 Low Flow	Area 4 Low Flow Range	End Flow High Flow	End Flow High Flow Range	End Flow Low Flow	End Flow Low Flow Range
EEU	43.8	38.5/49.5	49.9	43.3/57.0	59.3	56.4/64.0	64.3	61.6/68.0
PRAT	43.7	38.2/50.0	49.7	45.0/59.0	60.8	58.0/67.5	64.6	62.0/69.5
S/N 1009	42.8	39.0/50.5	49.1	45.0/56.5	60.5	56.0/66.0	64.4	62.0/69.0
S/N 1010	42.1	38.0/46.5	49.1	44.0/59.0	59.6	56.0/62.5	64.7	62.0/69.0
S/N 1011	42.8	38.5/49.0	48.8	44.9/58.2	60.0	56.0/64.0	63.8	60.0/69.5
S/N 1012	43.8	37.8/49.5	49.0	44.4/59.2	61.4	56.1/64.6	64.4	59.6/69.0
S/N 1013	44.2	37.2/49.2	48.9	45.7/54.0	59.7	55.7/64.5	63.4	59.3/69.2
S/N 1014	44.5	38.2/50.8	48.9	43.1/56.4	59.5	55.0/64.4	65.0	59.8/69.1
EEUR	45.3	39.3/50.5	49.1	45.4/55.7	61.7	57.4/64.5	64.1	61.9/70.7

TABLE IX

SECTION VI

ENGINEERING EVALUATION UNIT REBUILD (EEUR) LIFE EVALUATION TEST

The EEUR was subjected to an acceptance test, and a mission test to establish f... relationships and to evaluate total life characteristics. The former included eight firings, two from ambient temperatures; the first five were at 290 psia propellant pressure and the last three were at 105 psia propellant pressure. These represent the high and low ends of the normal operating range.

The mission test presented in Table X includes 124 firings, of which 63 were started from ambient temperature. The first two firings were of 30,000 lb-sec and 4000 lb-sec duration. The next 60 pair firings were nominally of 11,000 lb-sec and 1000 lb-sec duration with 45 minutes off-time between pairs. The last two firings were 2400 second duration endurance runs to test EEUR washout resistance.

Propellant temperature on all firings except the last firing was 70°F. Propellant temperature for the last firing was reduced to 52°F in an attempt to reduce operating time to washout. While the lower temperature did reduce the specific impulse level throughout the run it did not produce washout performance as defined (a fall-off of 10 points below the peak value attained during a run).

The mission propellant pressure profile included an initial decaying pressure phase from 284 ±4 psia down to 75 ±3 psia, a repressurization to 400 ±5 psia after the 38th firing and a final decaying pressure phase from 400 ±5 psia to 124 ±3 psia at the beginning of the first 2400 second firing. During both 2400 second firings, the propellant pressure was allowed to decay from 124 ±3 psia to 100 ±3 psia at which point the pressure was regulated to hold 100 ±3 psia for the duration of the firing. The decaying pressure portion of these runs lasted approximately 1000 seconds.

All testing was completed successfully. The acceptance test hot firing compared favorably with prior acceptance test data. Initial catalyst bed ΔP at 20 seconds into the first firing was 20.6 psia, a mid-range value. Figure 17 shows the initial catalyst bed pressure drop as well as a histogram of this pressure drop over the life of the unit. Propellant flow is also included in this figure. In the first 300,000 lb-sec of the mission test the catalyst bed pressure drop increased slowly as propellant pressure and flow dropped off rapidly. With repressurization, the flow increased 160 percent and the catalyst bed pressure drop increased 73%. Thereafter, the catalyst bed pressure drop decreased with flow until the first deboost firing where a test procedural problem was encountered.

Figure 18 presents the catalyst bed pressure drop history normalized to eliminate the influence of the continuously changing flow profile of a decaying pressure propellant supply. The normalization method shown is one method of several which may be used to extract the influence of changing flow. Normalization is discussed as a separate subject in Appendix VI.

TABLE X

PLANNED EEUR DUTY CYCLE

Pulse No.	Propellant Pressure (psia)	On-Time (Seconds)	Off-Time (Minutes)	Pulse No.	Propellant Pressure (psia)	On-Time (Seconds)	Off-Time (Minutes)
1	285 ±4	142 ±.1	45 ±5	25	97 ±4	85.8 ±.1	45 ±5
2	210 ±4	20.6 ±.1	-	26	93 ±4	8.1 ±.1	-
3	202 ±4	57.0 ±.1	45 ±5	27	93 ±4	88.1 ±.1	45 ±5
4	185 ±4	5.6 ±.1	-	28	89 ±4	8.3 ±.1	-
5	184 ±4	59.6 ±.1	45 ±5	29	89 ±4	90.5 ±.1	45 ±5
6	168 ±4	5.7 ±.1	-	30	86 ±4	8.5 ±.1	-
7	167 ±4	62.7 ±.1	45 ±5	31	86 ±4	92.8 ±.1	45 ±5
8	154 ±4	6.0 ±.1	-	32	83 ±3	8.8 ±.1	-
9	153 ±4	65.8 ±.1	45 ±5	33	83 ±3	96.5 ±.1	45 ±5
10	144 ±4	6.3 ±.1	-	34	80 ±3	9.2 ±.1	-
11	143 ±4	68.4 ±.1	45 ±5	35	80 ±3	107.3 ±.1	45 ±5
12	133 ±4	6.5 ±.1	-	36	77 ±3	10.0 ±.1	-
13	132 ±4	71.0 ±.1	45 ±5	37	77 ±3	106.0 ±.1	45 ±5
14	125 ±4	6.7 ±.1	-	38	75 ±3	10.4 ±.1	-
15	125 ±4	73.0 ±.1	45 ±5	39	400 ±5	40.1 ±.1	45 ±5
16	117 ±4	6.9 ±.1	-	40	372 ±5	3.7 ±.1	-
17	117 ±4	75.2 ±.1	45 ±5	41	370 ±5	41.5 ±.1	45 ±5
18	110 ±4	7.2 ±.1	-	42	356 ±5	3.9 ±.1	-
19	110 ±4	78.3 ±.1	45 ±5	43	355 ±5	42.5 ±.1	45 ±5
20	105 ±4	7.4 ±.1	-	44	341 ±5	4.1 ±.1	-
21	105 ±4	80.8 ±	45 ±5	45	340 ±5	43.3 ±.1	45 ±5
22	101 ±4	7.6 ±.1	-	46	327 ±5	4.1 ±.1	-
23	101 ±4	83.5 ±.1	45 ±5	47	326 ±5	44.1 ±.1	45 ±5
24	97 ±4	7.9 ±.1	-	48	314 ±5	4.1 ±.1	-

TABLE X

PLANNED EEUR DUTY CYCLE

Pulse No.	Propellant Pressure (psia)	On-Time (Seconds)	Off-Time (Minutes)	Pulse No.	Propellant Pressure (psia)	On-Time (Seconds)	Off-Time (Minutes)
49	313 ±5	45.2 ±.1	45 ±5	73	207 ±3	55.7 ±.1	45 ±5
50	301 ±5	4.1 ±.1	-	74	202 ±3	5.2 ±.1	-
51	300 ±5	46.3 ±.1	45 ±5	75	201 ±3	56.5 ±.1	45 ±5
52	291 ±4	4.3 ±.1	-	76	195 ±3	5.2 ±.1	-
53	290 ±4	47.2 ±.1	45 ±5	77	195 ±3	57.3 ±.1	45 ±5
54	281 ±4	4.4 ±.1	-	78	190 ±3	5.3 ±.1	-
55	280 ±4	48.1 ±.1	45 ±5	79	190 ±3	58.2 ±.1	45 ±5
56	271 ±4	4.5 ±.1	-	80	185 ±3	5.4 ±.1	-
57	270 ±4	49.0 ±.1	45 ±5	81	185 ±3	58.9 ±.1	45 ±5
58	261 ±4	4.6 ±.1	-	82	180 ±3	5.5 ±.1	-
59	260 ±4	49.9 ±.1	45 ±5	83	180 ±3	59.7 ±.1	45 ±5
60	251 ±4	4.7 ±.1	-	84	176 ±3	5.5 ±.1	-
61	250 ±4	50.8 ±.1	45 ±5	85	176 ±3	60.5 ±.1	45 ±5
62	242 ±4	4.7 ±.1	-	86	173 ±3	5.6 ±.1	-
63	241 ±4	51.8 ±.1	45 ±5	87	173 ±3	61.2 ±.1	45 ±5
64	235 ±4	4.8 ±.1	-	88	170 ±3	5.7 ±.1	-
65	234 ±4	52.6 ±.1	45 ±5	89	170 ±3	62.1 ±.1	45 ±5
66	228 ±4	4.9 ±.1	-	90	167 ±3	5.8 ±.1	-
67	227 ±4	53.5 ±.1	45 ±5	91	167 ±3	62.9 ±.1	45 ±5
68	222 ±4	5.0 ±.1	-	92	164 ±3	5.8 ±.1	-
69	221 ±4	54.2 ±.1	45 ±5	93	164 ±3	63.7 ±.1	45 ±5
70	215 ±4	5.0 ±.1	-	94	161 ±3	5.9 ±.1	-
71	214 ±3	55. ±.1	45 ±5	95	161 ±3	64.4 ±.1	45 ±5
72	208 ±3	5.1 ±.1	-	96	158 ±3	6.0 ±.1	-

TABLE X (Cont)

PLANNED EEUR DUTY CYCLE

Pulse No.	Propellant Pressure (psia)	On-Time (Seconds)	Off-Time (Minutes)	Pulse No.	Propellant Pressure (psia)	On-Time (Seconds)	Off-Time (Minutes)
97	158 ±3	65.1 ±.1	45 ±5	111	137 ±3	69.8 ±.1	45 ±5
98	155 ±3	6.0 ±.1	-	112	135 ±3	6.4 ±.1	-
99	155 ±3	65.7 ±.1	45 ±5	113	135 ±3	70.5 ±.1	45 ±5
100	152 ±3	6.1 ±.1	-	114	133 ±3	6.5 ±.1	-
101	152 ±3	66.3 ±.1	45 ±5	115	133 ±3	71.2 ±.1	45 ±5
102	149 ±3	6.1 ±.1	-	116	131 ±3	6.6 ±.1	-
103	149 ±3	67.0 ±.1	45 ±5	117	131 ±3	71.8 ±.1	45 ±5
104	146 ±3	6.2 ±.1	-	118	129 ±3	6.6 ±.1	-
105	146 ±3	67.6 ±.1	45 ±5	119	129 ±3	72.3 ±.1	45 ±5
106	143 ±3	6.3 ±.1	-	120	127 ±3	6.7 ±.1	-
107	143 ±3	68.4 ±.1	45 ±5	121	127 ±3	72.8 ±.1	45 ±5
108	140 ±3	6.3 ±.1	-	122	124 ±3	6.7 ±.1	-
109	140 ±3	69.1 ±.1	45 ±5	123	124 ±3	2400	-
110	137 ±3	6.4 ±.1	-	124	124 ±3	2400	-

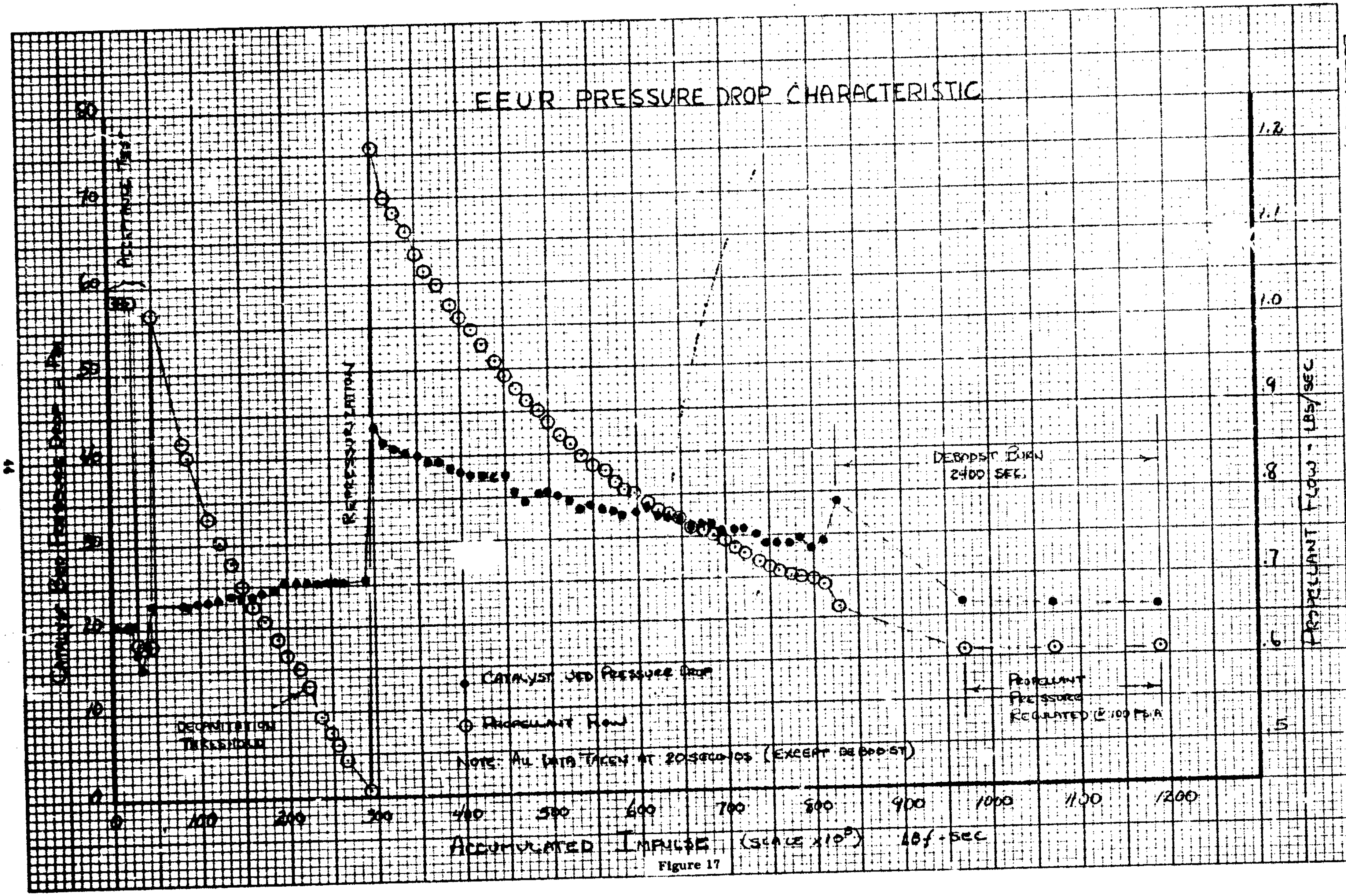

EEUR PRESSURE DROP CHARACTERISTIC
ACCEPTANCE TEST
REPRESSURIZATION
DEBOOST BURN
2400 SEC.
DEPOSITION THRESHOLD
CATALYST BED PRESSURE DROP
PROPELLANT FLOW
NOTE: ALL DATA TAKEN AT 20 SECONDS (EXCEPT DEBOOST)
PROPELLANT PRESSURE REGULATED @ 100 PSIA
ACCUMULATED IMPULSE (SCALE x10^3) LBf - SEC
PROPELLANT FLOW - LBS/SEC

Figure 17

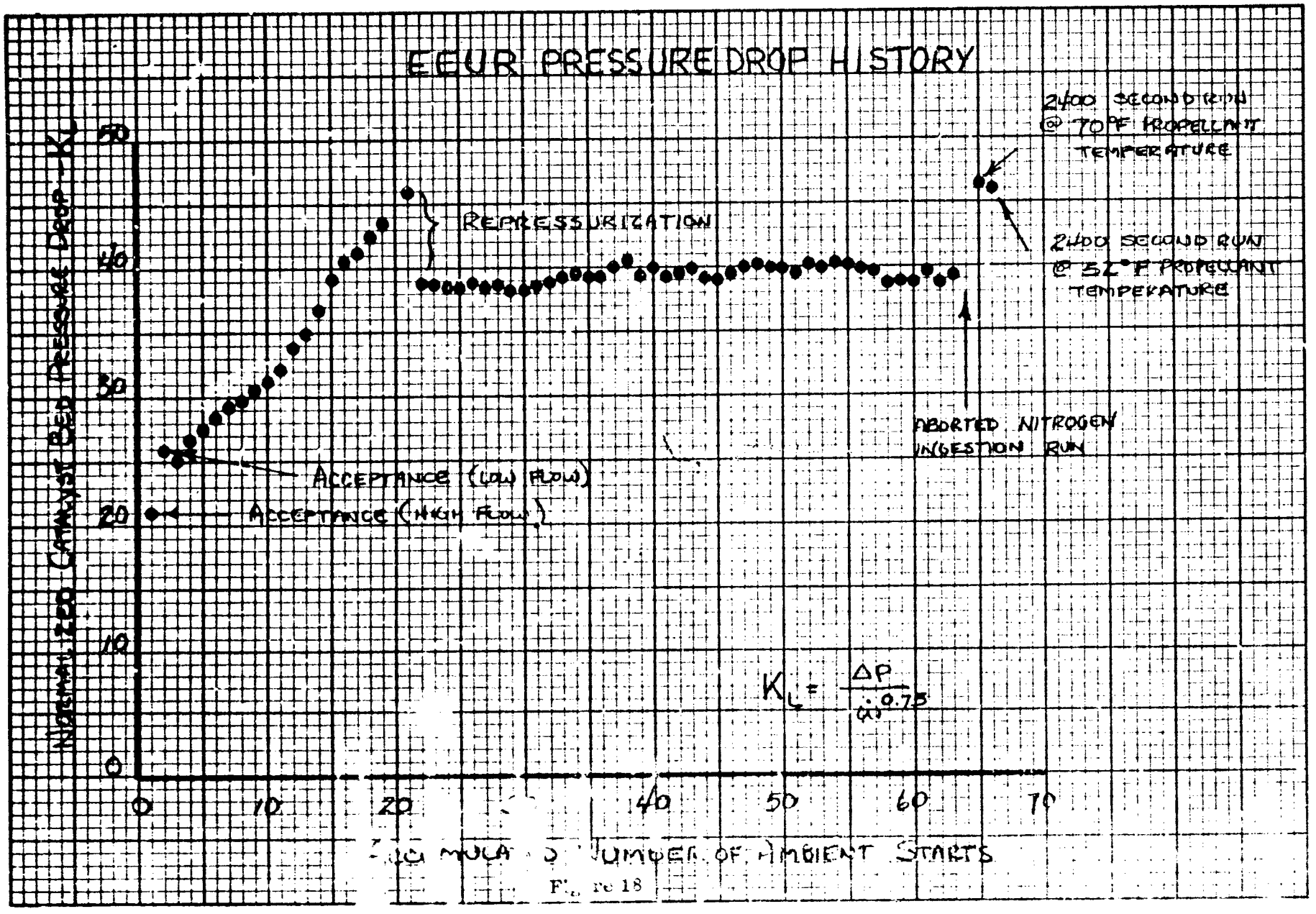
EECOM PRESSURE DROP HISTORY
2400 SECOND RUN @ 70°F PROPELLANT TEMPERATURE
2400 SECOND RUN @ 52°F PROPELLANT TEMPERATURE
REPRESSURIZATION
ABORTED NITROGEN INGESTION RUN
ACCEPTANCE (LOW FLOW)
ACCEPTANCE (HIGH FLOW)
$K_L = \frac{\Delta P}{\dot{w}^{0.75}}$
50
40
30
20
10
0
0
10
20
40
50
60
70
CUMULATIVE NUMBER OF AMBIENT STARTS

Figure 18

In the process of revamping ullage tankage to meet changed endurance firing requirements, a bleed line normally left open should have been closed, but was overlooked. When the first endurance firing was attempted, nitrogen passed through the bleed line from an ullage tank and joined the propellant entering the engine. The result was a nitrogen ingestion firing which produced low flow, low thrust and erratic stability. The unit was shut down after 85 seconds of operation under this condition and recycled through the cooldown process. The problem was discovered and corrected before the cooldown was completed.

Subsequently a successful endurance firing was accomplished without any sign of washout performance characteristics. However, a step change in the 20 second data slice ΔP characteristic was noted which probably occurred because the catalyst bed was reoriented by a nitrogen ingestion firing. The remainder of the points are in-run pressures showing the decay and regulated portions of the first endurance run.

Performance characteristics are presented on Figure 19 and in Table XI. The plot shows a smooth propellant pressure-thrust characteristic down to about 140 lbs thrust where venturi decavitation occurs causing an inflection in the flow characteristic. Specific impulse characteristics also presented generally follow the same type characteristic, though the scatter in data is more severe. However, when decavitation occurs, the specific impulse also shows a significant decrease. Table XI presents corresponding 20 second data and the total impulse accumulated during each run.

Catalyst bed and manifold temperature characteristics are presented in Figure 20 at the end of each mission firing. The levels attained in this test series are all well within acceptable units as is expected from a relatively low catalyst bed pressure drop engine. The effects of repressurization are not noticeable in manifold metal temperatures, but are of significance in the catalyst bed temperatures, especially the mid-bed temperature. This factor indicates the greater use of the bed due to increased upstream injection with increased flow.

Oscillograph traces presented in Figures 21, 22, and 23 show start, in-run, and shutdown characteristics for high and low thrust runs in the acceptance test, comparable thrust level runs in later life, and the minimum and maximum thrust level runs in the mission which occurred just prior to and just after repressurization.

Figure 21 compares a high thrust acceptance test run and a similar thrust level run about 350,000 lb-secs later in the mission after repressurization. Startup, stability and shutdown characteristics are comparable. Figure 22 compares a low thrust acceptance test firing with the second 2400 second endurance firing which present the comparison of characteristics over approximately 1.5 million pound-seconds of operation. Characteristics shown are equivalent and most satisfactory. Figure 23 compares minimum thrust characteristics before repressurization (propellant pressure 75 psia) with maximum thrust characteristics after repressurization (propellant pressure 406 psia). These results show no overshoot at startup and no significant oscillation over the complete operating range of the thrust chamber.

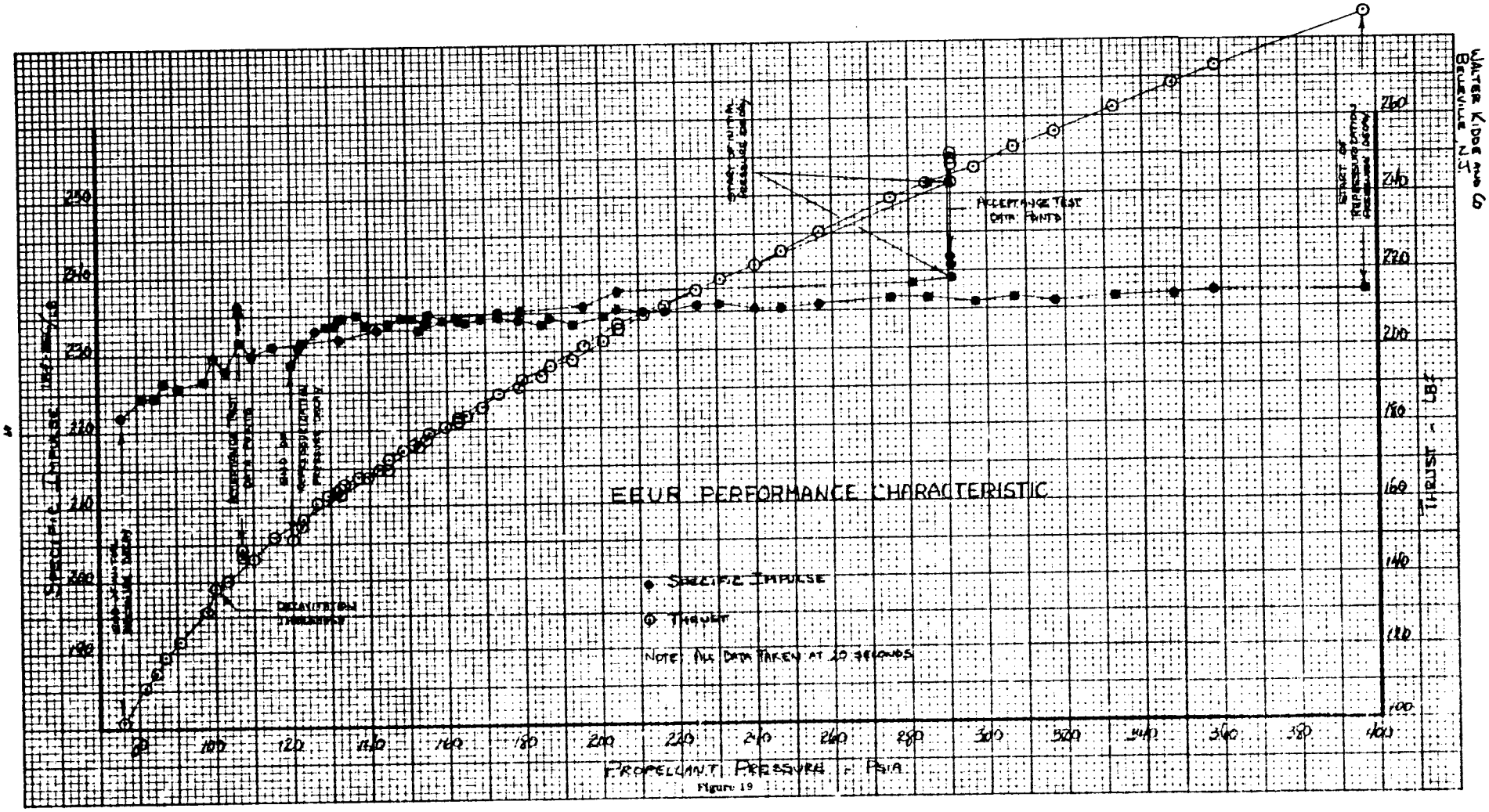
EEUR PERFORMANCE CHARACTERISTIC
SPECIFIC IMPULSE
THRUST
NOTE: ALL DATA TAKEN AT 20 SECONDS
PROPELLANT PRESSURE - PSIA
ACCEPTANCE TEST DATA POINTS
WALTER KIDDE AND CO
BELLEVILLE, N.J.

Figure 19

TABLE XI

EEUR PERFORMANCE DATA

Run No.	Propellant Pressure at 20 Sec. (psia)	On-Time (Seconds)	Thrust at 20 Sec. (Lbs)	Chamber Pressure at 20 Sec. (psia)	Catalyst Pressure Drop at 20 Sec. (psia)	Specific Impulse at 20 Sec. (Sec)	Total Impulse (Lb-Sec)
3332	280.8	142	243	74.0	25.6	238.5	33780
3333	204.5	20.6	207	64.1	25.3	237.7	4208
3334	195.8	57.0	201.5	62.0	23.8	235.8	11430
3335		5.6					1025
3336	179.6	59.6	192.7	59.4	23.8	235.3	11430
3337		5.7					992
3338	162.3	62.7	183.1	56.6	23.7	234.6	11440
3339		6.0					999
3340	152.5	65.8	175.6	55.0	23.6	232.9	11520
3341		6.3					1008
3342	142.1	68.4	169.5	52.7	23.5	233.0	11560
3343		6.5					993
3344	132.4	71.0	162.4	50.6	23.4	231.8	11150
3345		6.7					994
3346	122.7	73.0	156.5	48.9	23.3	231.4	11380
3347		6.9					990
3348	115.6	75.2	151.8	47.4	23.6	231.0	11380
3349		7.2					991
3350	109.9	78.3	146.0	45.7	24.3	229.8	11430
3351		7.4					961
3352	103.1	80.8	140.3	43.9	24.3	227.8	11380
3353		7.9					1003
3354	99.7	83.5	138.0	43.2	24.7	229.6	11550

TABLE XI (Cont)

EEUR PERFORMANCE DATA

Run No.	Propellant Pressure at 20 Sec. (psia)	On-Time (Seconds)	Thrust at 20 Sec. (Lbs)	Chamber Pressure at 20 Sec. (psia)	Catalyst Pressure Drop at 20 Sec. (psia)	Specific Impulse at 20 Sec. (Sec)	Total Impulse (Lb-Sec)
3355		8.1					982
3356	97.5	85.8	131.4	41.5	26.1	226.5	11450
3357		8.3					953
3358	90.6	88.1	122.9	38.9	25.6	225.7	10960
3359		8.5					936
3360	87.0	90.5	118.9	37.6	25.7	226.3	10900
3361		8.8					932
3362	84.7	92.8	114.6	36.3	25.8	224.3	10820
3363		9.2					941
3364	81.7	96.5	110.4	35.2	25.8	224.4	10850
3365		10.0					994
3366	-	-	Lost Data		-	-	-
3367		10.0					951
3368	76.0	106.0	101.4	32.1	25.6	221.9	11080
3369		10.4					956
3370	397.3	40.1	286.9	87.8	44.8	237.1	11410
3371		3.7					954
3372	358.6	41.5	273.2	83.7	43.0	237.2	11250
3373		3.9					984
3374	347.9	42.3	268.2	81.9	42.0	236.7	11320
3375		4.1					1015
3376	332.8	43.3	262.2	80.5	41.4	236.5	11260
3377		4.1					982
3378	317.8	44.1	256.1	78.9	41.3	236.0	11230

TABLE XI (Cont)

EEUR PERFORMANCE DATA

Run No.	Propellant Pressure at 20 Sec. (psia)	On-Time (Seconds)	Thrust at 20 Sec. (Lbs)	Chamber Pressure at 20 Sec. (psia)	Catalyst Pressure Drop at 20 Sec. (psia)	Specific Impulse at 20 Sec. (Sec)	Total Impulse (Lb-Sec)
3379		4.1					963
3380	307.0	45.2	252.2	77.4	40.2	236.5	11310
3381		4.1					944
3382	296.9	46.3	247.0	75.7	40.1	235.9	11380
3383		4.3					984
3384	284.6	47.2	243.0	74.8	38.9	236.6	11400
3385		4.2					982
3386	275.5	48.1	239.2	73.3	38.5	236.7	11410
3387		4.2					984
3388	267.4	49.0	227.3	72.0	38.5	228.5	11460
3389		4.2					991
3390	256.6	49.9	230.3	70.9	38.6	235.7	11430
3391		4.2					990
3392	247.0	50.8	225.4	69.2	38.0	235.2	11410
3393		4.2					979
3394	240.0	51.8	222.0	68.2	38.0	235.3	11450
3395		4.2					986
3396	230.7	52.6	218.6	67.5	37.1	236.0	11430
3397		-					
3398	225.3	53.5	215.5	66.3	36.6	235.9	11470
3399		5.0					988
3400	218.7	54.2	211.8	65.5	37.0	235.1	11450
3401		5.0					976

TABLE XI (Cont)

EEUR PERFORMANCE DATA

Run No.	Propellant Pressure at 20 Sec. (psia)	On-Time (Seconds)	Thrust at 20 Sec. (Lbs)	Chamber Pressure at 20 Sec. (psia)	Catalyst Pressure Drop at 20 Sec. (psia)	Specific Impulse at 20 Sec. (Sec)	Total Impulse (Lb-Sec)
3402	211.3	55.0	-	64.3	36.9	-	11440
3403		5.1					980
3404	204.5	55.7	205.5	63.5	36.0	235.3	11400
3405		5.2					986
3406	200.9	56.5	202.4	62.8	35.9	234.5	11370
3407		5.2					958
3408	192.8	57.3	197.7	61.4	34.7	233.4	11300
3409		5.3					971
3410	187.1	58.2	196.1	60.7	34.8	234.3	11390
3411		5.4					973
3412	184.6	58.9	193.5	60.1	34.7	233.6	11370
3413		5.5					974
3414	178.4	59.7	190.9	59.0	33.7	234.1	11360
3415		5.5					964
3416	173.6	60.5	189.0	58.6	33.4	234.5	11410
3417		5.6					975
3418	17.7	61.2	188.7	58.2	33.6	235.1	11520
3419		5.7					992
3420	169.2	62.1	185.7	57.4	33.7	234.3	11520
3421		5.8					994
3422	165.1	62.9	183.5	56.8	33.5	233.9	11540
3423		5.8					982
3424	163.0	63.7	182.0	56.7	33.1	234.1	11560

TABLE XI (Cont)

EEUR PERFORMANCE DATA

Run No.	Propellant Pressure at 20 Sec. (psia)	On-Time (Seconds)	Thrust at 20 Sec. (Lbs)	Chamber Pressure at 20 Sec. (psia)	Catalyst Pressure Drop at 20 Sec. (psia)	Specific Impulse at 20 Sec. (Sec)	Total Impulse (Lb-Sec)
3425		5.9					996
3426	159.5	64.4	180.6	55.5	32.9	234.2	11650
3427		6.0					1008
3428	155.5	65.1	179.3	55.2	32.2	235.0	11650
3429		6.0					994
3430	154.5	65.7	177.1	55.3	32.7	233.8	11640
3431		6.1					1004
3432	151.3	66.3	176.0	54.5	32.2	234.5	11650
3433		6.1					992
3434	148.5	67.0	174.4	54.6	32.1	234.6	11660
3435		6.2					1000
3436	144.9	67.6	172.7	53.4	32.0	233.9	11630
3437		6.3					997
3438	144.5	68.4	169.5	53.0	31.7	231.7	11560
3439		6.3					980
3440	139.7	69.1	167.3	52.0	31.1	232.7	11530
3441		6.4					992
3442	137.2	69.8	167.6	52.0	30.2	235.0	11650
3443		6.4					982
3444	133.2	70.5	165.8	51.7	30.2	234.7	11700
3445		6.5					982
3446	132.3	71.2	164.6	51.4	30.0	234.4	11700
3447		6.6					992

TABLE XI (Cont)

EEUR PERFORMANCE DATA

Run No.	Propellant Pressure at 20 Sec. (psia)	On-Time (Seconds)	Thrust at 20 Sec. (Lbs)	Chamber Pressure at 20 Sec. (psia)	Catalyst Pressure Drop at 20 Sec. (psia)	Specific Impulse at 20 Sec. (Sec)	Total Impulse (Lb-Sec)
3448	131.6	71.8	163.9	51.2	30.6	233.7	11740
3449		6.6					994
3450	129.3	72.3	162.9	50.8	29.6	233.5	11770
3451		6.7					993
3452	126.4	72.8	160.9	49.9	29.9	233.0	11680
3453		6.7					978
3454	-	-	Aborted	-	-	-	-
3455	120.0	2400	151.0	47.8	34.1	228.2	358700
3456	122.2	2400	154.7	48.2	34.2	230.7	362700

WALTER KIDDE & Co
BELLEVILLE, N.J.

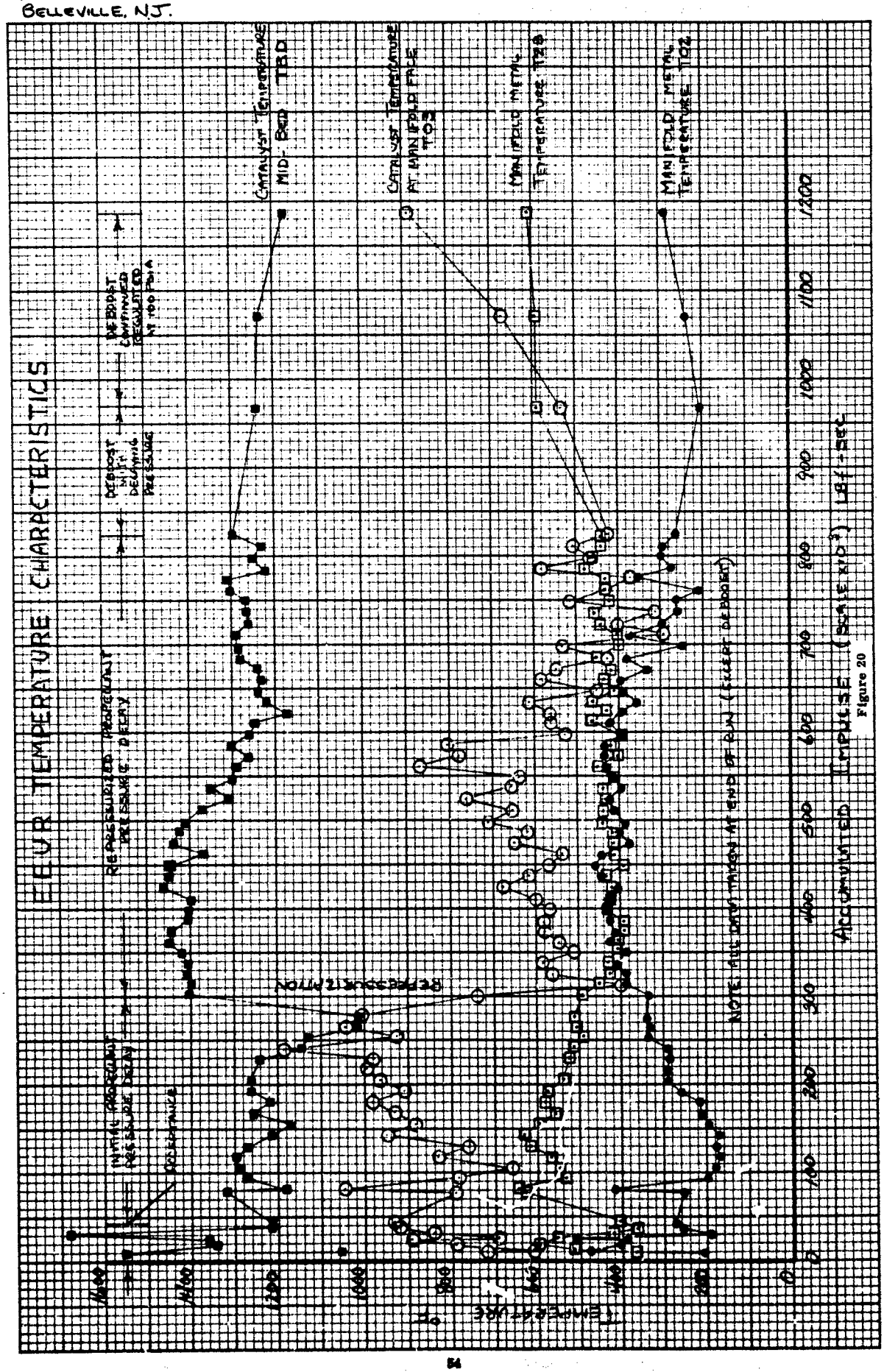

Figure 20

RUN 3326 ENGINEERING EVALUATION UNIT REBUILD ACCEPTANCE TEST – HIGH THRUST

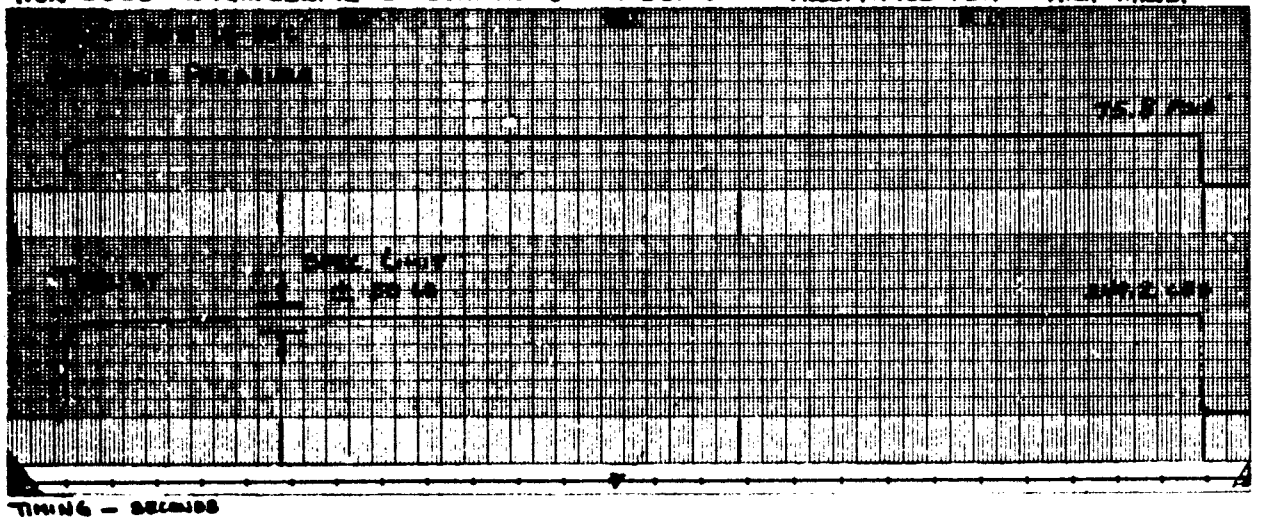

TIMING – SECONDS

RUN 3384 ENGINEERING EVALUATION UNIT REBUILD MID-WAY THROUGH MISSION TEST

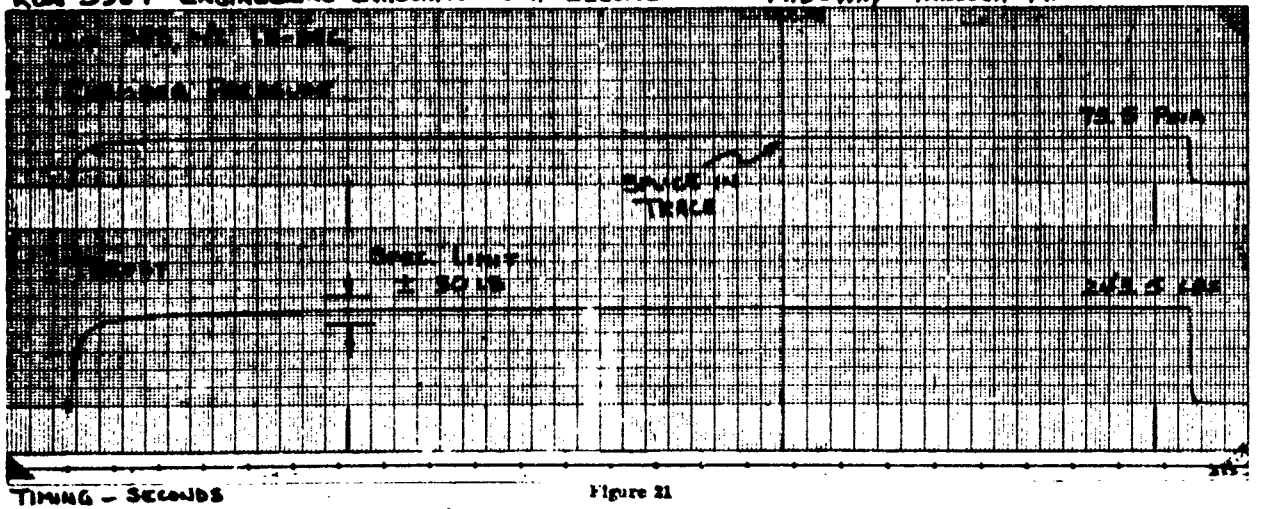

TIMING – SECONDS

Figure 21

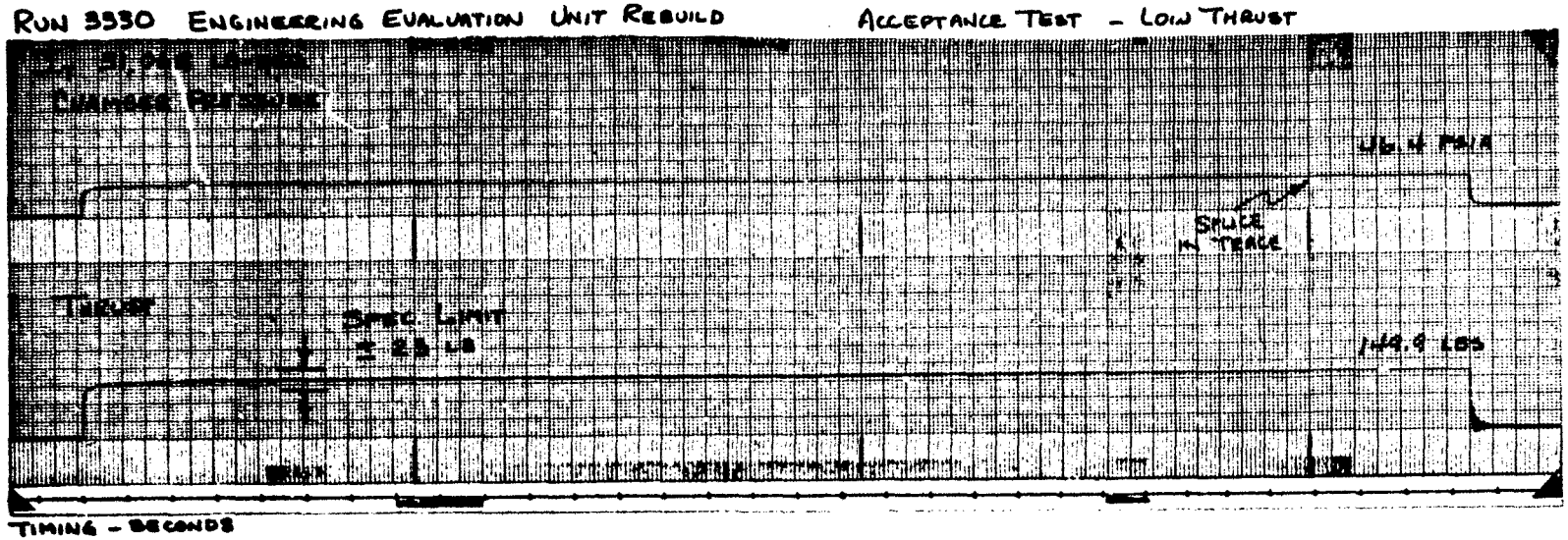
RUN 3330 ENGINEERING EVALUATION UNIT REBUILD
ACCEPTANCE TEST - LOW THRUST
CHAMBER PRESSURE
46.4 PSIA
SPLICE IN TRACE
THRUST
SPEC. LIMIT ± 2.5 LB
149.9 LBS
TIMING - SECONDS

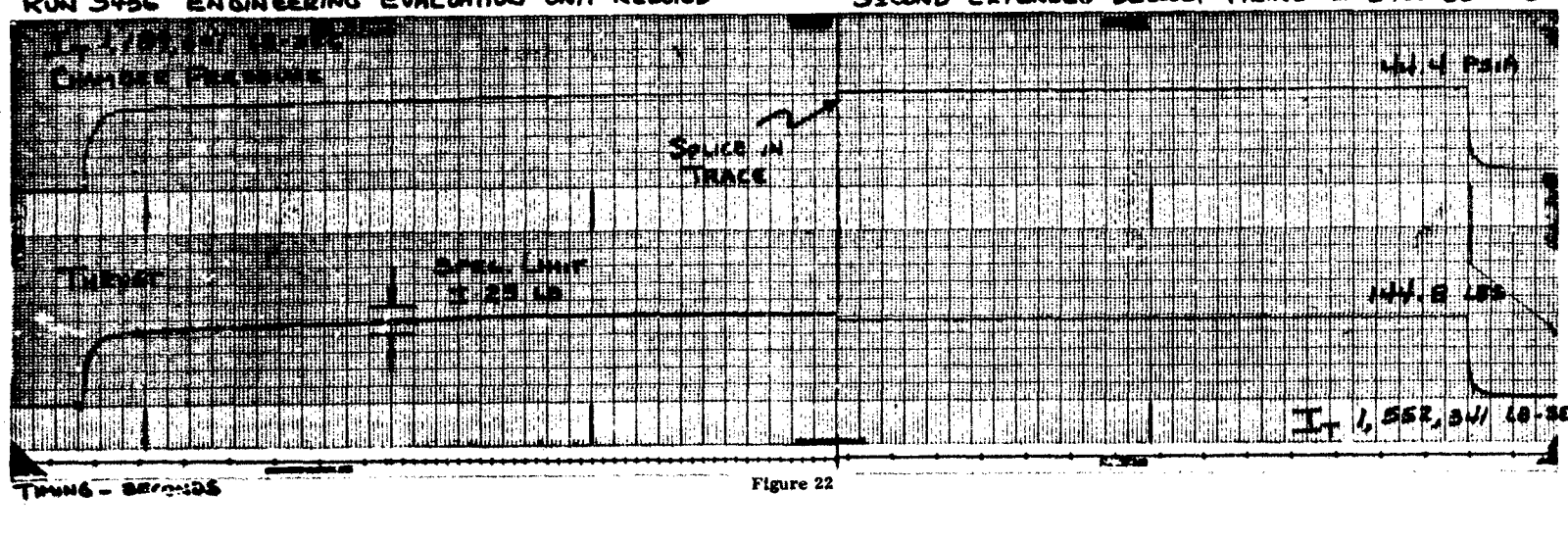
RUN 3456 ENGINEERING EVALUATION UNIT REBUILD
SECOND EXTENDED DEBOOST FIRING - 2400 SECONDS
CHAMBER PRESSURE
144.4 PSIA
SPLICE IN TRACE
THRUST
SPEC. LIMIT ± 2.5 LB
144.8 LBS
I_T 1,552,941 LB-SEC
TIMING - SECONDS

Figure 22

RUN 3368 ENGINEERING EVALUATION UNIT REBUILD – BEFORE REPRESSURIZATION

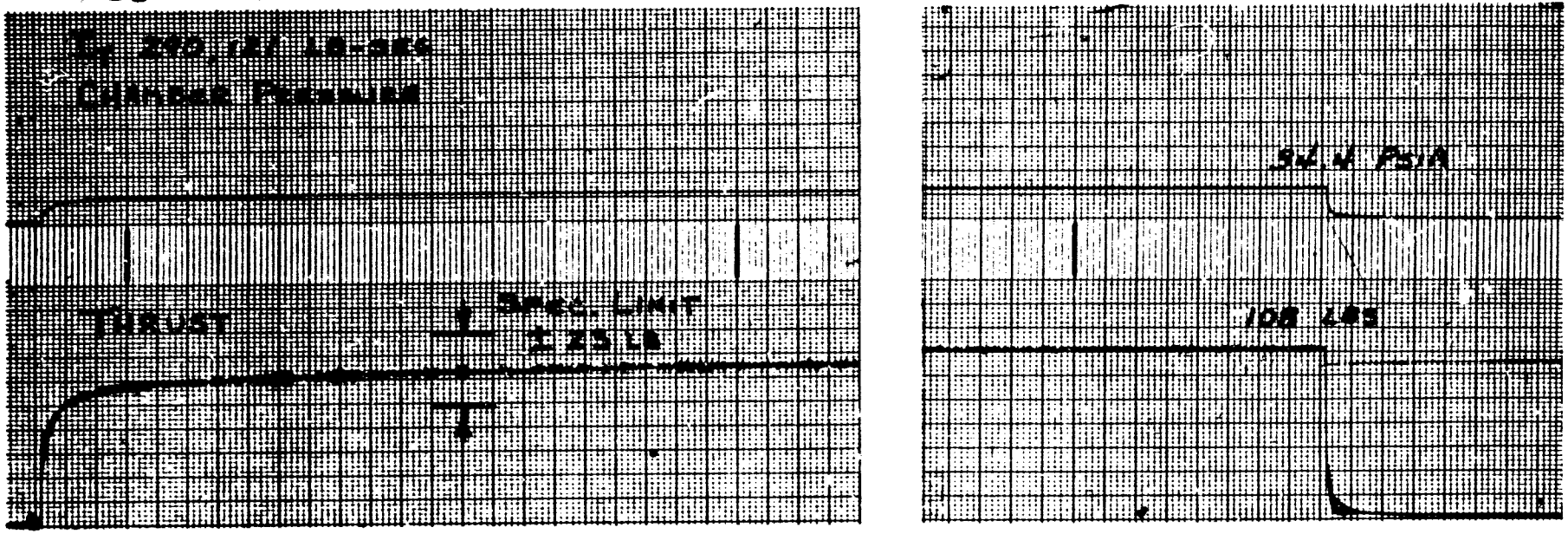

RUN 3372 ENGINEERING EVALUATION UNIT REBUILD – AFTER REPRESSURIZATION

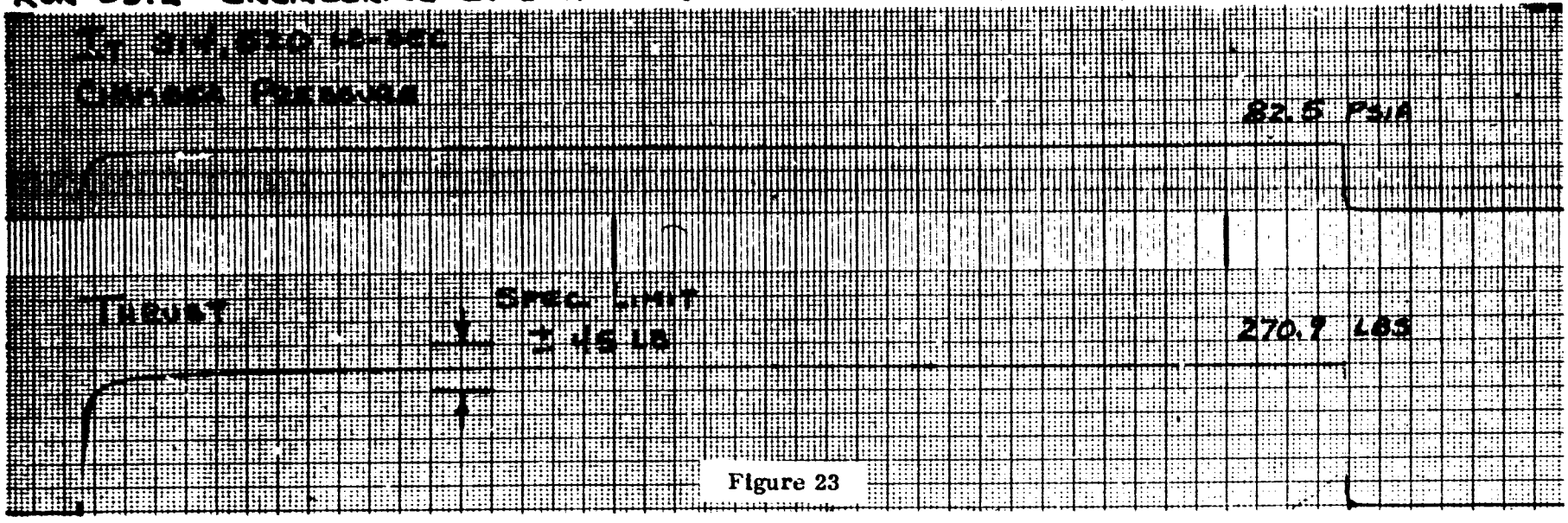

Figure 23

Figure 17 67

The 125 firings conducted on the EEUR, including 66 ambient temperature starts accumulated 1,552,341 lb-sec total impulse. Total propellant consumed was 6572 pounds producing an average specific impulse of 236 lb-sec/lb over the acceptance and mission task. The two 2400 second burns produced single firing total impulse of 358,700 lb-sec and 362,700 lb-sec. respectively.

SECTION VII

PERFORMANCE ANALYSIS

This program was a continuation of performance evaluation on a thrust chamber design with a sizable previous test experience. Based upon this experience, specific problem areas are known, and analysis methods have been established. Therefore, analysis of results under this program takes the form of comparing these results with prior analysis in specific areas of concern, namely, washout, catalyst bed pressure drop, specific impulse and manifold temperature.

1. WASHOUT CHARACTERISTICS

a. Washout Capability

The occurrence of washout in the engine is characterized by a continual downstream movement of the average decomposition zone in the catalyst bed which eventually results in some undecomposed propellant leaving the bed. As the decomposition zone moves downstream, the catalyst bed pressure drop decays due to the shortened bed length through which the decomposition gases pass. The specific impulse during the firing reflects the downstream movement of the decomposition zone in that it first increases in value due to reduced ammonia dissociation as the effective bed length becomes shortened, and then it decreases in value as undecomposed propellant begins to leave the bed. A 10 lb-sec/lb decay in specific impulse has been arbitrarily designated as "washout". However, when specific impulse has reached a peak value and begins to decay, the bed has begun to discharge undecomposed propellant so that the engine is operating in "incipient" washout even though a 10 lb-sec/lb decay has not yet occurred in the firing.

The Engineering Evaluation Unit (EEU) was subjected to two 5000 second duration firings to determine its washout capability. The unit had completed a 45 pair firing mission and deboost firing prior to these washout firings. The first washout firing was performed with 70°F propellant and a plot of its specific impulse and catalyst bed pressure drop is shown in Figure 24. The shape of the specific impulse and the pressure drop are characteristic of the washout phenomena of the engine. Pressure drop continually decays with time from the start of the firing while specific impulse climbs to a peak value and then slowly decays until washout occurs. The peak value corresponds to the final condition where propellant is not leaving the bed in an undecomposed state. Thereafter, the decay in specific impulse occurs because increasingly more propellant is leaving the bed undecomposed. The decay in the bed pressure drop reflects the downstream movement of the mean decomposition zone.

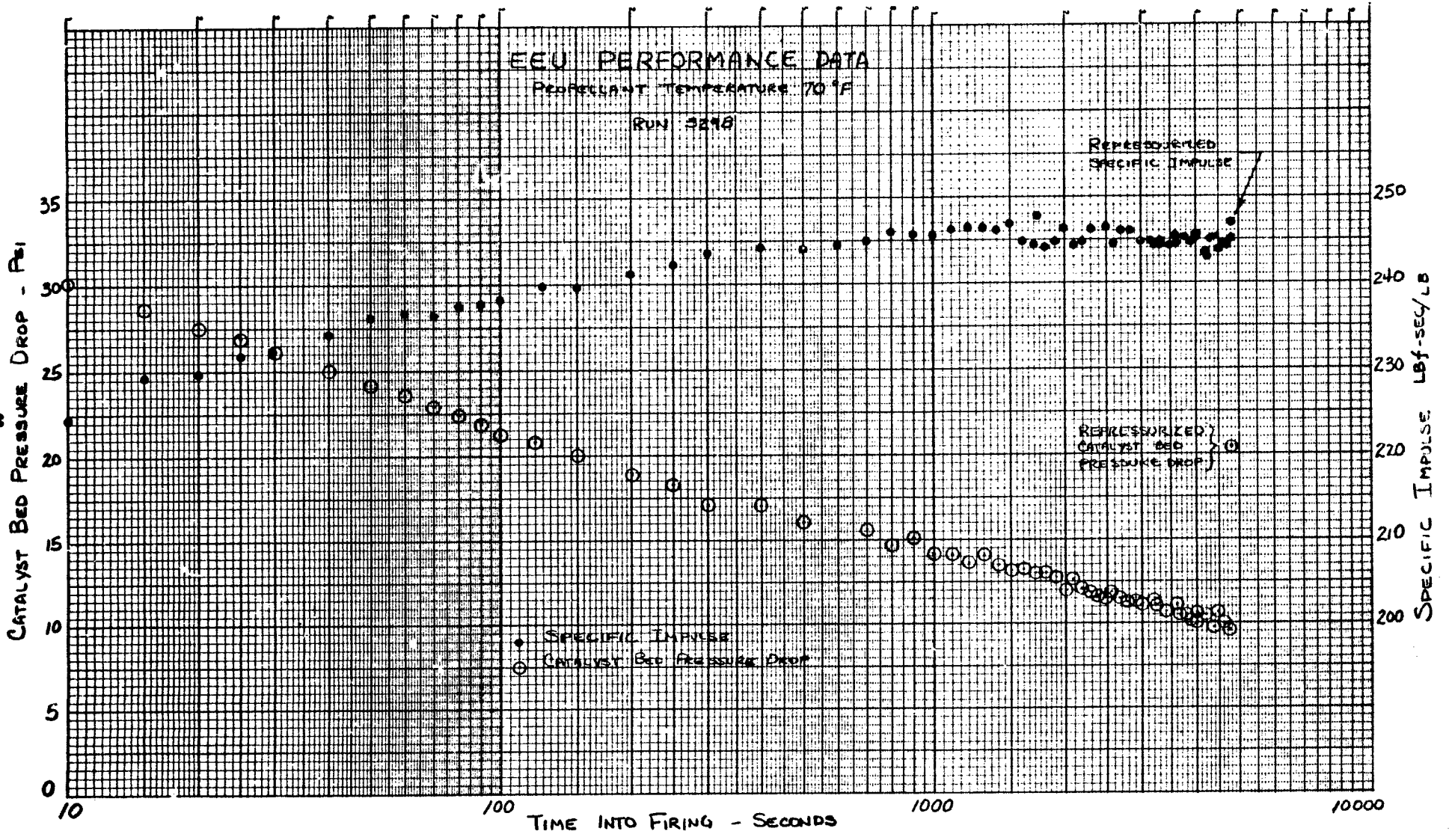
EEU PERFORMANCE DATA
PROPELLANT TEMPERATURE 70 °F
RUN 3298
REPRESSURIZED SPECIFIC IMPULSE
REPRESSURIZED CATALYST BED PRESSURE DROP
SPECIFIC IMPULSE
CATALYST BED PRESSURE DROP
CATALYST BED PRESSURE DROP - PSI
SPECIFIC IMPULSE LBf-SEC/LB
TIME INTO FIRING - SECONDS
0
5
10
15
20
25
30
35
200
210
220
230
240
250
10
100
1000
10000

Figure 24

The maximum decay from the peak value of specific impulse in the 70°F firing was 4.6 seconds which is less than the arbitrarily established washout definition of a 10 second decay in specific impulse; therefore, the engine did not washout according to this definition; however, the washout decay phenomena in both specific impulse and bed pressure drop were evident and show that the engine was in an incipient washout mode and that if the firing were to continue long enough, the washout specification of a 10 second specific impulse decay would eventually be reached. A rough estimate of about 10,000 seconds run time to washout can be made by extrapolation to the time where the bed pressure drop would have equaled the retainer screen pressure drop indicating passage of the decomposition zone out of the bed.

Referring to Figure 24, this estimation can be visualized by noting that the bed pressure drop is approximately 10 psi at 4800 seconds into the firing and would be 7 psi if the firing had extended to 10,000 seconds and if the pressure drop had continued to decay as indicated by the slope of the pressure drop plot. The 7 psi value is arrived at by extrapolating the bed pressure drop from 4800 seconds to 10,000 seconds firing time at the same slope of the plot preceding 4800 seconds firing time. This 7 psi bed pressure drop includes the pressure drop across the retainer screen located at the downstream end of the bed. However, the retainer screen pressure drop was separately measured and recorded as test data, and its value during the test firing was approximately constant at 7 psi. Since total bed pressure drop extrapolated to 10,000 seconds firing time equals the constant retainer screen pressure drop of 7 psi, it would be expected that decomposition gases would be flowing only through the screen and not through any portion of the bed at 10,000 seconds firing time. This condition can exist only if the bed is on the verge of washout. Therefore, 10,000 seconds would be a reasonable estimation of the expected time to washout in this firing. This estimated washout time is shown in Figure 25.

During development of the engine, washout occurred earlier in life on some engines especially for firings with low propellant temperatures, indicating that parameters other than operation time were significant in determining the occurrence of washout. Consequently, a correlation was formulated based on operational and configuration parameters which best described the conditions under which washout could be expected to occur. This correlation is presented in Figure 25. An overall washout correlation parameter (W) is calculated based on the propellant temperature during the particular firing under consideration, the total impulse accumulated up to the firing, the number of ambient starts accumulated up to the firing, and the particular engine configuration

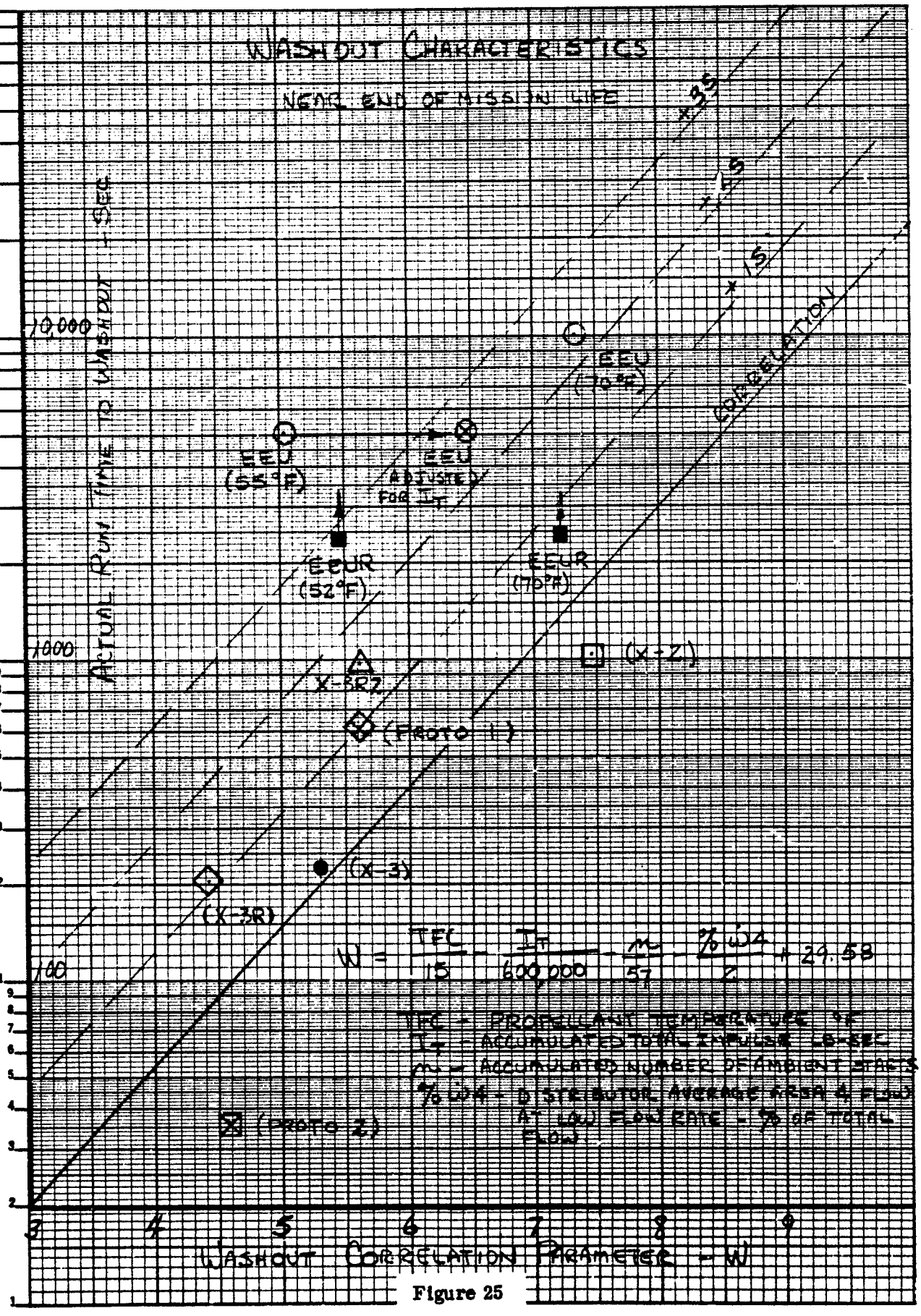
WASHOUT CHARACTERISTICS
NEAR END OF MISSION LIFE
ACTUAL RUN TIME TO WASHOUT - SEC
10,000
1000
100
EEU (55°F)
EEU ADJUSTED FOR T_T
EEU (70°F)
EEUR (52°F)
EEUR (70°F)
X-3R2
(PROTO 1)
(X+Z)
(X-3)
(X-3R)
(PROTO 2)
W = TFC/15 - T_T/600,000 - m/57 - %DA/2 + 29.58
TFC = PROPELLANT TEMPERATURE °F
T_T = ACCUMULATED TOTAL IMPULSE LB-SEC
m = ACCUMULATED NUMBER OF AMBIENT STARTS
%DA = DISTRIBUTOR AVERAGE AREA AT LOW FLOW RATE - % OF TOTAL FLOW
3 4 5 6 7 8 9
WASHOUT CORRELATION PARAMETER - W

Figure 25

build distributor tube average end flow. An influence coefficient for each parameter was derived from the development engine's test data to obtain a best fit for the correlation which results in a direct linear relationship of the logarithm of the time to washout with the overall washout parameter W.

This type of plot permits direct comparison of the results to correlation criteria or "family" characteristics obtained from the family of engines. Final burn washout times for engines which have washed out and have sufficient associated data with which to calculate a washout correlation parameter value are shown for reference purposes. Pertinent correlation criteria are the deviations of the test results from the mean correlation. The statistical one, two and three standard deviation lines of the correlation are shown for reference. As a simplified criterion, the three standard deviation limit is recognized as the boundary of random variations with the probability of conformance to the correlation increasing as the deviation decreases. A result lying beyond the three standard deviation line is taken to be definite evidence that the result belongs to a different characteristic. The estimated time of washout for the unit at 70°F propellant temperature is seen to lie outside previous engine data scatter at approximately the two standard deviation line indicating a possibility, but a low probability, that the result conforms to the correlation. An additional 5000 second duration firing of the Engineering Evaluation Unit (EEU) was performed with 55°F propellant to attempt to definitely establish an actual time to washout. The specific impulse and bed pressure drop for this firing are plotted in Figure 26 and show the same general characteristics as those obtained with 70°F propellant. However, the peak value of specific impulse occurs earlier and its decay thereafter is steeper than that which occurred with 70°F propellant, such that the maximum specific impulse decay was 9.9 seconds, practically reaching the washout definition of a 10 second decay.

These observations indicate an actual definition washout time of about 5000 seconds for the second firing and this estimated time is so plotted in Figure 25. This result lies outside the bounds of the correlation indicating that another characteristic is operable. If it is assumed that the impulse added by the long duration final mission burn and the first washout firing are non-influential, the calculated washout parameter value would be increased as indicated in Figure 25, resulting in a new plot of this result, which would then lie within the correlation bounds but, even so, would not probably be characterized by the correlation.

The rebuilt Engineering Evaluation Unit (EEUR) was subjected to two 2400 second duration extended firings, one with 70°F propellant temperature and the second with 52°F propellant. The unit had completed a

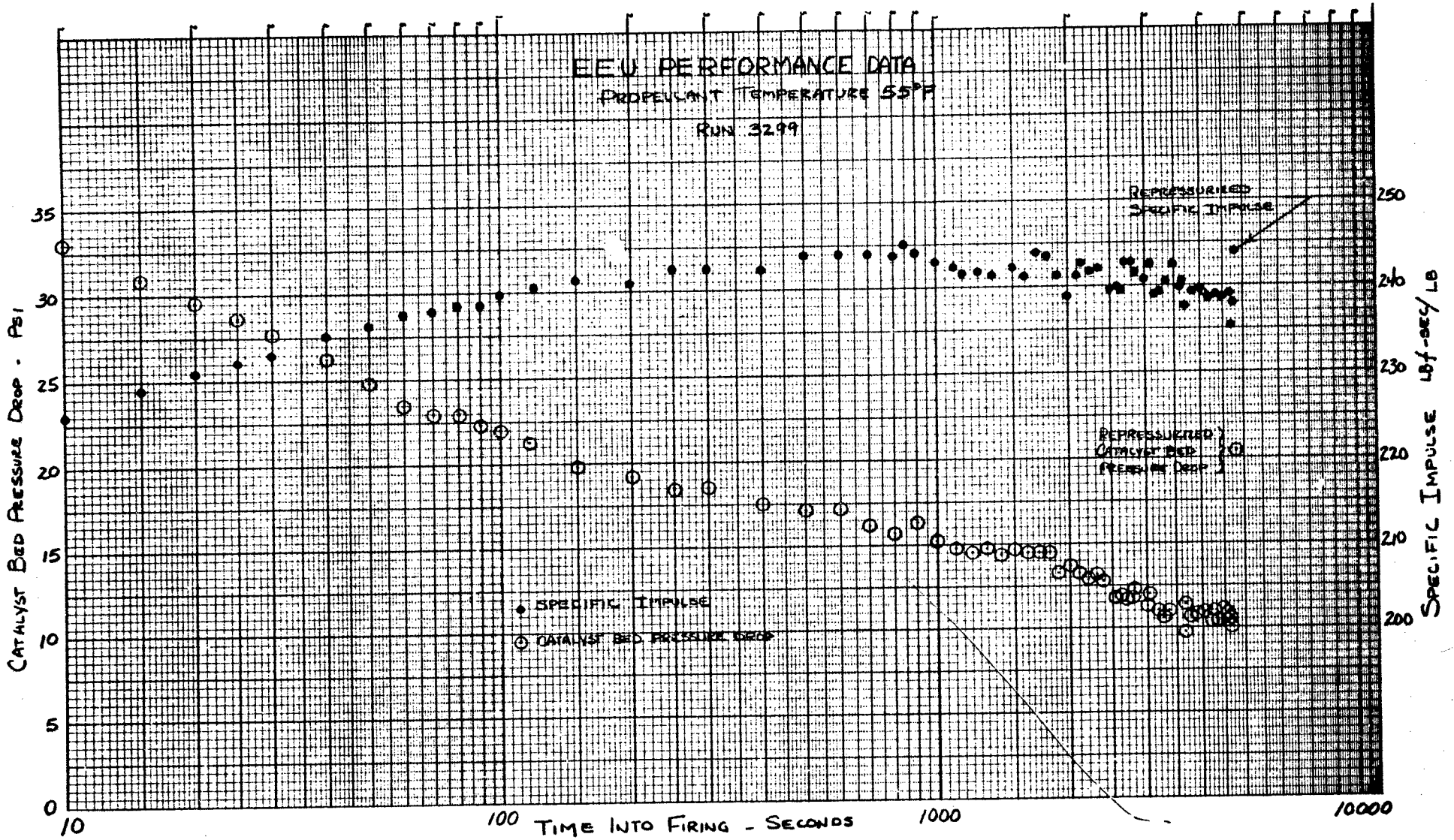
EEW PERFORMANCE DATA
PROPELLANT TEMPERATURE 55°F
RUN 3299
REPRESSURIZED SPECIFIC IMPULSE
REPRESSURIZED CATALYST BED PRESSURE DROP
SPECIFIC IMPULSE
CATALYST BED PRESSURE DROP
CATALYST BED PRESSURE DROP - PSI
SPECIFIC IMPULSE LBf-SEC/LB
TIME INTO FIRING - SECONDS
0
5
10
15
20
25
30
35
200
210
220
230
240
250
10
100
1000
10000

Figure 26

60 pair firing mission, including a repressurization after 18 pairs, and an aborted final burn. The specific impulse and bed pressure drop decay results are shown in Figures 27 and 28. The general character of the plots is very similar to that of the EEU.

Since the firing durations of the EEUR tests were only half those of the EEU, though the washout parameter values are about equal, evaluation of the washout capability of the EEUR is not as readily obtained as that of the EEU. The EEUR actual washout times are shown in Figure 25 as 2400 seconds, the run time, with arrow symbols indicating additional capability of uncertain magnitude. About the most that can be ascertained is that the EEUR results indicate a slightly lesser time to washout by their earlier peaks and somewhat faster decay of specific impulse values.

The validity of the EEUR deboost firing results is obscured by the preceding aborted final burn which involved surging propellant flow and thrust, which evidently resulted in an appreciable rise in bed pressure drop, the effect of which could conceivably be significant. Since there is no known valid method of determining any added influence due to this aborted run, it is presumptuous to evaluate the results directly, since this effect would have to be ignored. Nevertheless, the results do suggest that the EEUR capability is probably comparable to that of the EEU, and that the conclusions relative to the EEU probably apply to the EEUR.

b. Washout Recovery

Although a "washout", (arbitrarily defined as a 10 lb-sec/lb decay in specific impulse during a firing) was not obtained in these tests, the specific impulse decay during the 5000 second duration firings of the EEU was sufficient to consider that the inception of the washout mode of operation had occurred near the end of the firings such that undecomposed propellant was beginning to leave the bed. The unit was repressurized at the end of each firing to determine if the bed would recover from this incipient washout condition; and it did recover. However, the fact that the engine was not in a deep washout operating condition reduces the significance of the test result. Consequently, the results are presented as applicable to "incipient" washout rather than full washout. However, the results do tend to substantiate the gas pore-filling theory of washout which would also apply to recovery from full washout.

At 4800 seconds into the firings of the EEU, the engine inlet pressure was suddenly (in approximately 0.1 second) raised from the 100 psia level to the 290 psia level resulting in an immediate increase in specific impulse and bed pressure drop as shown in Figures 29 and 30. The specific impulse in both repressurizations recovered to near the peak value obtained previously

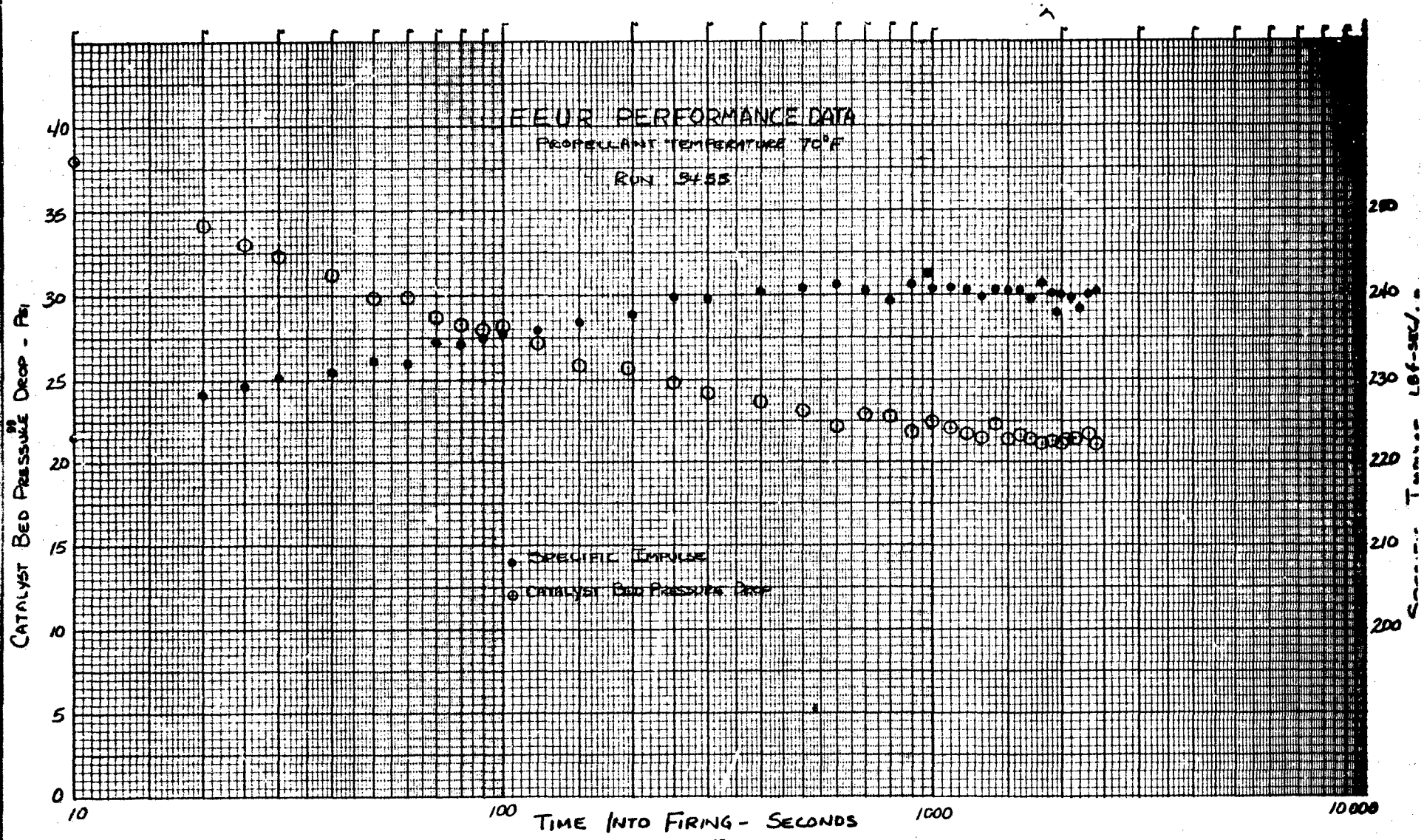
EEUR PERFORMANCE DATA
PROPELLANT TEMPERATURE 70°F
RUN 54-55
SPECIFIC IMPULSE
CATALYST BED PRESSURE DROP
CATALYST BED PRESSURE DROP - PSI
TIME INTO FIRING - SECONDS
0
5
10
15
20
25
30
35
40
10
100
1000
10000
200
210
220
230
240

Figure 27

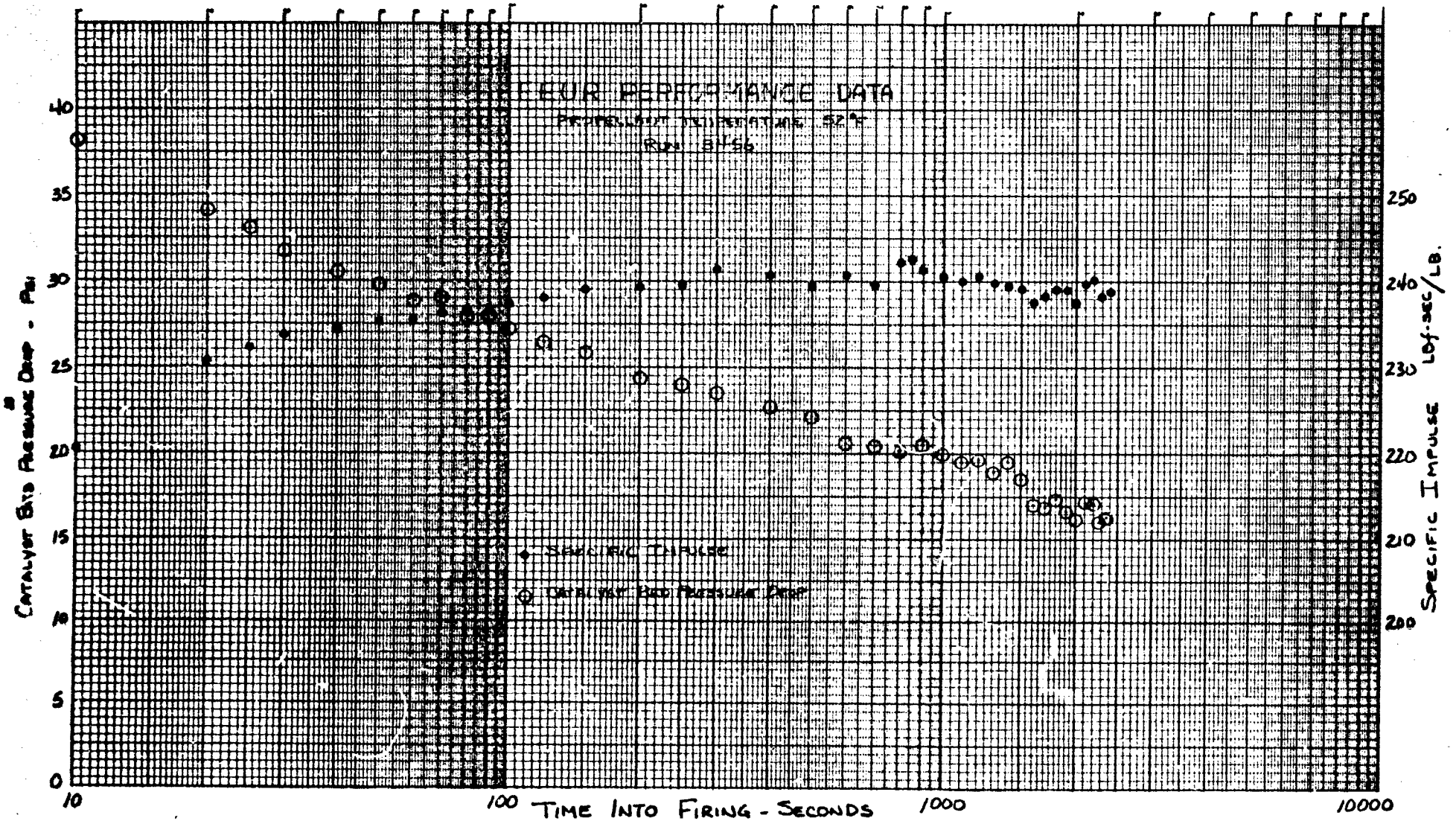
FEUR PERFORMANCE DATA
PROPELLANT TEMPERATURE 52°F
RUN 8156
CATALYST BED PRESSURE DROP - PSI
SPECIFIC IMPULSE LBF-SEC/LB.
TIME INTO FIRING - SECONDS
SPECIFIC IMPULSE
CATALYST BED PRESSURE DROP
0
5
10
15
20
25
30
35
40
200
210
220
230
240
250
10
100
1000
10000

Figure 28

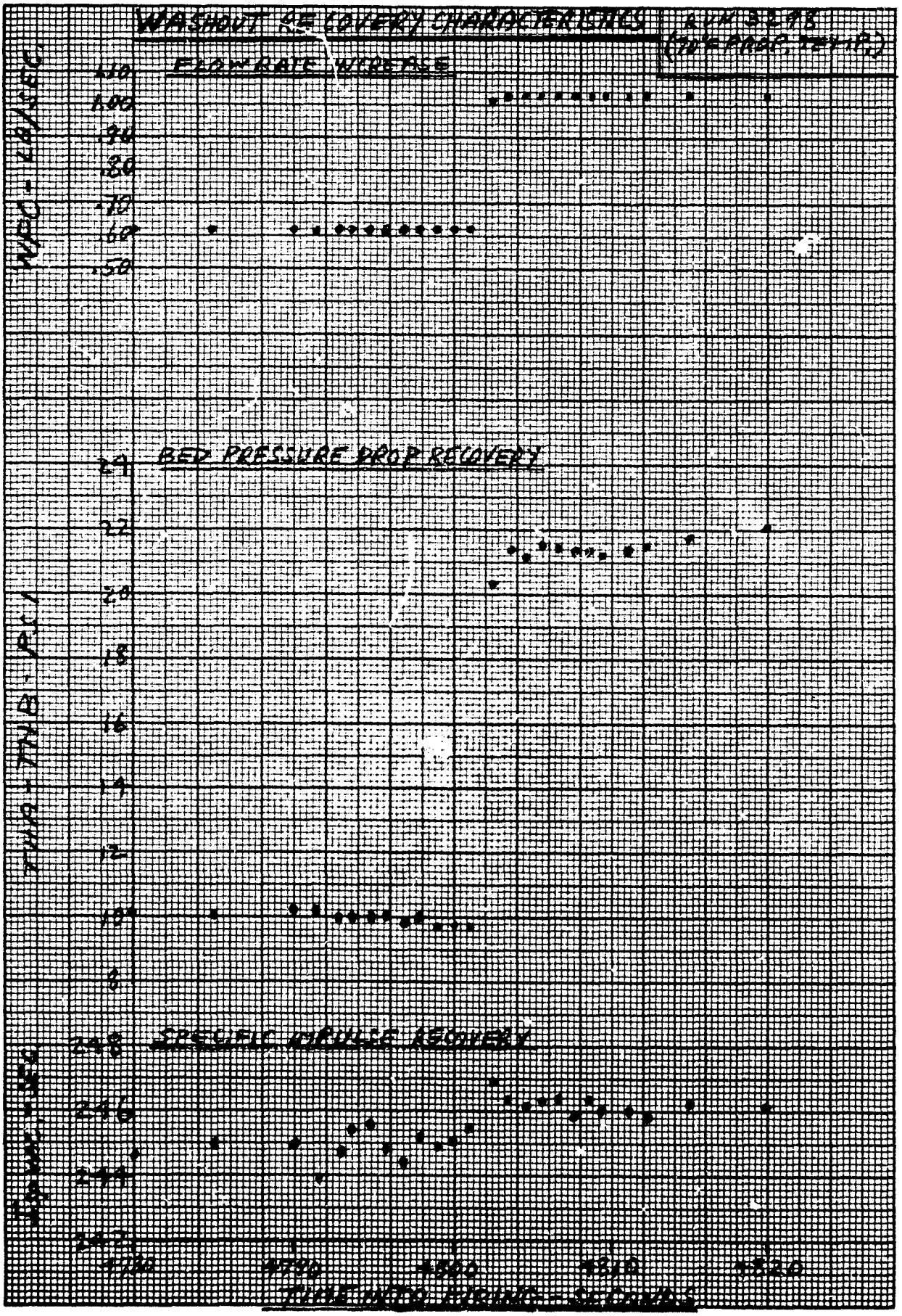
WASHOUT RECOVERY CHARACTERISTICS
FLOW RATE INCREASE
WEIGHT FLOW, LBM/SEC
BED PRESSURE DROP RECOVERY
TUBE PRESSURE DROP, PSI
SPECIFIC IMPULSE RECOVERY
SPECIFIC IMPULSE, SEC
TIME INTO FLIGHT - SECONDS

Figure 29

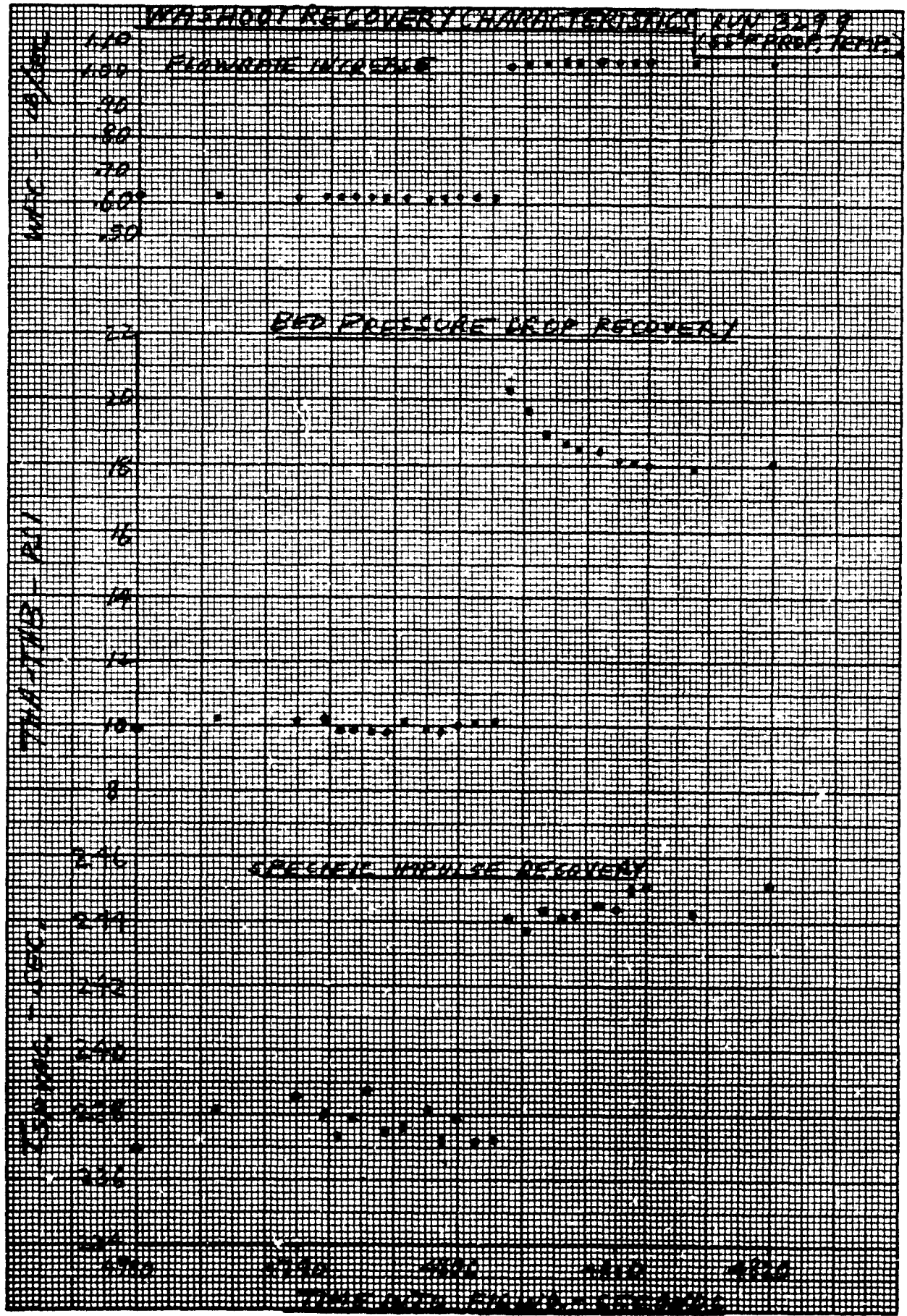
WASHOUT RECOVERY CHARACTERISTICS (RUN 32)
(65°F REF. TEMP.)
FLOWRATE INCREASE
BED PRESSURE DROP RECOVERY
SPECIFIC IMPULSE RECOVERY

Figure 30

during the firing before incipient washout began. The normalized bed pressure drop increased markedly, the increase being 20 to 50% in excess of that attributable to the flow rate increase, depending upon the method used to normalize pressure drop.

The results indicate that the decomposition zone moved back upstream farther into the bed, evidently bringing the engine back out of the incipient washout mode for the remaining 200 seconds of firing time. These recovery results indicate practical as well as academic phenomena:

(1) An engine can be repressurized during a single firing and partially recover some of its run time to washout and performance capability in that particular firing. The degree of recovery of run time to washout cannot be determined from these results as the remaining firing duration of 200 seconds was too short.

(2) The evident movement of the decomposition zone upstream into the bed upon repressurization tends to substantiate the gas pore-filling theory of washout which is that the filling of the pores of the catalyst with decomposition gases greatly reduces the accessibility of the hydrazine to the major part of the catalyst activated area, thereby effectively partially de-activating the catalyst for the remainder of the run. Shutdown of the engine permits expulsion of the pore gases and enables restarting of the bed. Likewise, repressurization to a higher level of flow rate results in a sudden increase in chamber pressure above that existing in the catalyst pores such that hydrazine can again flow into the pores as in starting.

2. CATALYST BED PRESSURE DROP

A normalized pressure drop technique is used to evaluate the catalyst bed pressure drop test results. The derivation and rationale for the use of this technique are presented in Appendix VI. Essentially this method evaluates bed pressure drop, normalized for flowrate and chamber gas temperature, as a function of the number of accumulated ambient start firings.

The results of the PRAT TCA tests in terms of the normalized pressure drop evaluation methods are shown in Figure 31. The initial firing of the program shows a step increase in normalized pressure drop R_c of about 5%. This firing was made with a 290 psia TCA inlet pressure as compared to the 134 psia inlet pressure for the last firing of the prior engine tests. Subsequent firings at higher (up to 400 psia) inlet pressures show even larger increases in R_c. However, subsequent reduction in inlet pressure resulted in reduced R_c, indicating a different influence of flow rate on R_c after the Δ P buildup has occurred.

WALTER KIDDE & CO
BELLEVILLE, N.J.

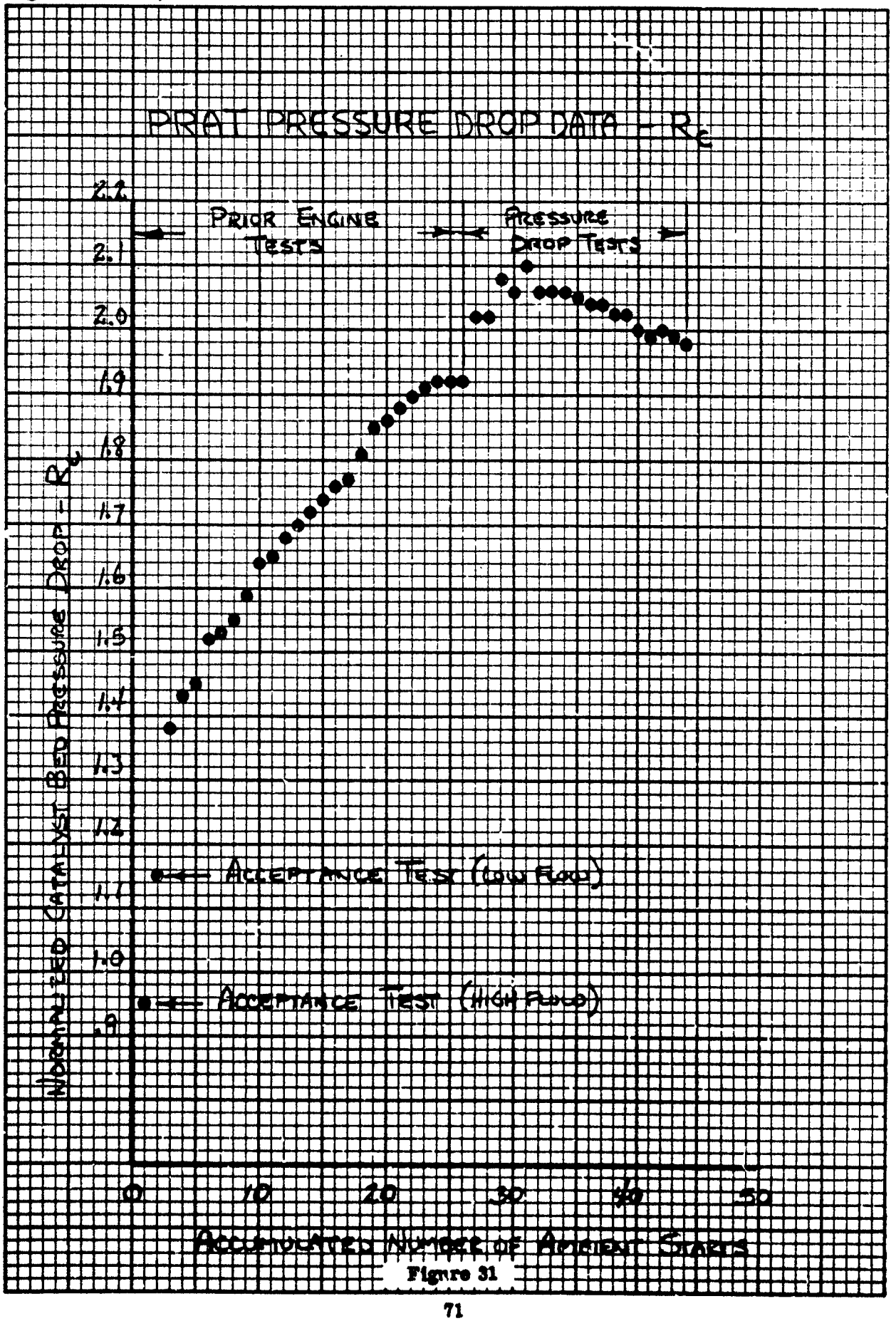

Figure 31

Review of data from similar repressurizations occurring on other TCAs after mission completion and Δ P buildup indicated similar increases in R_c. These increases were plotted non-dimensionally as a function of flow rate in Figure 32, and this plot is considered to be an additional empirically determined influence coefficient to be applied to R_c results obtained with repressurization after Δ P buildup has occurred. Application of this additional correction factor to the PRAT TCA data results in the Plot of Figure 33 of R_{cc} versus the number of ambient starts. Also shown on this plot is the ΔR_c correlation, previously established, for single ambient firings plotted for $\Delta R_c = 0$ for the initial mission firing. It is apparent that the R_c buildup follows the ΔR_c correlation within 3% of R_c throughout. It is conceivable that the increase in bed pressure drop at repressurization could have been related to the coincident resumption of test and the interim removal of the unit from the test stand, however, the repressurization correlations established herein tend to disprove this hypothesis.

The duty cycle of the PRAT test program was largely based upon events and results occurring during the test program and recognition of the nature of the operational characteristics and requirements of the engine. The original test plan called for 20 single ambient starts at 100°F propellant temperature, to determine if the leveling-off of R_c after 30 starts observed with 70°F propellant temperature also occurs with 100°F propellant. The first firing at 290 psia inlet pressure resulted in an 850°F manifold temperature kill. Recognizing that the repressurization was the probable cause of the excessive manifold temperature, the inlet pressure was raised to the maximum value of 400 psia to test the run time to kill at the most adverse condition, with subsequent firings following a blowdown mode. After 12 firings, some of which experienced manifold temperature kills, it was considered proven that R_c had reached a plateau. Subsequently, 5 pair firings, followed by 20 hot starts, followed by an ambient start firing were performed to determine if ΔP could be altered by these types of firings at this stage in life. No significant change in normalized ΔP occurred during these tests.

These results demonstrate the following:

a. The bed pressure drop R_c buildup characteristic for single ambient starts applies over the range of 58 to 100°F propellant temperature. However, R_c must be corrected for repressurization in accordance with Figure 32.

b. Pair firing or hot pulsing have no significant effect on single ambient start pressure drop buildup after it reaches its R_c plateau.

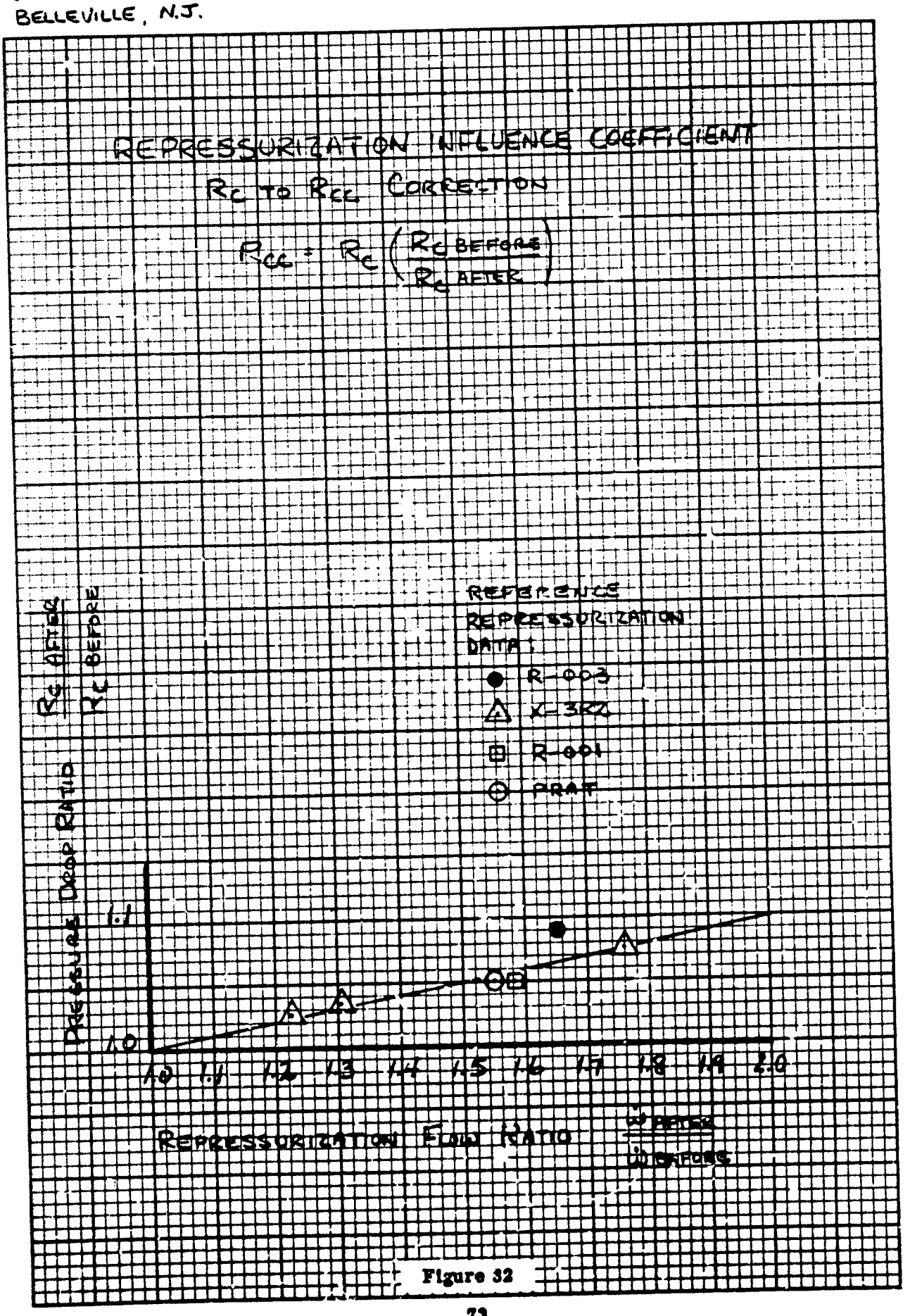
REPRESSURIZATION INFLUENCE COEFFICIENT
R_C TO R_{CC} CORRECTION
$R_{CC} = R_C \left(\frac{R_C \text{ BEFORE}}{R_C \text{ AFTER}} \right)$
REFERENCE REPRESSURIZATION DATA:
R-003
X-3RZ
R-001
PRAT
R_C AFTER / R_C BEFORE
PRESSURE DROP RATIO
1.0
1.1
1.2
1.3
1.4
1.5
1.6
1.7
1.8
1.9
2.0
REPRESSURIZATION FLOW RATIO
W BEFORE / W AFTER

Figure 32

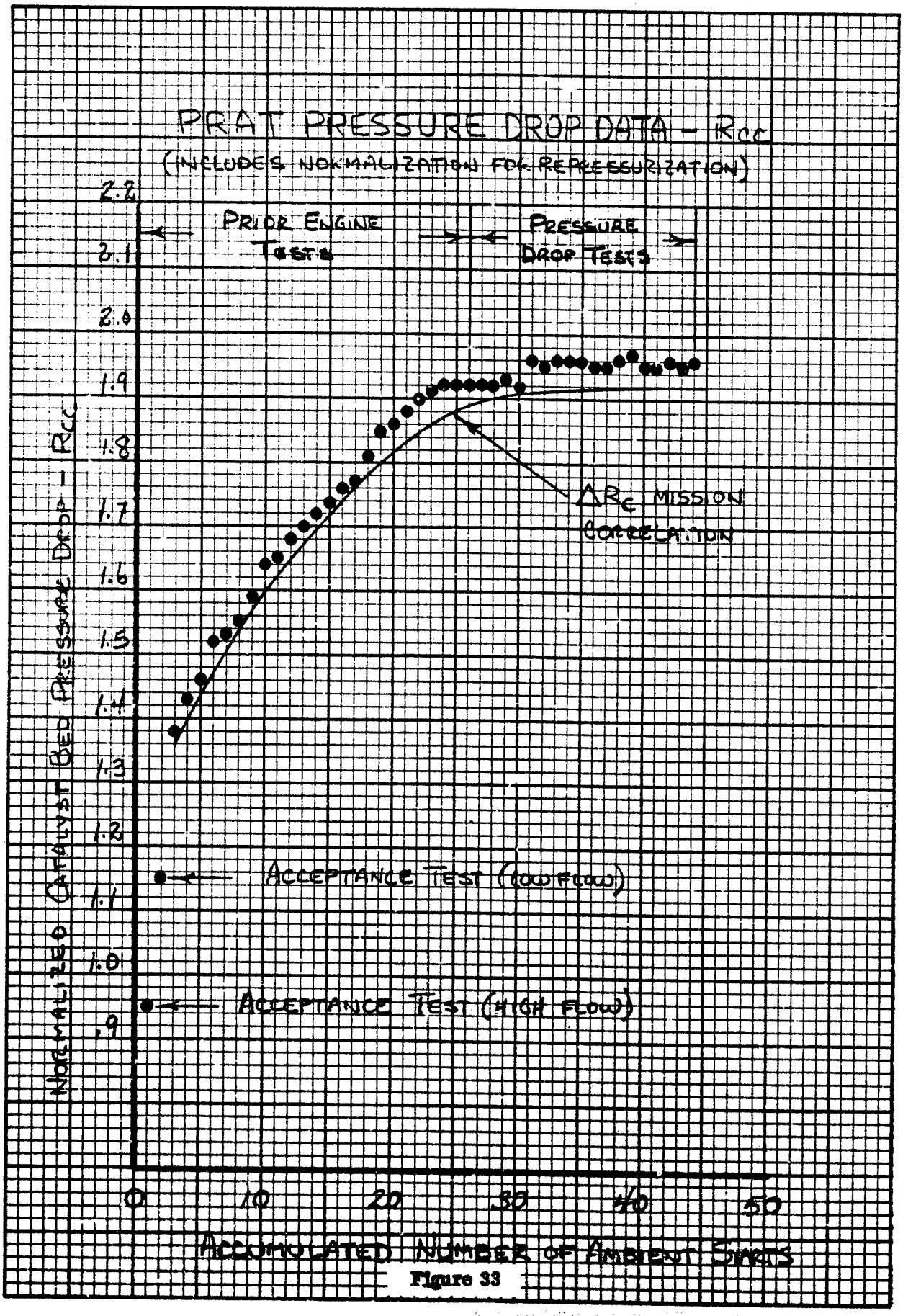
PRAT PRESSURE DROP DATA - R_{cc}
(INCLUDES NORMALIZATION FOR REPRESSURIZATION)
PRIOR ENGINE TESTS
PRESSURE DROP TESTS
ΔR_c MISSION CORRELATION
ACCEPTANCE TEST (LOW FLOW)
ACCEPTANCE TEST (HIGH FLOW)
NORMALIZED CATALYST BED PRESSURE DROP R_{cc}
2.2
2.1
2.0
1.9
1.8
1.7
1.6
1.5
1.4
1.3
1.2
1.1
1.0
.9
0
10
20
30
40
50
ACCUMULATED NUMBER OF AMBIENT STARTS

Figure 33

Figure 34 is a plot of R_c versus the number of ambient starts for the Engineering Evaluation Unit (EEU) mission. The 54th and 55th ambient starts were performed under the test program and represent the two washout duration tests. The 54th start normalized pressure drop shows about a 5% decline from the previous firing of the EEU mission. No specific reason for the decline in normalized pressure drop for the 54th start is known; it is presumably associated with the interim removal of the TCA from the test stand.

The pressure drop results of the rebuilt Engineering Evaluation Unit (EEUR) in accordance with the normalization method are shown in Figure 35, with the repressurization correction being applied to Figure 35 to obtain Figure 36 Superimposed on Figure 36 are the EEU results in terms of the established ΔR_c correlation and also the absolute value of R_c. The data for the two engines compared on an absolute R_{cc} basis (Figure 36) indicates that although the rebuild engine started with the lower value, its higher buildup rate attending the unusually low propellant flow rate of the final half of the initial blowdown, caused the normalized ΔP to reach the same absolute value as the EEU at repressurization. It appears that the rebuild engine normalized pressure drop peaked earlier than the EEU. The step increase in the bed pressure drop occurring after the aborted gas surging deboost firing (start number 64) is reflected in the R_c results.

The most reasonable interpretation of the pressure drop differences between the EEU and the EEUR is that the EEUR pressure drop was initially lower, followed the established ΔR_c correlation up to the ambient start where the inlet pressure became less than that previously tested (85 psia) at about the 15th start where the flow rate was thereafter definitely decavitated and markedly lower than that experienced in the EEU tests. It is surmised that this low flow rate resulted in a more rapid buildup in normalized pressure drop than had occurred with the EEU. The cause of this increased buildup rate is uncertain; perhaps it is the result of the longer gas bed length attending low flow rates and consequent degradations of portions of the bed not normally used. The more rapid buildup rate could conceivably lead to the earlier peak or plateau of the EEUR normalized pressure drop as compared to the EEU.

In summary, it appears that the rebuild unit EEUR normalized bed pressure drop results generally followed the EEU results which are the basis of the pair firing correlation, except that the lower decavitated flow rate of the last part of the initial blowdown apparently caused a more rapid buildup than would be accounted for by the correlation. This rapid buildup evidently resulted in an earlier plateau and peak value of normalized pressure drop. It is worth indicating that these differences are minor compared to the differences between the single and pair firings pressure drop correlations. The increase in the pressure drop of the two final burn firings are the result of surging thrust chamber operation in the preceding firing caused by pressurant gas in the feed system.

WALTER KIDDE & CO
BELLEVILLE, N.J.

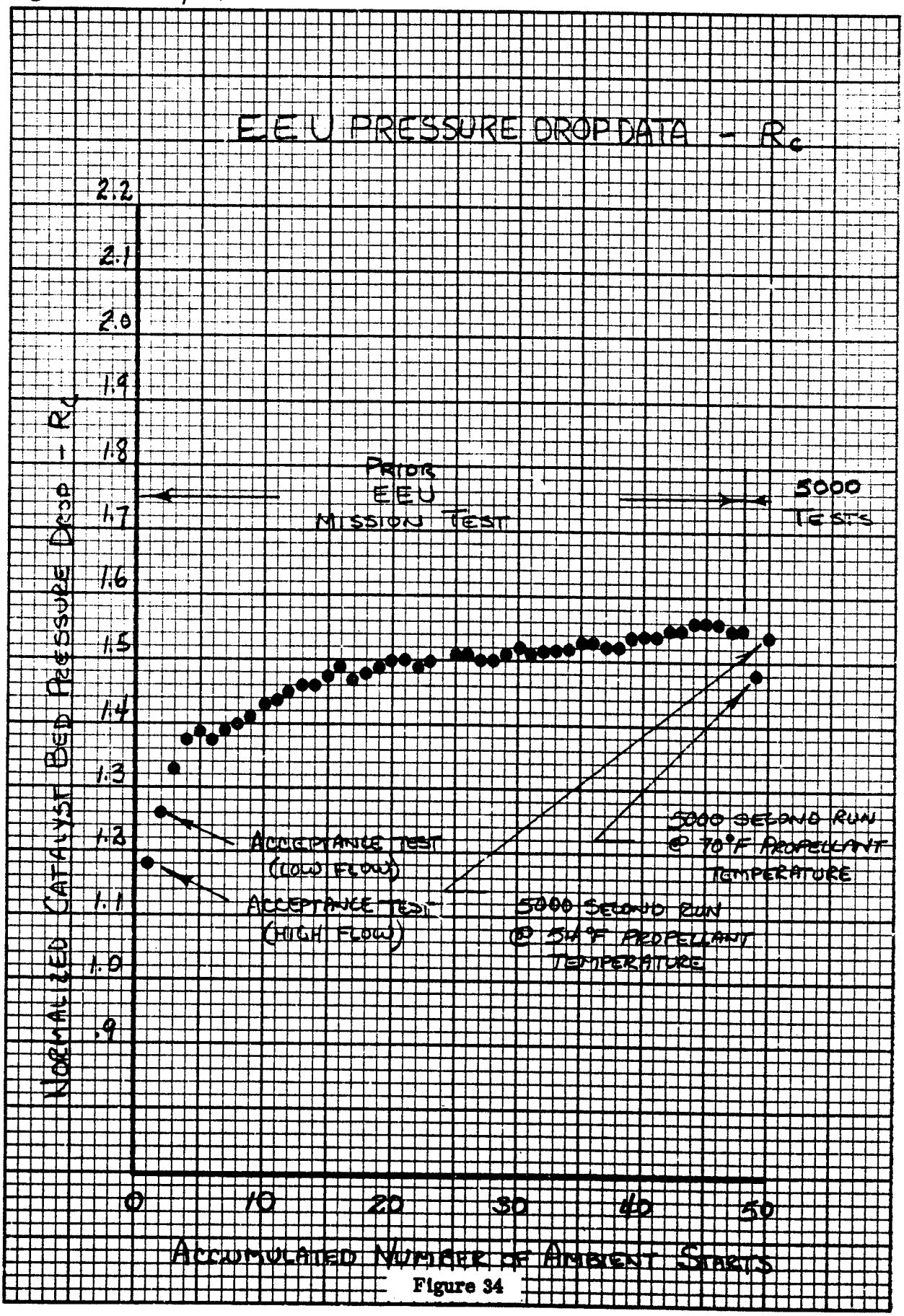

Figure 34

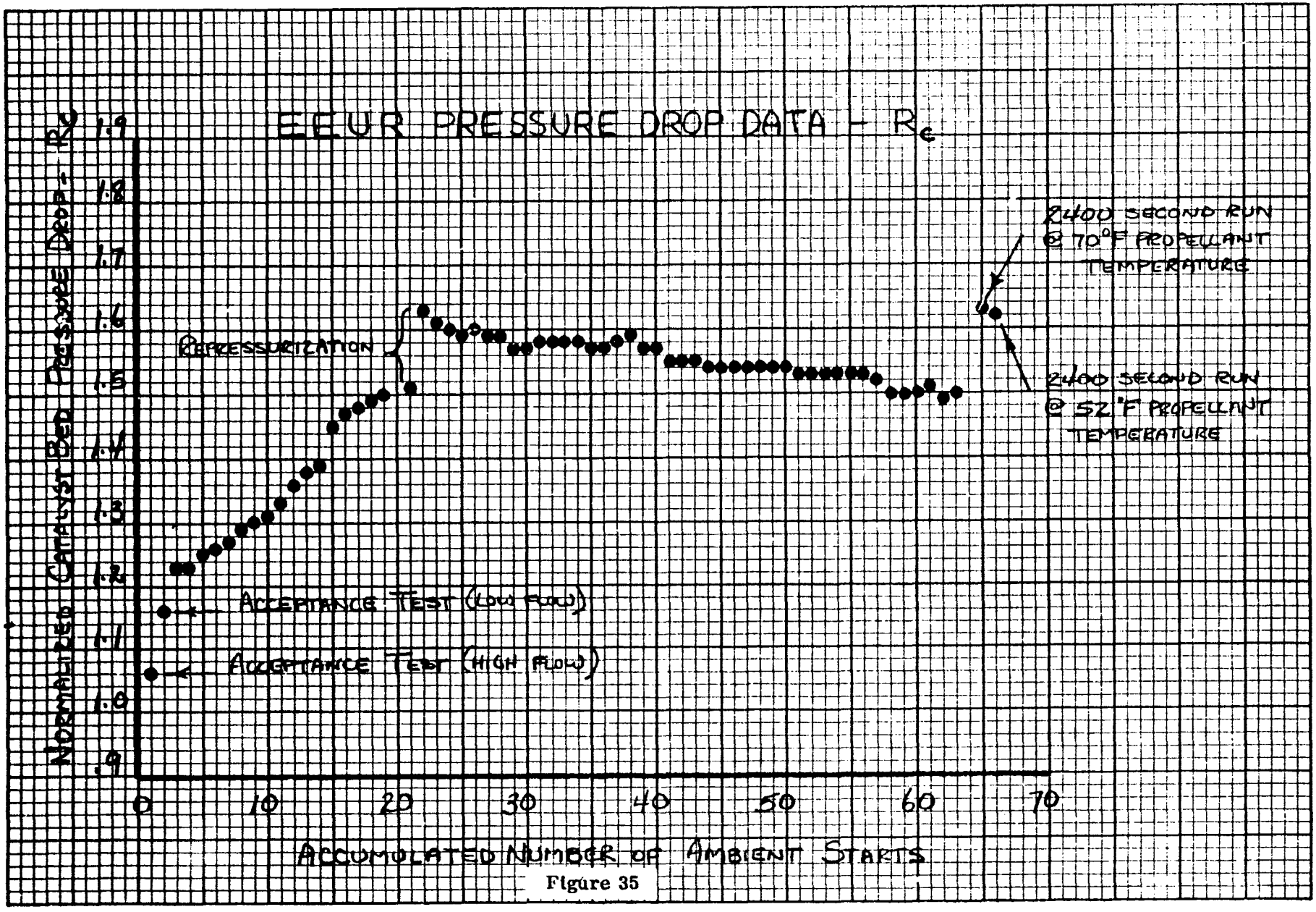
EEUR PRESSURE DROP DATA - R_c
NORMALIZED CATALYST BED PRESSURE DROP - R_p
1.9
1.8
1.7
1.6
1.5
1.4
1.3
1.2
1.1
1.0
.9
REPRESSURIZATION
ACCEPTANCE TEST (LOW FLOW)
ACCEPTANCE TEST (HIGH FLOW)
2400 SECOND RUN @ 70°F PROPELLANT TEMPERATURE
2400 SECOND RUN @ 52°F PROPELLANT TEMPERATURE
0
10
20
30
40
50
60
70
ACCUMULATED NUMBER OF AMBIENT STARTS

Figure 35

WALTER KIDDE & CO
BELLEVILLE, N.J.

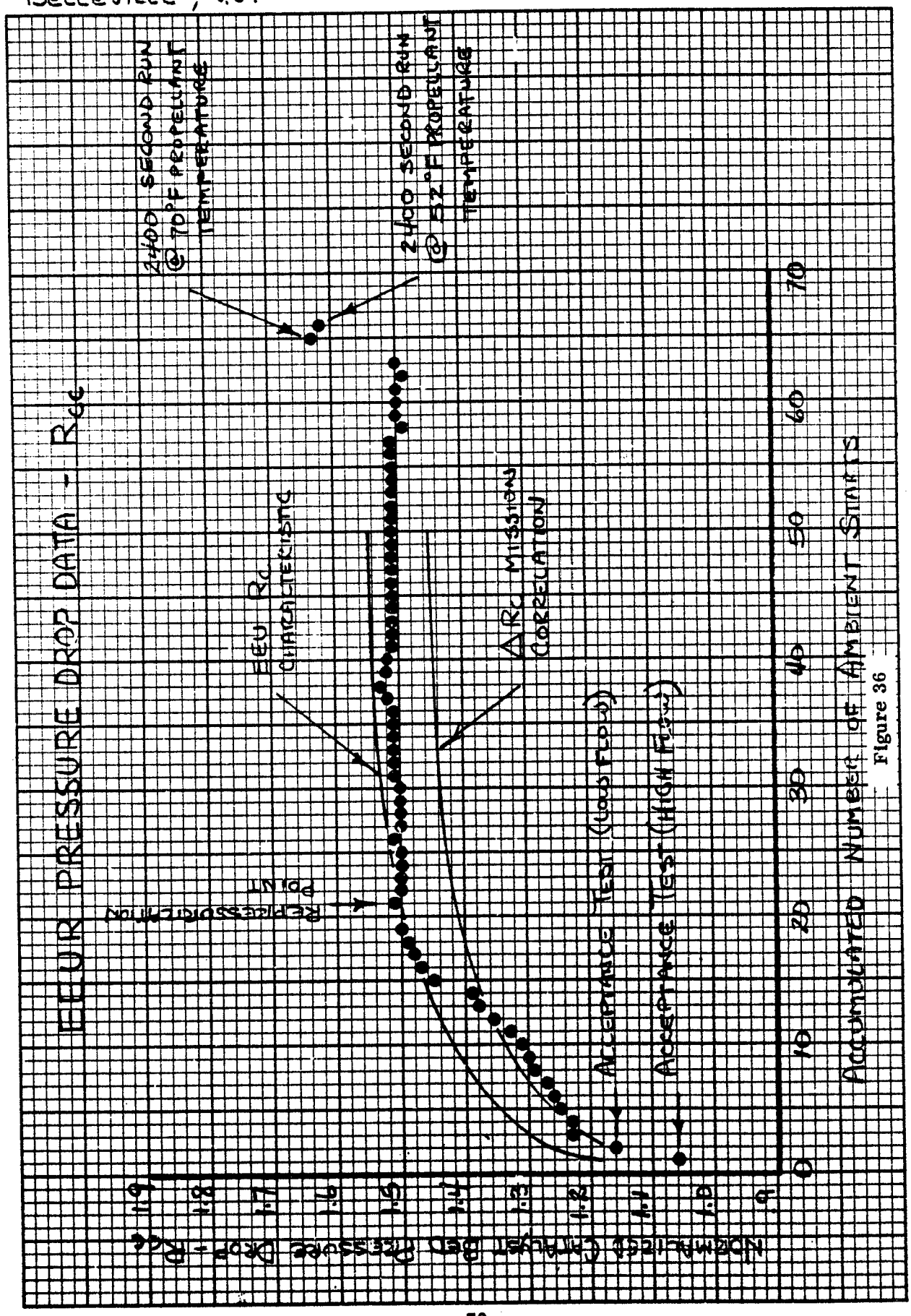

Figure 36

3. SPECIFIC IMPULSE PERFORMANCE

Thruster performance as measured by instantaneous specific impulse is plotted in Figures 37, 38, and 39 for the three units. Superimposed on the plots is the correlation established for the instantaneous specific impulse at 20 seconds after the start of the firing. The correlation is based upon the results of TCA's X3R2, 1001, 1002, R001, R003 and is given in terms of thrust as

$$F' = 247.921\ WFC - 12.848 \pm 1.77s$$

where:

F' = Vacuum thrust - LB

WFC = Flow rate - LB/SEC

s = Standard deviation

The specific impulse is obtained by dividing F' by WFC.

Figure 37 shows that the data from the Engineering Evaluation Unit tests all lie between the correlation average and the upper limit, with most being very close to the average. The two test results are 1 or 2 seconds higher than the bulk of the prior results which can be attributed to normal variation.

Figure 38 shows that practically all of the results of the Engineering Evaluation Unit Rebuild test data lie between the correlation average and the upper limit with the great majority being close to the average.

Figure 39 shows that all of the PRAT unit results fall easily within the correlation limits with the great majority being close to the average. The initial test results are somewhat lower than the corresponding PRAT results perhaps due to the effect of increased bed pressure drop on bed stay time, however, the differences are small and within normal variation.

These results show that the test thrusters performances conform to the established correlation. Extended missions and repressurization net effects are within normal variations of the correlation.

WALTER KIDDE & CO
BELLEVILLE, N.J.

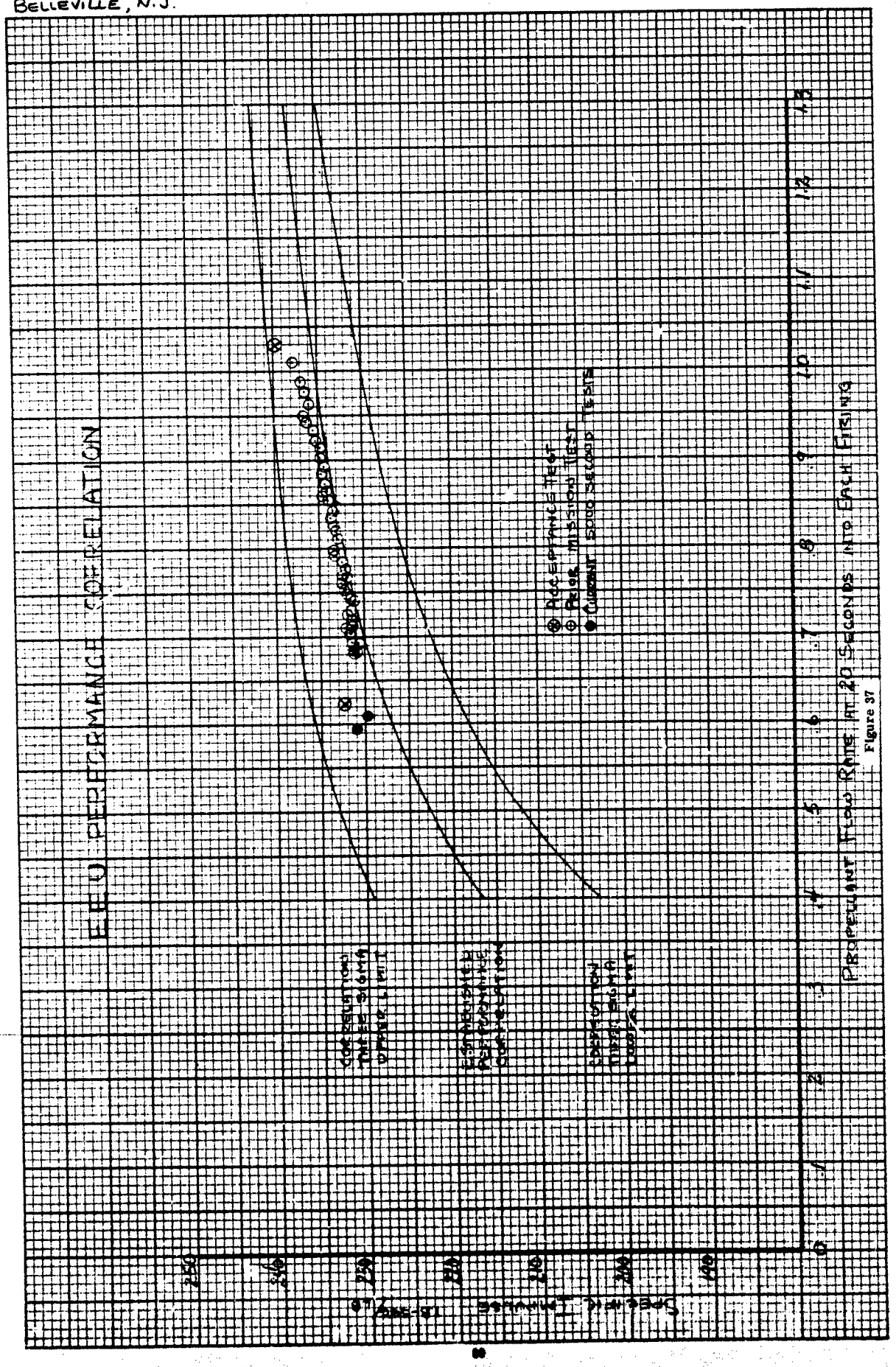

Figure 37

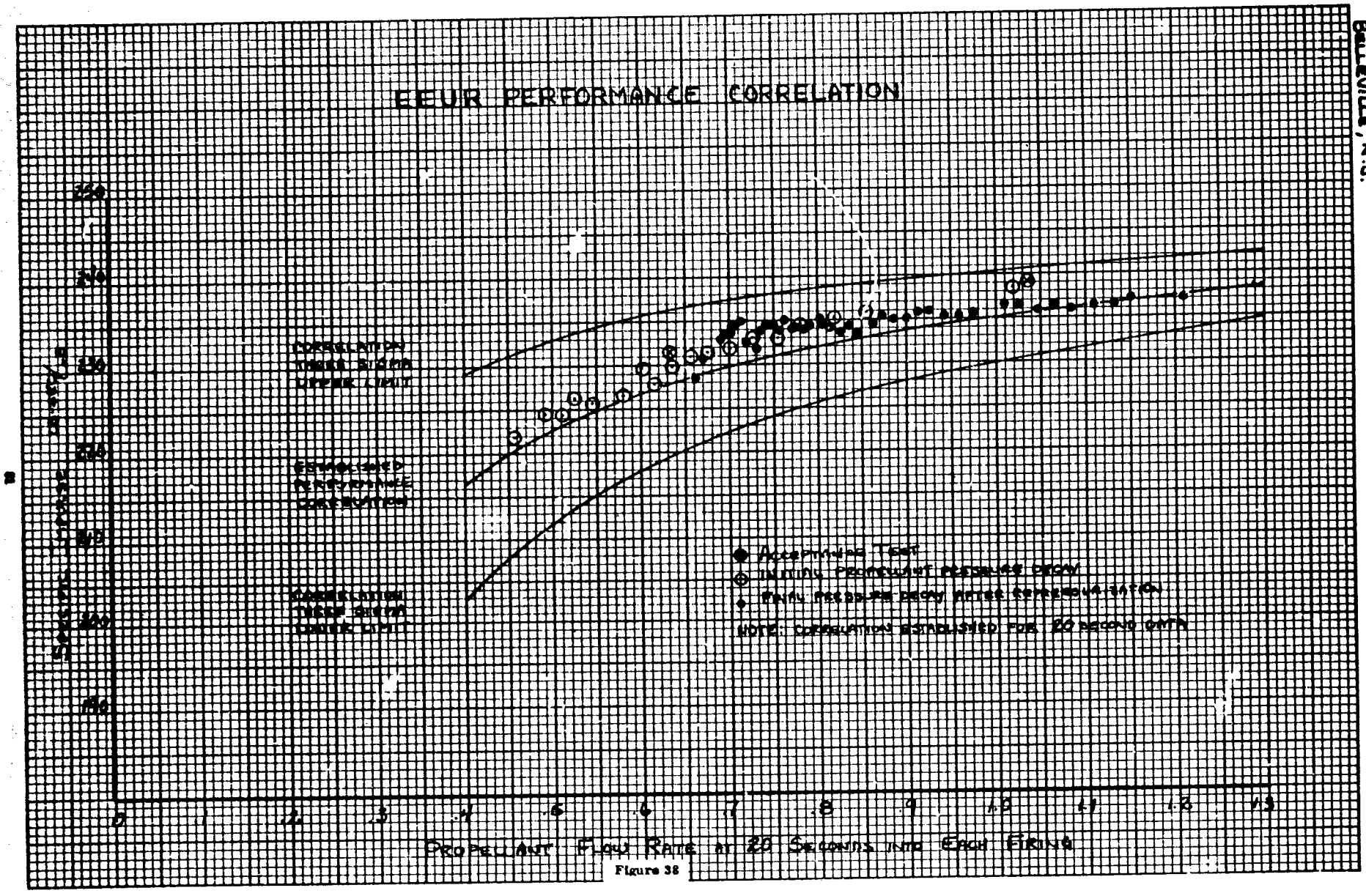
EEUR PERFORMANCE CORRELATION
WALTER KIDDE & CO
BELLEVILLE, N.J.
250
240
230
220
210
200
190
CORRELATION
THRUST SIGMA
UPPER LIMIT
CORRELATION
THRUST SIGMA
LOWER LIMIT
◆ ACCEPTABLE TEST
⊙ RUNNING PROPELLANT PRESSURE DROP
◆ RUNNING PRESSURE DROP WITHIN CORRELATION LIMITS
NOTE: CORRELATIONS ESTABLISHED FOR 20 SECOND BURN
0
1
2
3
4
5
6
7
8
9
1.0
1.1
1.2
1.3
PROPELLANT FLOW RATE AT 20 SECONDS INTO EACH FIRING

Figure 38

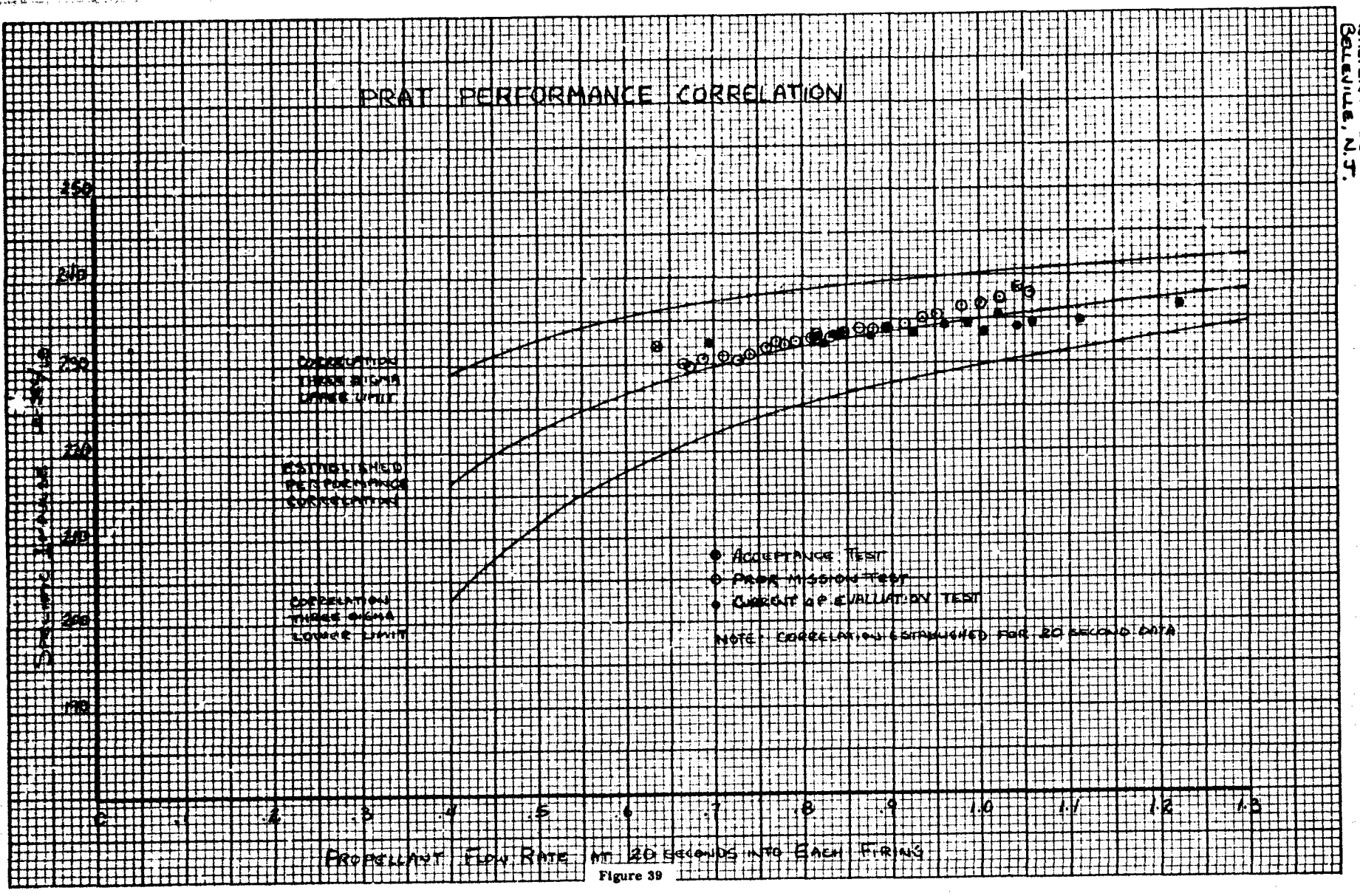
PRAT PERFORMANCE CORRELATION
WALTER KIDDE & CO
BELLEVILLE, N.J.
150
200
250
220
240
260
CORRELATION THREE SIGMA LOWER LIMIT
ESTABLISHED PERFORMANCE CORRELATION
CORRELATION THREE SIGMA LOWER LIMIT
ACCEPTANCE TEST
PEAK MISSION TEST
CURRENT QUALIFICATION TEST
NOTE: CORRELATION ESTABLISHED FOR 20 SECOND DATA
.1
.2
.3
.4
.5
.6
.7
.8
.9
1.0
1.1
1.2
1.3
PROPELLANT FLOW RATE AT 20 SECONDS INTO EACH FIRING

Figure 39

4. MANIFOLD TEMPERATURE

The initial firing of the PRAT bed pressure drop test series resulted in automatic abort when the outermost manifold temperature (T2B) reached 850°F a few seconds before the completion of the 22,000 lb-sec impulse firing. This 850°F "kill" temperature is based upon experience in that safe shutdowns have been performed up to this temperature. Only the outermost of the three manifold temperatures (T2B, T2A, TO2 as shown in Figure 47) reached the limit, probably due to heat feed back from the chamber wall. Manifold temperatures T2A and TO2 located more towards the center of the manifold were well below the "kill" limit as shown in Figure 40. No unsafe shutdowns have been encountered so the true safe upper limit for manifold temperature is unknown. Since prior operation of this TCA at the same 100°F propellant temperature and firing impulse but at a low inlet pressure had not resulted in a manifold temperature kill, it was surmised that the high inlet pressure of 290 psia was the cause of the kill of the initial firing. Consequently, the inlet pressure was raised to the highest level (406 psia) anticipated in the vehicle system, and fired until a manifold temperature kill occurred at about 89 seconds into the firing which corresponds to approximately 26,000 lb-sec impulse.

A blowdown cycle of inlet pressure was thereafter followed until kills no longer occurred. In all, four firings resulted in manifold temperature kills. These results are plotted in Figure 40 and the three manifold temperature transients for the maximum pressure firing are plotted in Figure 40. Table XII summarizes the results which indicate a somewhat erratic pattern to the kills.

Chronologically, a kill occurred during every other firing while the firing impulse varied from 18,000 to 26,000 lb-seconds with no correspondence to pressure level. However, below an inlet pressure level of 280 psia no kills were encountered.

WALTER KIDDE & CO
BELLEVILLE, N.J.

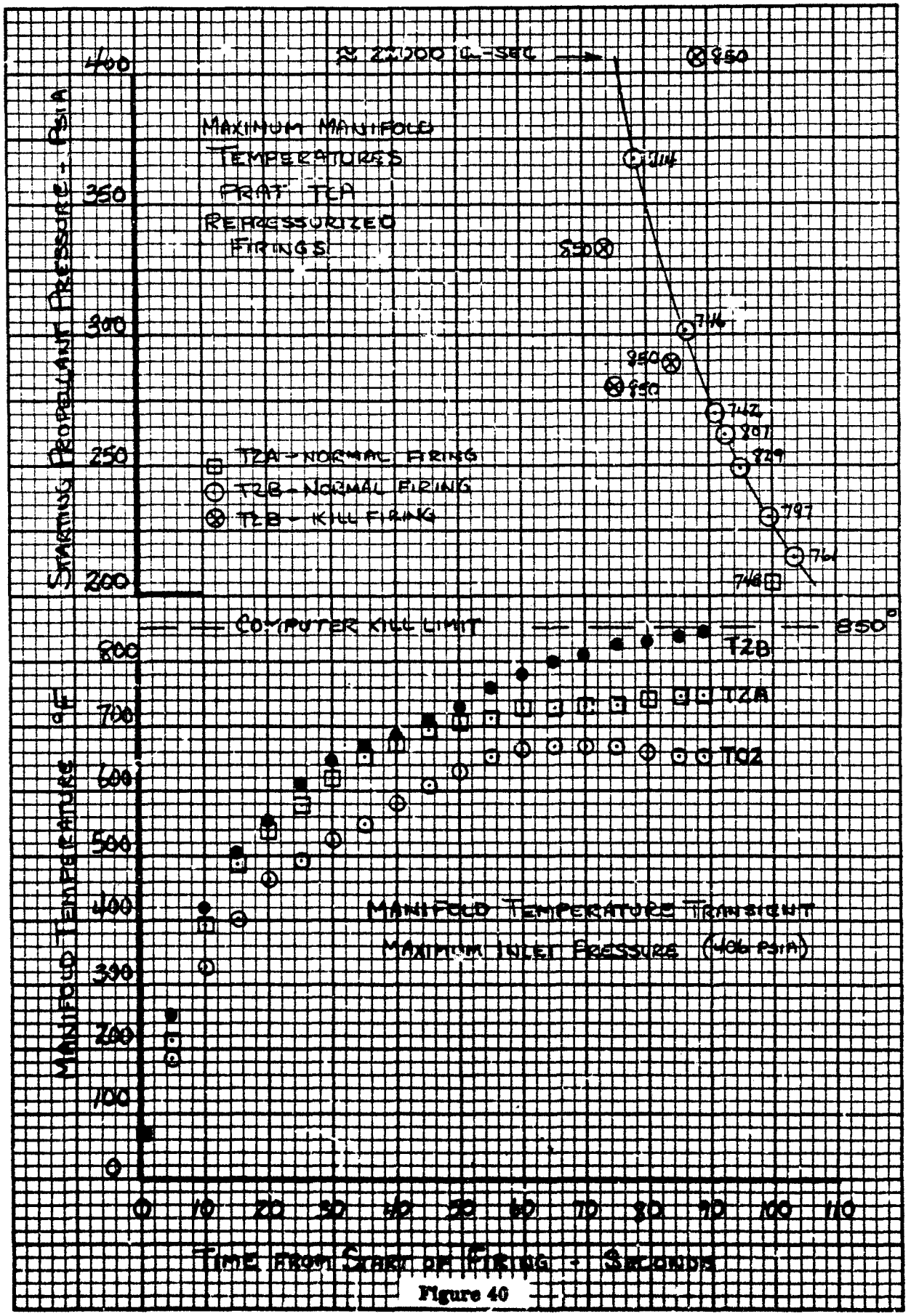

Figure 40

TABLE XII

LONG DURATION PRAT TESTS - MAXIMUM MANIFOLD TEMPERATURES

Run No.	Start Inlet Pressure psia	Maximum Manifold Temperature °F	Thermo-couple	Time into Run at Max. Temperature Seconds	Type of Shutdown
3300	289	850	T2B	84.1	Kill
3301	271	742	T2B	91.3	Normal
3302	406	850	T2B	86.8	Kill
3303	367	814	T2B	79.8	Normal
3304	333	850	T2B	73.4	Kill
3305	301	746	T2B	86.6	Normal
3306	280	850	T2B	75.2	Kill
3307	262	807	T2B	92.9	Normal
3308	249	829	T2B	95.1	Normal
3309	230	797	T2B	99.6	Normal
3310	214	761	T2B	103.7	Normal
3311	206	748	T2A	100.0	Normal

Prior experience with high manifold temperatures has shown that the maximum temperature experienced during a firing increases with increasing bed pressure drop. The PRAT TCA had the high bed pressure drop associated with single starts and experienced a maximum manifold temperature (T2B) of 734°F during final burn at low inlet pressure. Increasing the inlet pressure to 280 psia on the next run evidently provided sufficient additional heat input to increase this temperature to the 850°F kill limit, which is in agreement with the general trend of manifold temperature effects of inlet pressure level.

The erratic behavior of manifold temperature transient with respect to the known causal factor of inlet pressure is unresolved and indicates that an area of uncertainty exists in terms of the critical conditions of the causal factors. It may be that if the kill limit was safely raised somewhat, all potential causal factor conditions could be tolerated within this limit. The nature of the transients indicates a peak followed by a slight decline in manifold temperature during the firing. Based upon Figure 40, the peak is likely not far above 850°F, in all likelihood less than 1000°F which level may be safe for shutdown and tolerant of all potential conditions which could be verified by appropriate tests and evaluations.

SECTION VIII

CONCLUSIONS

1. WASHOUT CAPABILITY

The results demonstrate the ability of the engine to meet the requirements of future missions with extended life capabilities of up to 66 ambient starts and 2.3 million lb-seconds total impulse. The evaluated washout capability of the Engineering Evaluation Unit and the Rebuild Unit lie outside the previous range of engine results but still possibly within the limits of the overall washout correlation except for the influence of long duration firing impulse accumulation which seems to be negligible. The questionable validity and the statistical inadequacy of the results provide only a suggestion of trend as to the exact extent of influence of the various contributing factors. Nevertheless, it is highly probable that the 49% area 4 end flow engines exhibit a different characteristic than that previously obtained with the higher end flow (53 to 56%) engines of the same design, such that the influence of cold starts and firing impulse may be substantially reduced. Also, the recent narrowing of the range of individual distributor tube end flows could be a factor in the improvement in washout capability above that predicted for these tests.

2. WASHOUT RECOVERY

Repressurization of the EEU engine when operating in an incipient washout condition resulted in recovery of specific impulse and bed pressure drop, indicating the following:

a. An engine operating with incipient washout can be repressurized during a single firing and partially recover some of its run time to washout and performance capability in that particular firing.

b. The recovery of specific impulse and evident bed length recovery upon repressurization tend to substantiate the gas pore-filling theory of washout.

3. BED PRESSURE DROP

a. The PRAT TCA catalyst bed pressure drop confirmed the established single firing normalized pressure drop correlation for 100°F propellant.

b. Pair firings or hot pulsing have no significant effect on single ambient start duty cycle pressure drop after it reaches its plateau. Pressure drop management by pair firing must be accomplished early in the mission to be effective.

c. The Engineering Evaluation Unit Rebuild TCA exhibited a faster normalized pressure drop buildup rate than that of the Engineering Evaluation Unit with a consequent earlier plateau and peak, these effects evidently being the result of uniquely low decavitated flow rates during the latter half of the initial blowdown cycle. Otherwise, the results were in general agreement with the pressure drop correlation for pair firings.

4. SPECIFIC IMPULSE

The performance of the thrusters during the extended mission tests was normal and well within limits of the established instantaneous specific impulse correlation.

5. MANIFOLD TEMPERATURE

Repressurization with high bed pressure drop of the level associated with single start missions can result in manifold temperature levels above those demonstrated to be safe, depending upon the repressurization pressure level and firing duration. Demonstrations of safe shutdown capability at these high manifold temperature conditions seems appropriate.

APPENDIX I

THRUST CHAMBER COMPONENT AND UNIT ASSEMBLY

The Walter Kidde & Company 300-lb thrust chamber design is presented on drawing 894849. The basic parts are the inlet bell, the inlet tube assembly, the manifold assembly, the shell assembly, the partition assemblies which contain the distribution tubes, the catalyst, the catalyst retainer screens, the retainer plate, the support plate and the nozzle assembly. Materials of construction are presented on Table XIII. Propellant enters the unit through the inlet tube. The flow is divided into 37 flow paths in the manifold and directed into the distribution tubes through orifice tubes contained in the manifold face.

The distribution tubes serve to distribute propellant over the fine mesh catalyst contained within the partition assembly where decomposition is initiated. Fluid flow proceeds radially out of the partitions into the coarse catalyst or main catalyst bed and turns to flow axially out of the catalyst bed through the retaining screens and plates.

The critical performance components in the fabrication of the thrust chamber are the manifold and distribution tubes. These form the injection system. Each component of this system is subjected to component testing against established limits as a basis for acceptance or rejection. The manifold is flow tested to obtain element flow and total flow using a weighing system. Flow from each injection point in the manifold is simultaneously collected over a closely controlled time interval and the flow from each point is weighed to determine flow rate. A total flow is also accomplished at two fluid pressure levels representing low and high thrust levels and the results are compared with established limits as indicated on Figure 41, the Manifold Flow Calibration Sheet. The ratio limits, which are the acceptance criteria, have been established based upon previous build data and the correlation of this data with resultant test experience. The limits vary from point to point based upon location with respect to the inlet (point 1) as indicated in Figure 42. Water at 70°F is used for flow testing.

Kidde drawing 279079 presents the distribution tube detail showing the inlet and the exits. This tube is pressed into a bushing and an 80 mesh cylindrical screen and end screen are tack welded to the tube to form the distribution tube assembly shown on Figure 43. Each distribution tube assembly is subjected to a flow test inspection using the Distribution Tube Flow Rig shown on Figure 43. This rig provides means to control inlet pressure and back pressure as well as time and collect fluid flow from four areas on each distribution tube. Fluid collected from each area is drawn from each tank and weighed. Data obtained is recorded on the Distribution Water Flow Test Data sheet also shown on Figure 43.

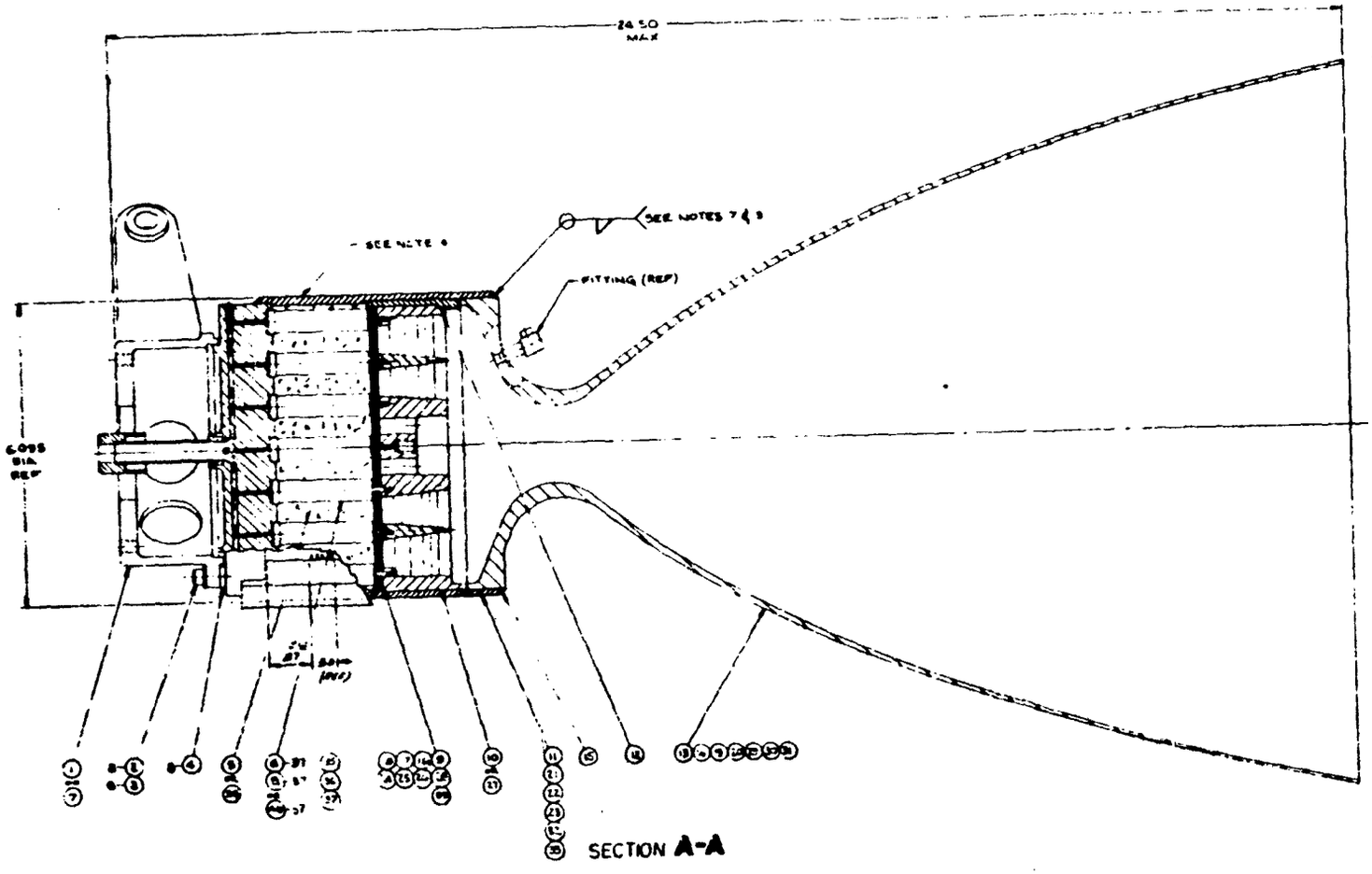

THRUST CHAMBER 894849

TABLE XIII

THRUST CHAMBER CONSTRUCTION MATERIALS

Final Assembly	Major Sub-Assemblies	Sub-Assemblies	Major Parts	Raw Materials
Thrust Chamber	Shell Assembly	Manifold Assembly	Manifold	CRES 304L
			Inlet fitting	CRES 304L
			Inlet tube	CRES 17-4 PH
			Orifice tube	Inconel 600
			Shell	Hastelloy X
			Inlet bell	CRES 17-4 PH
	Partition Assembly	Distribution Assembly	Tube	Inconel 600
			End screen	Hastelloy C
			Side screen	Hastelloy C
			Plug (1)	Inconel 600
			Partition	Hastelloy C
			Plug (2)	Inconel 600
			Fine catalyst	Shell type 405
		Nozzle Assembly	Nozzle	Hastelloy X
			Fitting	Hastelloy X
			Support Plate	Hastelloy X
			Retainer Plate	TZM
			Screen (1)	Hastelloy C
			Screen (2)	Hastelloy C
			Screen (3)	Hastelloy C
			Coarse catalyst	Shell type 405

MANIFOLD FLOW CALIBRATION SHEET
FIGURE 35

P/N _____ S/N _____ DATE _____

SINGLE POINT FLOW-HIGH

INLET PRESSURE _____ PSIG TIME _____ SEC.

INJECTOR	1	2	3	4	5	6	7	8	9	10	11	12	13	14	15	16	17	18	19	20	21	22	23	24
GROSS																								
TARE																								
NET-LBS.																								
RATIO $\frac{NET}{Avg}$																								
RATIO LIMITS	.88 .88	1.09 .89	1.09 .89	1.09 .89	1.09 .89	1.09 .89	1.09 .89	1.11 .91	1.13 .93	1.11 .91	1.13 .92	1.11 .91	1.12 .92	1.11 .91	1.12 .92	1.11 .91	1.12 .92	1.11 .91	1.12 .92	1.13 .93	1.06 .86	1.06 .86	1.13 .93	1.06 .86

INJECTOR	25	26	27	28	29	30	31	32	33	34	35	36	37
GROSS													
TARE													
NET-LBS.													
RATIO $\frac{NET}{Avg}$													
RATIO LIMITS	1.06 .86	1.13 .93	1.06 .86	1.06 .86	1.13 .93	1.06 .86	1.06 .86	1.13 .93	1.06 .86	1.06 .86	1.13 .93	1.06 .86	1.06 .86

TOTAL FLOW (NET) LBS. ÷ TIME SEC. = FLOW RATE LBS./SEC. *

_____ ÷ _____ = _____

TOTAL FLOW (NET) LBS. ÷ 37 = AVG FLOW (NET) LBS.

_____ ÷ 37 = _____

TOTAL FLOW INLET PRESSURE _____ PSIG TIME _____ SEC.

GROSS _____

TARE _____

NET _____ LBS.

RATE _____ LBS./SEC. *

SINGLE POINT FLOW-LOW

INLET PRESSURE _____ PSIG TIME _____ SEC.

INJECTOR	1	2	3	4	5	6	7	8	9	10	11	12	13	14	15	16	17	18	19	20	21	22	23	24
GROSS																								
TARE																								
NET-LBS.																								
RATIO $\frac{NET}{Avg.}$																								
RATIO LIMITS	.88 .88	1.09 .89	1.09 .89	1.09 .89	1.09 .89	1.09 .89	1.09 .89	1.13 .93	1.18 .98	1.13 .93	1.18 .98	1.13 .93	1.18 .98	1.13 .93	1.18 .98	1.13 .93	1.18 .98	1.13 .93	1.18 .98	1.18 .98	1.06 .86	1.06 .86	1.16 .96	1.06 .86

INJECTOR	25	26	27	28	29	30	31	32	33	34	35	36	37
GROSS													
TARE													
NET-LBS.													
RATIO $\frac{NET}{Avg.}$													
RATIO LIMITS	1.06 .86	1.16 .96	1.06 .86	1.06 .86	1.16 .96	1.06 .86	1.06 .86	1.16 .96	1.06 .86	1.06 .86	1.16 .96	1.06 .86	1.06 .86

TOTAL FLOW (NET) LBS. ÷ TIME SEC. = FLOW RATE LBS./SEC. *

_____ ÷ _____ = _____

TOTAL FLOW (NET) LBS. ÷ 37 = AVG. FLOW (NET) LBS.

_____ ÷ 37 = _____

TOTAL FLOW INLET PRESSURE _____ PSIG TIME _____ SEC.

GROSS _____

TARE _____

NET _____ LBS.

RATE _____ LBS./SEC. *

TEST CONDUCTOR _____

WK INSPECTOR _____

LMSC QA REP _____

ACCEPTABLE _____ UNACCEPTABLE _____

* PLOT ON GRAPH - (PAGE 1C)

Figure 41

INJECTOR LOCATION

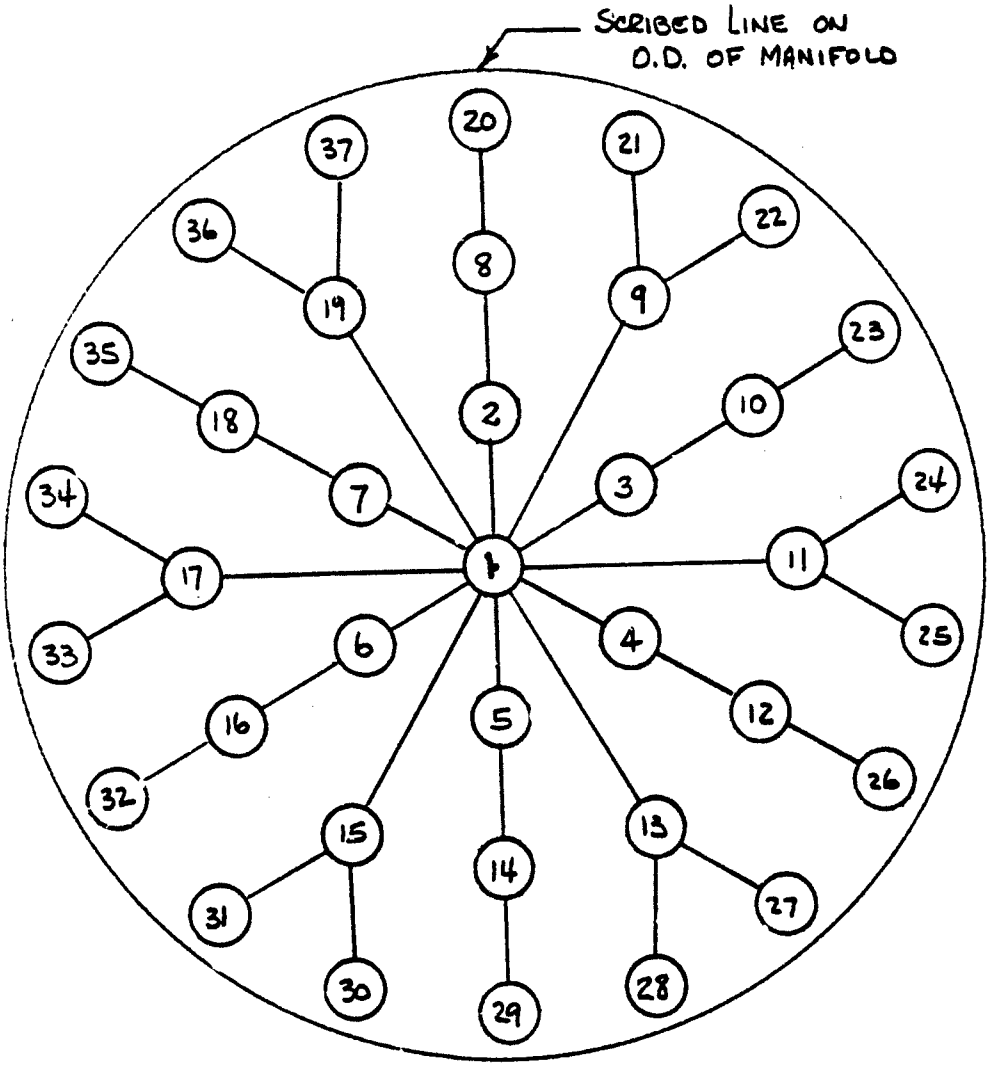

Figure 42

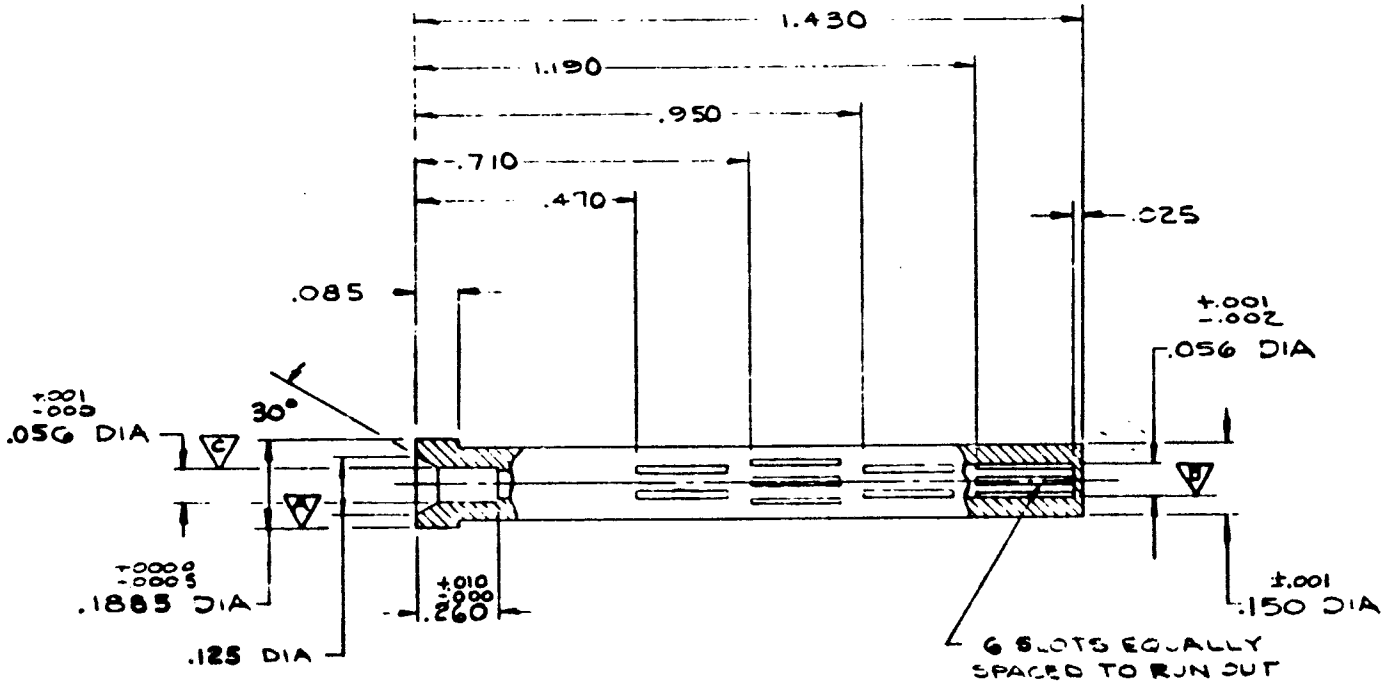
1.430
1.190
.950
.710
.470
.025
.085
+.001
-.002
.056 DIA
+.001
-.005
.056 DIA
30°
+.0005
-.0005
.1885 DIA
.125 DIA
+.010
-.000
.260
±.001
.150 DIA
6 SLOTS EQUALLY
SPACED TO RUN OUT
TUBE DISTRIBUTION 279079

Figure 52

Walter Kidde & Company, Inc.

DISTRIBUTOR WATER FLOW
TEST DATA

Distributor Tube Assembly P/N_____ S/N_____

Project_____
Phase_____
Date_____
Test Conductor_____
WK Inspector_____
Accept_____
Reject_____
Reflow_____

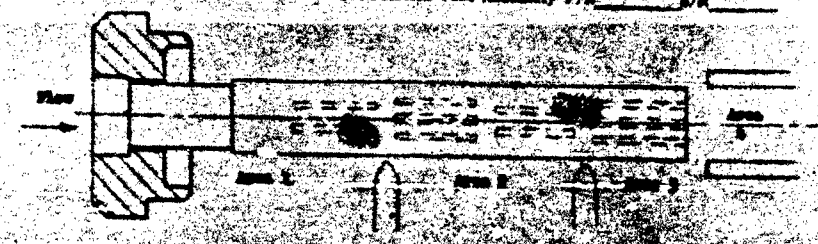

Inlet Press (psig)	Back Press (psig)	Press Drop (psi)	Flow Time (sec)	Body Flow (lb) 1	3	Total	End Flow (lb) 5	6	Total	Total Flow (lbs)	Area 4 Flow (%)	End Flow (%)	Reflow Limits Total Flow (lbs)	Reject Limits Area 4 Flow (%)	End Flow (%)
196	81	35	60										1.075 1.307	84 26	72 86
"	"	"	"										"	"	"
55	45	10	60										1.154 988	81 47	77 52
196	81	35	60										1.075 1.307	84 26	72 86
"	"	"	"										"	"	"
55	45	10	60										1.154 988	81 47	77 52

153974 Sheet 6 Rev C

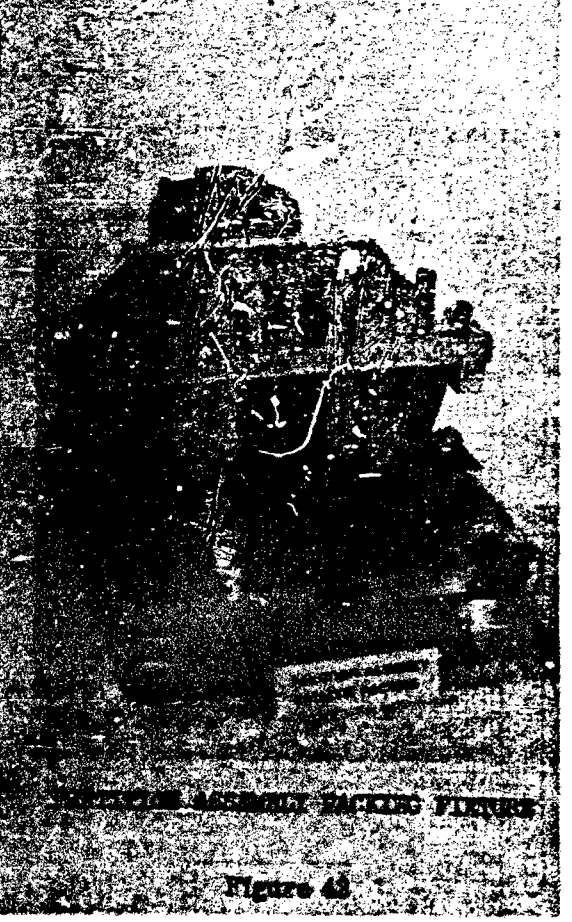

DISTRIBUTOR ASSEMBLY PACKING FIXTURE

Figure 43

Four flow tests are conducted on each distribution tube; two at high flow and two at low flow with respect to the operating range. Inlet pressure is set to obtain the required flow and back pressure is adjusted to simulate the thrust chamber operating pressure. The distribution tube is fixtured to collect flow from each of four areas indicated in Figure 43. The data obtained is analyzed to obtain total flow and percentage of total flow in area 4 and the sume of area 3 plus area 4. These values are compared with limits printed at the right of the flow sheet as the basis for acceptance.

Accepted distribution tube assemblies are selected for partition assembly based upon attainment of a ship-set average area 4 flow at low flow conditions of 49 - 50% for the 37 elements required. The ship-sets selected are then built into partition assemblies shown on drawing 876062 using the Partition Assembly Packing Fixture shown on Figure 43. Partitions are packed in lots of eight units using a prescribed procedure containing incremental additions of catalyst and alternate periods of vibration with the catalyst weighed down as indicated. The completed modules are bagged and sealed following assembly, and retained for installation in the thrust chamber at final assembly.

At final assembly, the shell assembly is installed in the packing fixture as indicated in Figure 44. Subsequently, the partitions are installed, the instrumentation is installed and the catalyst packing is accomplished. Retainer screens, retainer plate support plate and the nozzle assembly are then installed, with the latter being welded to the shell assembly to complete the thrust chamber assembly. Kidde drawing 894849 presents a sectional view of the total assembly.

A nitrogen gas purge is provided through the manifold inlet which flowed out through the orifice tubes preventing catalyst particle migration upstream during the catalyst packing procedure. Partitions are installed in counterbores in the manifold face as indicated in Figure 45. Instrumentation is then installed through the various ports in the shell wall. Two classes of instrumentation may be installed, the flight instrumentation and the ground test instrumentation, some of the latter being redundant with flight measurements. Figure 46 presents a schematic of the flight instrumentation showing location and method of installation. Internal thermocouples TF4 and TF5 are symmetrically located and provide flight measurement redundancy.

The non-flight instrumentation is a carry-over from initial development testing and provides greater depth of measurement. Figure 47 includes a schematic of non-flight instrumentation in the catalyst bed and in the manifold area. The catalyst bed thermocouples provide a thermal profile of the catalyst bed during operation, while the manifold thermocouples monitor manifold metal temperatures during operation, shutdown and restart phases of testing.

Catalyst is installed around partitions and instrumentation in steps following a prescribed procedure which includes vibration step with weight on the catalyst to settle the catalyst in layers until the prescribed depth is attained. Figure 45 shows a shell

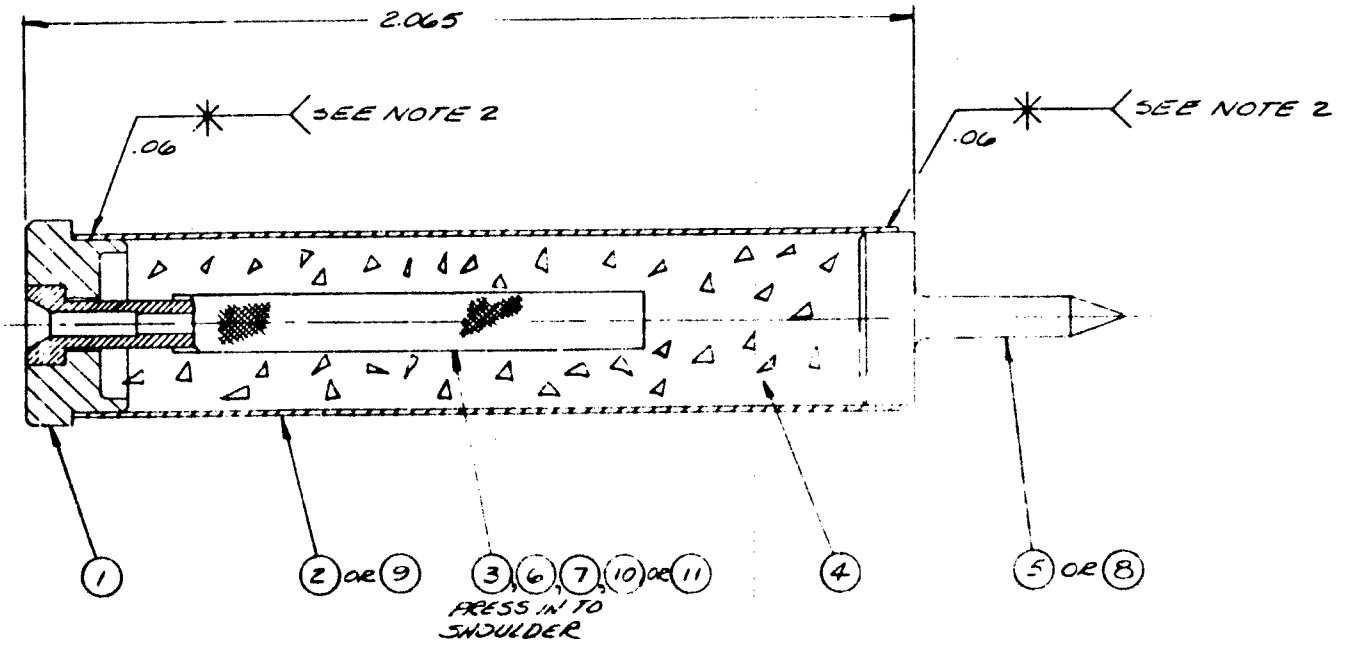

PARTITION ASSEMBLY 876062

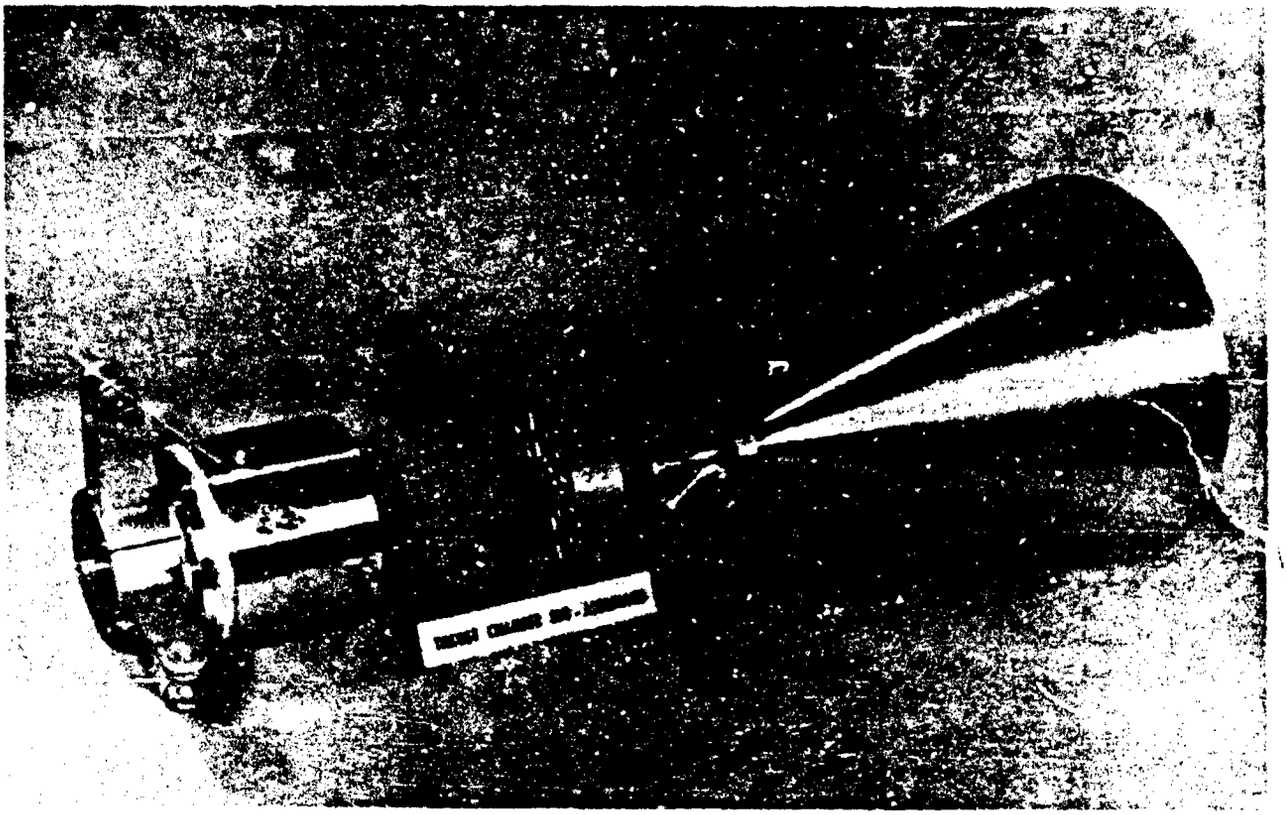

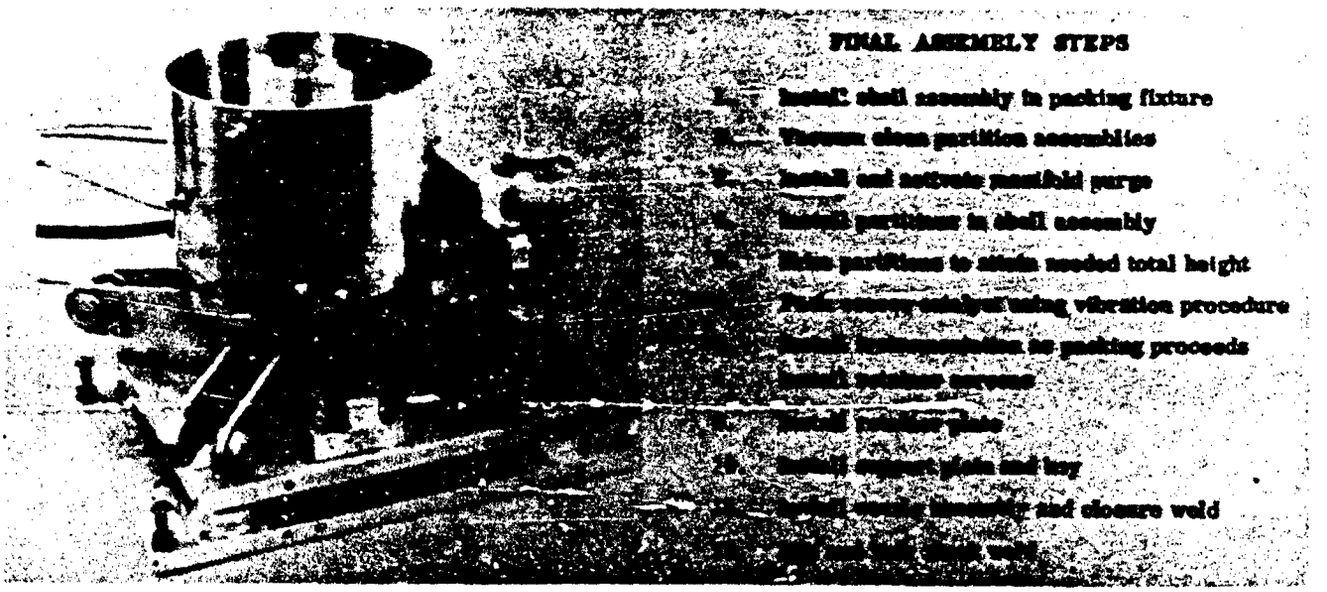
FINAL ASSEMBLY STEPS

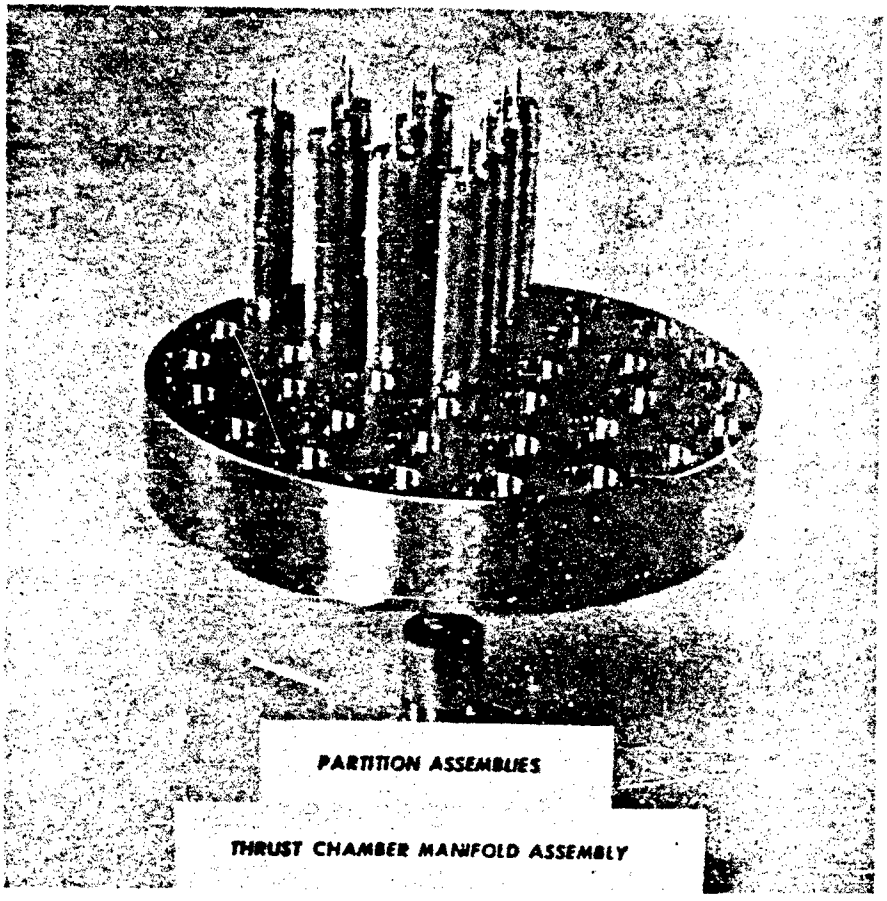
PARTITION ASSEMBLIES
THRUST CHAMBER MANIFOLD ASSEMBLY


THRUST CHAMBER
CATALYST INSTALLED

FLIGHT INSTRUMENTATION
QUALIFICATION TEST HARDWARE

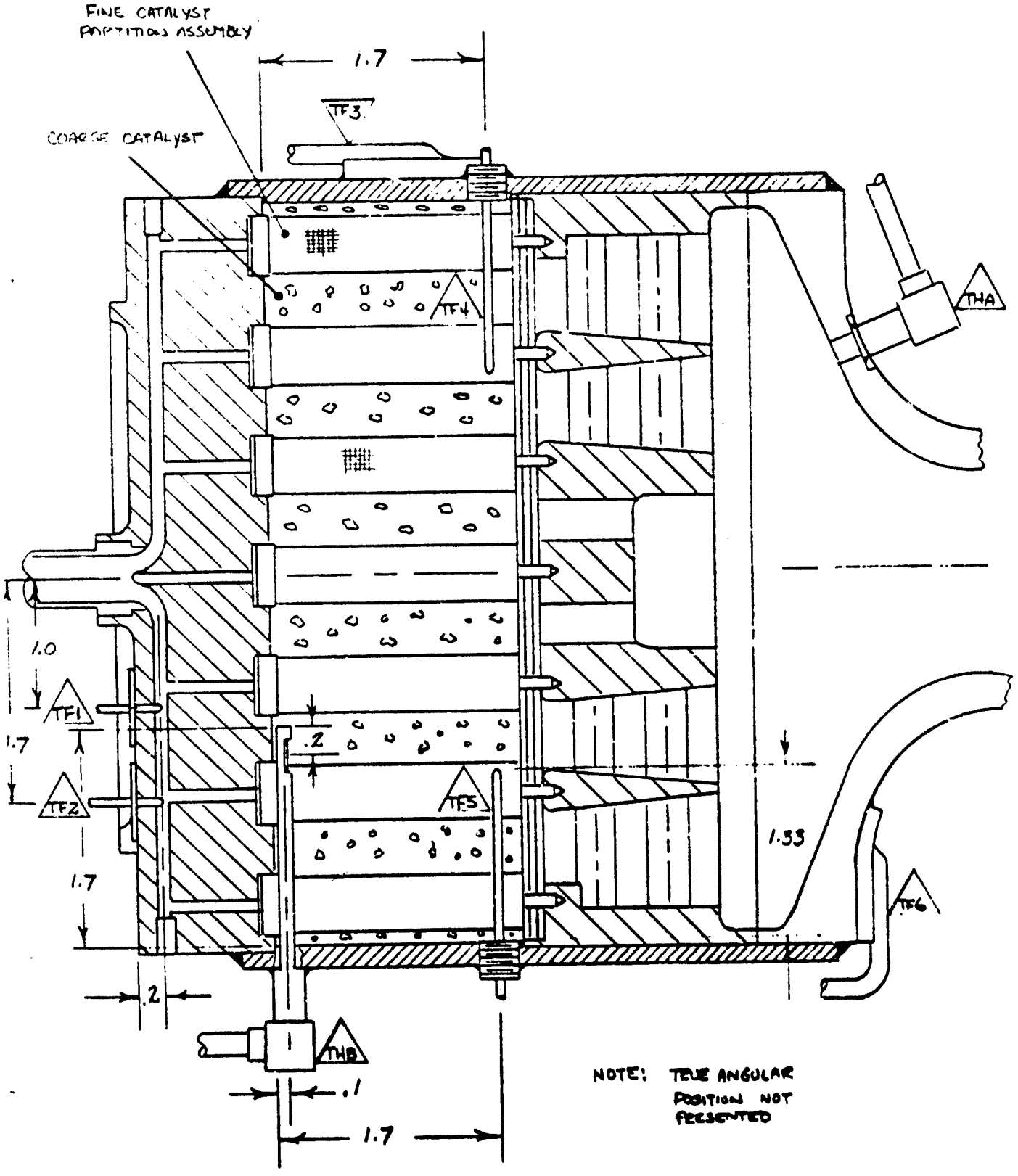

Figure 46

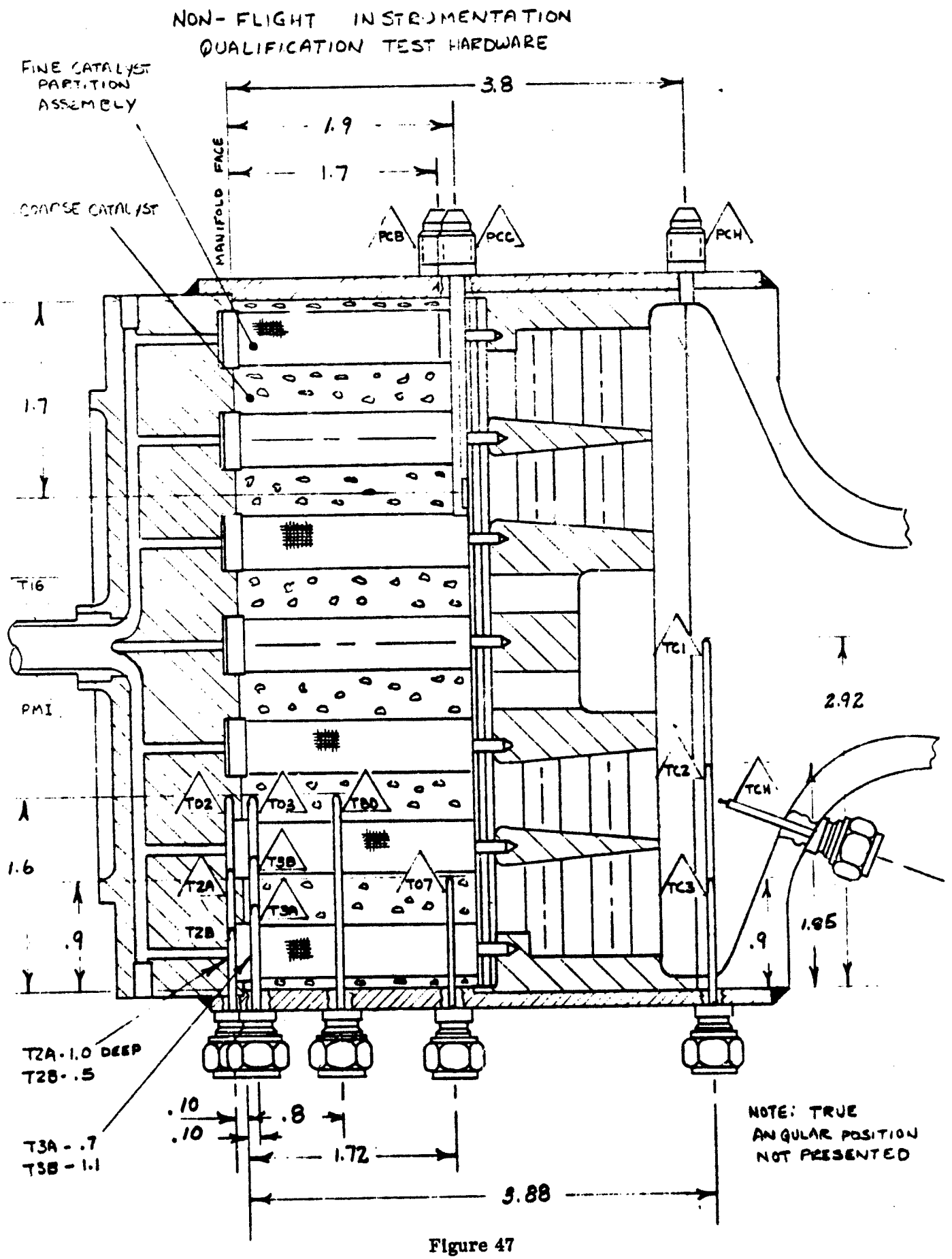
NON-FLIGHT INSTRUMENTATION
QUALIFICATION TEST HARDWARE
FINE CATALYST PARTITION ASSEMBLY
COARSE CATALYST
MANIFOLD FACE
3.8
1.9
1.7
PCB
PCC
PCH
1.7
T16
PMI
1.6
.9
T2A
T2B
T02
T03
T0D
T3B
T3A
T07
TC1
TC2
TCH
TC3
2.92
1.85
.9
T2A - 1.0 DEEP
T2B - .5
T3A - .7
T3B - 1.1
.10
.10
.8
1.72
3.88
NOTE: TRUE ANGULAR POSITION NOT PRESENTED

Figure 47

assembly with catalyst packed and ready for closure. The catalyst retention hardware is then installed and the engine closure is accomplished. Weld pressure and leak check is completed prior to assembly of the thrust chamber to the valve.

APPENDIX II

TEST FACILITY REQUIREMENTS AND PROCEDURES

Each TCA arriving at the test facility is accompanied by a test procedure which defines all the steps in preparation for testing as well as the actual test program and facility procedures to be followed under normal as well as unusual test conditions. The test program can be expected to change from unit to unit but the facility requirements remain basically the same for essentially identical test articles. In view of this, excerpts of the Requirements and Test Procedures sections of the test procedure prepared for the EEUR are included herein to define the test conditions maintained during this program.

4.0 REQUIREMENTS

This section delineates the general requirements that shall be adhered to during engineering evaluation testing.

4.1 Room Ambient Test Conditions

Unless otherwise specified herein, all test firings will be performed at an atmospheric pressure of between 650 and 810 torr, a temperature between +55° F to +95° F and a relative humidity of not more than 90%. Where tests are performed with atmospheric conditions different from the above values, appropriate corrections shall be made for measurements. The above test conditions will not be maintained during extended non-firing periods.

4.2 Environmental Tolerances

Unless otherwise specified the tolerances applied during actual testing shall be within the following limits:

a.	Temperature	±5° F
b.	Barometric Pressure	±5% 900 torr to 1 torr ±10% 1 torr to 10^{-5} torr
c.	Relative Humidity	±5% of RH

4.3 Accuracies

This section details the performance and environmental instrumentation accuracies that shall be maintained during testing.

4.3.1 Performance Accuracy

The instrumentation (end to end) used to measure the following parameters shall have accuracies within the following limits:

a.	Weight	±1%
b.	Voltage	0.25 volts
c.	Amperage	±0.1 amperes
d.	Temperature	±5°F within the range of -35°F to +160°F ±3% of the measured value at temperature greater than +160°F

Performance Accuracy (cont)

e.	Pressure	±1%
f.	Flow Rate	The accuracy of the flow measuring system shall comply with Section 4.3.1.2.
g.	Thrust	The accuracy of the thrust measuring system shall comply with Section 4.3.1.3.
h.	Flight Pressure Transducers	±0.8%
i.	Flight Pressure Transducers Output Measuring System	+.212% -.414%
j.	Flight Pressure Transducers Calibration System	±0.4%
k.	Simulated Thrust Loads	±1%

4.3.1.1 Response

4.3.1.1.1 Thrust Mount Response

1. Thrust mount response shall be determined by measurement of the system resonant frequency and damping. The measurement shall be performed in the test stand, with the engine assembly mounted, and all plumbing connected as for an engine test.

2. The measurement shall be made by suspending a dead weight from the thrust calibration rig, and cutting the suspension cord to apply an instantaneous change in weight to the mount.

3. Thrust mount resonant frequency shall be greater than 20 Hz.

4. Thrust mount damping shall be such that the amplitude of the thrust mount oscillation shall decay to less than 10% of the initial amplitude in 30 cycles.

4.3.1.1.2 Flow Data Response:

Response of turbine flowmeter signal conditioning systems shall be such that data response is greater than the limits shown below.

Time (secs)	Minimum Response % of S.S. Value
1.0	95.0
2.0	98.0
3.0	99.0

4.3.1.2 Flowmeter Calibration Control

Flowmeter calibration shall be performed in accordance with Procedure 152950. Flowmeter calibration data shall be reduced using computer program "WK-0010". The 3 sigma value computed by the program at each flow rate shall be less than the limiting value shown in the Table 4.3.1.2-I.

TABLE 4.3.1.2-I

Flow Rate	3 Sigma Limit
0.3 #/sec	1.10%
0.5	0.88
0.8	0.64
1.1	0.50
1.5	0.44

In addition, the value of "delta mean" computed when a flowmeter is recalibrated shall not exceed 2 sigma at more than one point in the calibration.

4.3.1.3 Thrust Calibration Control

Thrust calibration shall be performed in accordance with Procedure 152949. Variation and hystereses of thrust calibration data shall be evaluated prior to acceptance of the calibration. Variation of thrust calibration data shall be less than the limits shown in Table 4.3.1.3-I, for both increasing and decreasing calibrations.

TABLE 4.3.1.3-I

Thrust Level (lbs)	Variation Limit (%)
50	0.7
100	0.65
150	0.60
200	0.55
250	0.50
300	0.50

Hystereses shall not exceed 0.6% at any level.

4.3.2 Environmental Accuracy

Unless as otherwise specified in Section 4.3.1, the accuracy of each instrument used for test measurements shall be better than the tolerances stipulated for environmental conditions by a factor of three.

4.4 Instrumentation Calibration

Instrumentation shall conform to the calibration requirements of MIL-C-45662. Method of calibration for hot firings shall be done in accordance with procedures WK 152949, WK 152950 and TCC-RMD TER 85E.

4.5.3 Contamination

All fluids entering the TCA in servicing, checkout, operation, and cleaning shall not contain particulate contamination in excess of the limits specified in Table 4.5.3-I.

TABLE 4.5.3-I

Particle Size (Microns)	Number of Particles: Gases per 10 Standard Cubic Feet	Number of Particles: Liquid per 100 Milliliters
26 to 50	280	280
51 to 100	45	45
101 to 150	4	4
Over 150	0	0
Fibers*	1	1

*A fiber is a particle whose length-to-width ratio is 10:1 or greater, whose greatest dimension is in excess of 100 microns and whose width is not in excess of 20 microns.

4.6 Failure Reporting

a) Immediately after a test deviation occurs, a Trouble and Failure Report (TFR) shall be prepared by Walter Kidde & Co., Inc.

4.5 Liquids and Gases

4.5.1 Liquids

4.5.1.1 Propellant shall be hydrazine as specified in MIL-P-26536C except the constituent analysis shall be as follows:

% N_2H_4	98.0 minimum
% H_2O	1.5 maximum

4.5.1.2 Distilled water shall be as specified in WK 214693 except the particle count shall not be greater than that specified in Table 4.5.3-I for liquids.

Samples shall be taken downstream of 20 micron filter in feed system. The sample shall be collected in a 150 ml glass laboratory bottle cleaned to meet the requirements of Kidde Spec. 152786, para. 6.2.

4.5.2 Gases

4.5.2.1 The gases used in servicing, testing and cleaning of the TCA shall be nitrogen as specified in MIL-P-27401 or helium as specified in MIL-P-27407, except the particle count shall not be greater than that specified in Table 4.5.3-I for gases.

4.5.2.2 Samples shall be taken in accordance with Kidde Spec. 530015 by inserting a new 10 micron filter element or a new filter in the gaseous system and bleeding 10 standard cubic feet of gas through it.

5.0 TEST PROCEDURES

The TCA shall be subjected to the following tests in the sequence listed.

	Referenced Paragraph
5.1 Acceptance Test	
5.2 Simulated Mission Test	
5.3 Washout Resistance Evaluation Test	

5.1 Acceptance Test*

5.2 Simulated Mission Test*

5.2.2 Visicorder

Visicorder will be run at a paper speed of 10 inches per second (IPS) continuously for all firing except where on-times are such that one roll of visicorder paper (100 ft) is not enough for the firing at 10 IPS, in which case visicorder paper speed can be reduced to a max paper speed and still accommodate the continuous coverage. Speed change will be accomplished after the start transient.

5.2.3 FM Tape

FM analog tape will be run at a tape speed of 60 IPS continuously for all firings except where reel length is exceeded. In that case the tape reel will be replaced as soon as possible after the original tape is depleted.

5.2.4 Mission Duty Cycle

5.2.4.1 Critical Instrumentation

5.2.4.1.1 Flight Instrumentation

It is desirable that all flight instrumentation data acquisition systems be properly operating during all firings.

---

*Test steps would apply to specific duty cycle.

5.0 TEST PROCEDURES

The TCA shall be subjected to the following tests in the sequence listed:

Reference Paragraph	
5.1	Acceptance Test
5.2	Simulated Mission Test
5.3	Washout Evaluation Test

5.1 Acceptance Test

5.1.1 This test will be conducted in accordance with Kidde Specification 152800 with the following exceptions:

Referenced 152800	Change
5.0	Delete
6.0	Delete
7.0	Add 9.7 of 152800
7.3	Replace with 9.13 of 152800
Table 7.7.1-I	Table 5.1.1-I (This document)
8.1.1	5.1.2 (This document)
9.1 through 9.16	Delete

TABLE 5.1.1-I

PARAMETER LIST

PARAMETER	DESCRIPTION	OPERATING RANGE STEADY STATE	FM TAPE	LINE PRINTER	VISI-CORDER
PFI	Press, Fuel Inlet	105 - 290 psia	X	X	X
PMI	Press, Manifold Inlet	70 - 140 psia	X	X	X
THB	Press, Chamber Bed	60 - 100 psia	X	X	X
PCA	Press, Chamber Bed	60 - 100 psia		X	X
PCB	Press, Chamber Bed	60 - 100 psia		X	X
PCC	Press, Chamber Bed	60 - 100 psia		X	X
PCH	Press, Chamber Gas	40 - 80 psia		X	X
THA	Press, Chamber Gas	40 - 80 psia	X	X	X
DPA	Press, THB - PCB	10 - 20 psi	X	X	X
PFV	Press, Fuel Venturi	105 - 290 psia		X	X
ALT	Press, Altitude	100,000 ft (min)		X	
TFC	Tem. Fuel	CUC		X	

TABLE 5.1.1-I (Cont)

PARAMETER	DESCRIPTION	OPERATING RANGE STEADY STATE	FM TAPE	LINE PRINTER	VISI-CORDER
F	Thrust, Measured	150 - 240 lb_f	X	X	X
F'	Thrust at 450 K Ft	150 - 240 lb_f		X	
WFU	Flow Rate Up	1.1 - .64 lbs N_2H_4/sec	X	X	X
WFD	Flow Rate Down	1.1 - .64 lbs N_2H_4/sec	X	X	
WFC	$\frac{WFU + WFD}{2}$	1.1 - .64 lbs N_2H_4/sec		X	
C*	$\frac{THA\ (A_T)\ (32.174)}{WFC}$	4400 Ft/sec		X	
C_F	$\frac{F'}{THA\ (A_T)}$	1.74		X	
I_{SP}	$\frac{F'}{WFC}$	235 sec.		X	
RAT	$\frac{WFU}{WFD}$	1.00		X	
IV	Current, Total	5.3 amp at 28 vdc		X	X
IV1	Current, Solenoid 1	1.3 amp at 28 vdc			X
IV2	Current, Solenoid 2	1.3 amp at 20 vdc			X

TABLE 3.1.1-I (Cont)

PARAMETER LIST

PARAMETER	DESCRIPTION	OPERATING RANGE STEADY STATE	FM TAPE	LINE PRINTER	VISI-CORDER
T 02	Temp, 02	CA		X	
T 2A	Temp, 2A	CA		X	
T 2B	Temp, 2B	CA		X	
T 03	Temp, 03	CA		X	
T 3A	Temp, 3A	CA		X	
T3B	Temp, 3B	CA		X	
TBD	Temp, Bed	CA	X	X	
T 07	Temp, 07	CA		X	
T 10	Temp, Feed Tube	CuC		X	
TE1	Temp, Flight 1	CA		X	
TE2	Temp, Flight 2	CA		X	

TABLE 5.1.1-I (Cont)

PARAMETER	DESCRIPTION	OPERATING RANGE STEADY STATE	FM TAPE	LINE PRINTER	VIS-CORDER
TF3	Temp. Flight 3	CA		X	
TF4	Temp. Flight 4	CA		X	
TF5	Temp. Flight 5	CA		X	
TF6	Temp. Flight 6	CA		X	
TCH	Temp. Chamber Gas	CA	X	X	X
TV1	Temp. Valve 1	CuC		X	
TV2	Temp. Valve 2	CuC		X	
TE1	Temp. Envir. 1	CuC		X	

TABLE 5.1.1-I (Cont)

PARAMETER	DESCRIPTION	OPERATING RANGE STEADY STATE	FM TAPE	LINE PRINTER	VISICORDER
IV3	Current, Solenoid 3	1.3 amp at 28 vdc			X
IV4	Current, Solenoid 4	1.3 amp at 28 vdc			X
IP1	Position Sw. 1 ON			X*	X*
IP2	Position Sw. 1 OFF			X**	X**
IP3	Position Sw. 2 ON			X*	X*
IP4	Position Sw. 2 OFF			X**	X**
IP5	Position Sw. 3 ON			X*	X*
IP6	Position SW. 3 OFF			X**	X**
IP7	Position Sw. 4 ON			X*	X*
IP8	Position Sw. 4 OFF			X**	X**

*Record on 1 channel IP1, IP3, IP5, IP7 (TP2)

**Record on 1 channel IP2, IP4, IP6, IP8 (TP1)

TABLE 5.1.1-I (Cont)

PARAMETER	DESCRIPTION	OPERATING RANGE STEADY STATE	FM TAPE	LINE PRINTER	V... CO...
VM1	Valve Voltage Monitor 1	2.9 vdc		X***	X***
VM2	Valve Voltage Monitor 2	2.9 vdc		X***	X***
VM3	Valve Voltage Monitor 3	2.9 vdc		X***	X***
VM4	Valve Voltage Monitor 4	2.9 vdc		X***	X***
A1	Accelerometer 1	± 3 g's	X		
A2	Accelerometer 2	± 30 g's	X		
EV	Quad Valve Voltage	28 vdc		X	
DP 1	Press THB Press PCB	0-20 psi		X	
DP 2	Press PCB Press PCC	0-30 psi		X	
DP 3	Press THB Press THA	0-80 psi		X	
DP 4	Press PMI Press THB	0-50 psi		X	
DP 5	Press PCC Press THA	0-50 psi		X	
DP 6	Press PCC Press PCH	0-10 psi		X	

***Record on 1 channel VM 1 thru VM 4 (VVM)

5.1.2 Critical Instrumentation

5.1.2.1 Flight Instrumentation*

It is desirable that all flight instrumentation data acquisition systems be properly operating during all firings.

If there is a malfunction in the recording of data and the fault is due to the data acquisition system (non-TCA) testing shall be delayed and the malfunction shall be repaired. When the problem has been resolved and corrected, the "on-site WK engineer" in concurrence with the quality control representative shall decide whether or not the (those) firing(s) that were conducted with the malfunction shall be tested again.

If there is a TCA flight instrumentation malfunction, testing shall continue but a Trouble and Failure Report (TFR) shall be made out for the record.

5.1.2.2 Non-Flight Instrumentation

It is desirable that all non-flight instrumentation data acquisition systems be properly operating during all firings.

If there is a malfunction in the recording of data and the fault is due to the acquisition system (non-TCA) or to the non-flight instrumentation, testing

*Flight instrumentation is as indicated on WK 894571

shall be delayed and the problem shall be investigated. When the reason for the malfunction has been determined, Kidde Engineering in concurrence with the quality control representative shall decide whether the malfunction shall be repaired and whether the (those) firing(s) that were conducted with the malfunction shall be tested again.

5.2 Simulated Mission Test

5.2.1 This test shall be performed in accordance with the attached latest revision of Kidde Specification 152800 with the following exceptions:

Specification 152800:	Replace with:	
Section	Section	
4.3.1.1	Delete except for thrust calibration	
4.7, 4.8, 5.0, 6.0, 7.2, 7.3, 7.4, 7.5, 7.6	Delete.	
Table 7.7.1-I*	5.1.1-I	(This document)
7.7.2.1	5.2.2	(This document)
7.7.2.2	5.2.3	(This document)
8.0	5.2.4	(This document)
9.1 - 9.16	Delete.	

The above is based on the TCA's having just previously performed the Acceptance Test per paragraph 5.1

*Also where referenced.

The TCA's shall be visually inspected to assure that there is no damage to them or related test stand piping or instrumentation.

5.2.2 Visicorder

Visicorder will be run at a paper speed of 10 inches per second (IPS) continuously for all firing except where on-times are such that one roll of visicorder paper (100 ft) is not enough for the firing at 10 IPS, in which case visicorder paper speed can be reduced to a max paper speed and still accommodate the continuous coverage. Speed change will be accomplished after the start transient.

5.2.3 FM Tape

FM analog tape will be run at a tape speed of 60 IPS continuously for all firings except where reel length is exceeded. In that case the tape reel will be replaced as soon as possible after the original tape is depleted.

5.2.4 Mission Duty Cycle

5.2.4.1 Critical Instrumentation

5.2.4.1.1 Flight Instrumentation*

It is desirable that all flight instrumentation data acquisition systems be properly operating during all firings.

---

*Flight instrumentation is as indicated on WK 895471

If there is a malfunction in the recording of data and the fault is due to the data acquisition system (non-TCA) testing shall be delayed and the malfunction shall be repaired. When the problem has been resolved and corrected, the "on-site WK engineer" in concurrence with the quality control representative shall decide whether or not the (those) firing(s) that was (were) conducted with the malfunction shall be tested again.

If there is a TCA flight instrumentation malfunction, testing shall continue but a Trouble and Failure Report (TFR) shall be made out for the record.

5.2.4.1.2 Non-Flight Instrumentation

It is desirable that all non-flight instrumentation data acquisition systems be properly operating during all firings.

If there is a malfunction in the recording of data and the fault is due to the acquisition system (non-TCA) or to the non-flight instrumentation, testing shall be delayed and the problem shall be investigated. When the reason for the malfunction has been determined, Kidde Engineering in concurrence with the quality control representative shall decide whether the malfunction shall be repaired and whether the (those) firing(s) that was (were) conducted with the malfunction shall be tested again.

5.2.4.2 Kill Procedure

5.2.4.2.1 The no-go condition shall prevail if the following conditions exist: TF1, TF2, TO2, T2A or T2B is greater than 650°F or TV1 greater

than 225° F. The shut-down condition shall prevail if TF1, TF2, TO2, T2A or T2B is greater than 850° F or if TV1 is greater than 225° F.

5.2.4.2.2 The following steps shall be taken when a no-go ("Kill") condition is in evidence:

- In the event of a no-go "kill", immediately start the FM tape and visicorder recorders, record data for 30 seconds or until tape and visicorder paper are depleted. In the event of a shutdown "kill", continue running the FM tape until it is depleted.

- In the event of either a no-go or a shutdown "kill", immediately (within 100 milliseconds after "kill") start line printer recorder and record at a maximum data acquisition rate for the first 30-seconds, then reduce the rate to one print out every 15-seconds. Continue recording at this rate until the "kill" condition is eliminated.

  If TV2 appears to be approaching 250° F during shutdown, turn on bell purge when it reaches 240° F and continue bell purging until there is evidence that it will not exceed 250° F.

5.2.4.2.3 In the event that TF1, TF2, TO2, T2A or T2B provide the "kill" adhere to the following procedure:

- Cool TCA with an external GN_2 purge (bell purge) for 30 minutes (minimum). If TO7 has not cooled to 900° F at the completion of the 30 minute purge, continue external GN_2 purge until TO7 has decreased to 900° F.

- Then helium purge the TCA until TO7 decreases to 500° F. Continue the purge and begin cooling the TCA exterior with a GN_2 spray. If at any time TO7 exceeds TF3 by 200° or more, terminate the GN_2 spray. Continue cooling until TO7 decreases to the desired temperature prior to continuing the test effort.

5.2.4.2.4 Emergency Shutdowns

- If TV1 is equal to or greater than 225° F, shutdown TCA and immediately purge with 40 psig of helium internally and GN_2 bell purge externally. Continue purging until TV1 has decreased below 225° F.

- If TF1, TF2, TO2, T2A or T2B equals or exceeds 700° F during the first five minutes of shutdown, purge immediately (internal and external) until they have decreased below 500° F.

5.2.4.3 Ambient Cool Procedure

The ambient cool procedure will be conducted in accordance with paragraph 5.2.4.2.3 with line printer monitoring temperatures during cool downs. Except where soak data is specifically required, line printer coverage of

the cool downs is not necessary as long as TF1, TO3, TO7, and TF3 are monitored on DVMs.

5.2.4.4 Daily Shutdown Procedure

After completion of daily testing, the TCA will be secured in the following manner:

- Steam boiler and ejector are to maintain engine at altitude condition until temperature (TO7) drops to 900°F.

- Turn gaseous nitrogen, for external valve cooling purge, on at two minutes into cooldown.

- Turn on ambient helium purge when temperature (TO7) drops to 900°F with a minimum of 30 minutes into cooldown.

- When the preceding steps are complete:

  - Turn on mechanical vacuum pump. Maintain 80,000 feet minimum simulated altitude during shutdown period.

- Close vacuum isolation valve.

- Take steam boiler off line.

- Continue ambient helium purge and GN_2 bell cooling purge until engine reaches desired temperature, approximately 500° F.

- Turn off mechanical vacuum pump.

- Discontinue all cooling except blanket purge (para. 5.2.4.5).

- Open vacuum isolation bypass valve.

- Continuously record TF4, and PFI until the next test day.

5.2.4.5 TCA Helium Gas Blanket

A helium gas blanket system will be incorporated in the "HBP" port. (Ref. Drawing SKR 144309). It will be operated in the following manner.

When the TCA has completed the first two pulses (Reference Table 5.2.4.7-I), the helium blanket system will be energized (yielding a flow rate = 10 ± 1 scfh). This system will remain energized CONTINUOUSLY until the TCA is removed from the test cell. Just prior to inserting nozzle throat plug de-energize helium blanket system. Next open any one of the 1/8 inch ports on the thrust chamber and allow the catalyst bed to oxidize through this port for one hour.

5.2.4.6 Firing Requirements

5.2.4.6.1 The TCA shall be fired with voltage (EV at the valve connector) of 28 ±2 vdc.

5.2.4.6.2 Maintain 100,000 feet minimum simulated altitude during all firings.

5.2.4.6.3 Fire the TCA's in accordance with Table 5.2.4.7-I and the following minimum countdown indicated in Section 5.2.4.6.4.

5.2.4.6.4 Minimum Test Countdown Requirements:

(a) Vacuum isolation valves and bypass closed.

(b) Computer down to bring steam boiler on line

(c) Bring boiler on line and verify.

(d) OPEN Chapman valve and verify.

(e) Vacuum load propellant per para. 7.10 of specification 152800 if not already done.

(f) Computer on line - Take zero and R-cal and verify.

(g) Computer on line (Load operating program and profile for monitoring temperature with tape.

(h) Check engine temperature and purge as required per cool down procedure. (Computor in holding mode). Manifold heaters may be used to obtain required pre-run temperatures.

(i) Set tank pressure.

(j) Bleed fuel and check fuel temperature.

(k) Arm the Engine.

(l) Stand by for FIRE.

(m) Computer FIRE. (Transfer from holding to run mode). Bleed fuel for temperature check if required during countdown (9 seconds to 7 seconds). Test Conductor acknowledge -- (Start and Shutdown).

(n) At end of pulse cycle start waiting time for next Pulse or start cool-down Procedure.

5.2.4.7 Firing Tests

The TCA shall be fired to the duty cycle shown in Table 5.2.4.7-I. Total propellant loaded shall be 3800 lbs (454 gallons) and the initial ullage should be 48 gallons. After the 35K burn and 18 pairs of firings, the propellant

APPENDIX III

EEU BUILD DATA AND PRIOR PERFORMANCE

Manifold flow data for the EEU is presented on Figure 48, the Manifold Flow Calibration Sheet. This sheet gives individual injection point flow data as well as a total flow measured independently at each of two flow levels. All four total flows, those measured directly and the sum of the individual flows at each flow level must fall within prescribed limits for the manifold to pass acceptance test. This requirement is in addition to individual injection point flow requirements on Figure 48. Relative injection point location is presented on Figure 42.

Individual distribution tube flow data is presented on Table XIV, listed in element serial number order. Included are average area 4 flow, average end flow (area 3 plus area 4) and average body flow (area 1 plus area 2). The number in each location is the average of two flow measurements taken at that condition. The ship-set average area 4 flow at low flow for the EEU was 49.9%.

The EEU was subjected to a standard acceptance test including eight firings, two from ambient temperature; five were at 290 psia propellant pressure (250 lbs thrust) and three were at 105 psia propellant pressure (150 lbs thrust). Total accumulated impulse was 42,595 lb-sec in 227.6 seconds of accumulated run time.

The mission duty cycle conducted included an initial pair firing of 30,000 and 4000 lb-sec with 45 minutes off-time between firings. This pair was followed by 45 pair firings of 10,000 and 1000 lb-sec with the first firing of each pair accomplished with ambient temperature of 70 -90°F hardware and a 45-minute off-time between pair firings. Cooldown time between pair firings was approximately two hours. The final firing was of 1200 seconds duration from an ambient temperature start.

A listing of the mission accomplished is presented on Table XV. The initial propellant pressure was 278 psia and was allowed to decay throughout the mission, ending up at 102 psia at the end of the 1200 second firing. Propellant temperature through the mission was 70 ±5°F. A total of 93 firings were accomplished, including 47 ambient temperature starts. Total impulse accumulated was 696,686 lb-sec. in an accumulated run time of 3939 seconds.

The final 1200 second firing accumulated 185,400 lb-sec total impulse while using 778 lbs of propellant. This resulted in a total life accumulation of 4166 seconds of operation while accumulating 738,281 lb-sec total impulse and using 3178 lbs of propellant. Based upon these figures, the integrated specific impulse over the lifetime was 232 seconds.

MANIFOLD FLOW CALIBRATION SHEET
FIGURE

P/N 894998 S/N 015 DATE 9/9/70

SINGLE POINT FLOW-HIGH
INLET PRESSURE 42 PSIG TIME 60 SEC.

INJECTOR	1	2	3	4	5	6	7	8	9	10	11	12	13	14	15	16	17	18	19	20	21	22	23	24
GROSS	1.786	1.734	1.778	1.732	1.732	1.744	1.700	1.782	1.724	1.748	1.750	1.718	1.780	1.810	1.772	1.768	1.762	1.762	1.780	1.730	1.686	1.666	1.712	1.702
TARE	.196	.194	.194	.202	.204	.208	.206	.198	.204	.200	.204	.200	.200	.200	.200	.194	.196	.200	.208	.203	.194	.202	.194	.196
NET-LBS.	1.590	1.540	1.584	1.530	1.528	1.536	1.494	1.584	1.520	1.548	1.546	1.518	1.580	1.610	1.572	1.574	1.566	1.562	1.572	1.527	1.492	1.464	1.518	1.506
RATIO NET/Avg	.98	1.01	1.04	1.00	1.00	1.01	.98	1.04	1.00	1.01	1.01	1.00	1.04	1.06	1.03	1.04	1.03	1.02	1.00	1.00	.98	.96	1.01	.99
RATIO LIMITS	85 / 65	109 / 89	109 / 89	109 / 89	109 / 89	109 / 89	109 / 89	111 / 91	112 / 92	111 / 91	112 / 92	111 / 91	112 / 92	111 / 91	112 / 92	111 / 91	112 / 92	111 / 91	112 / 92	113 / 93	106 / 86	106 / 86	113 / 93	106 / 86

INJECTOR	25	26	27	28	29	30	31	32	33	34	35	36	37
GROSS	1.710	1.744	1.706	1.645	1.778	1.686	1.670	1.780	1.708	1.676	1.784	1.716	1.718
TARE	.196	.204	.196	.204	.208	.198	.194	.200	.200	.200	.196	.206	.200
NET-LBS.	1.514	1.540	1.510	1.450	1.570	1.488	1.476	1.580	1.508	1.476	1.588	1.510	1.518
RATIO NET/Avg	.99	1.01	.99	.95	1.03	.98	.97	1.04	.99	.97	1.04	.99	1.00
RATIO LIMITS	106 / 86	113 / 93	106 / 86	106 / 86	113 / 93	106 / 86	106 / 86	113 / 93	106 / 86	106 / 86	113 / 93	106 / 86	106 / 86

TOTAL FLOW (NET) LBS.	÷ TIME SEC.	= FLOW RATE LBS./SEC.	
56.389	÷ 60	= .940	*

TOTAL FLOW (NET) LBS.	÷37 = AVG. FLOW (NET) LBS.
56.389	÷37 = 1.524

TOTAL FLOW INLET PRESSURE 42 PSIG TIME 60 SEC.
GROSS 63.042
TARE 6.884
NET 56.158 LBS.
RATE .936 LBS/SEC.*

SINGLE POINT FLOW-LOW
INLET PRESSURE 14 PSIG TIME 90 SEC.

INJECTOR	1	2	3	4	5	6	7	8	9	10	11	12	13	14	15	16	17	18	19	20	21	22	23	24
GROSS	1.214	1.500	1.550	1.612	1.510	1.510	1.464	1.518	1.492	1.510	1.526	1.504	1.560	1.586	1.548	1.560	1.522	1.512	1.490	1.500	1.442	1.426	1.500	1.470
TARE	.196	.194	.194	.202	.204	.208	.206	.198	.204	.200	.204	.200	.200	.200	.200	.194	.196	.200	.208	.203	.194	.202	.194	.196
NET-LBS.	1.018	1.306	1.356	1.410	1.306	1.302	1.278	1.320	1.288	1.310	1.322	1.304	1.360	1.386	1.348	1.366	1.326	1.312	1.282	1.297	1.248	1.224	1.306	1.274
RATIO NET/Avg	.78	1.00	1.04	1.01	1.00	1.00	.98	1.01	.99	1.01	1.02	1.00	1.05	1.07	1.04	1.05	1.02	1.01	.99	1.00	.96	.94	1.00	.98
RATIO LIMITS	85 / 65	108 / 88	108 / 88	108 / 88	108 / 88	108 / 88	108 / 88	113 / 93	116 / 96	113 / 93	116 / 96	113 / 93	116 / 96	113 / 93	116 / 96	113 / 93	116 / 96	113 / 93	116 / 96	116 / 96	106 / 86	106 / 86	116 / 96	106 / 86

INJECTOR	25	26	27	28	29	30	31	32	33	34	35	36	37
GROSS	1.442	1.536	1.500	1.472	1.582	1.500	1.471	1.580	1.504	1.482	1.534	1.458	1.458
TARE	.196	.204	.196	.204	.208	.198	.194	.200	.200	.200	.196	.206	.200
NET-LBS.	1.246	1.332	1.304	1.268	1.374	1.302	1.277	1.380	1.304	1.282	1.338	1.252	1.258
RATIO NET/Avg	1.00	1.02	1.00	.97	1.06	1.00	.98	1.06	1.01	.99	1.03	.96	.97
RATIO LIMITS	106 / 86	116 / 96	106 / 86	106 / 86	116 / 96	106 / 86	106 / 86	116 / 96	106 / 86	106 / 86	116 / 96	106 / 86	106 / 86

TOTAL FLOW (NET) LBS.	÷ TIME SEC.	= FLOW RATE LBS./SEC.	
48.126	÷ 90	= .535	*

TOTAL FLOW (NET) LBS.	÷37 = AVG. FLOW (NET) LBS.
48.126	÷37 = 1.30

TOTAL FLOW INLET PRESSURE 14 PSIG TIME 90 SEC.
GROSS 54.626
TARE 6.884
NET 47.742 LBS.
RATE .530 LBS./SEC.*

ORIGINAL SIGNED BY
TEST CONDUCTOR M. ALTIS
WK INSPECTOR J. SOLDA
LMSC QA REP W. DOLL
ACCEPTABLE ✓ UNACCEPTABLE

* PLOT ON GRAPH-(PAGE)

Figure 48

152770 REV D
PAGE

WALTER KIDDE & CO. BELLEVILLE, N.J.

TABLE XIV

DISTRIBUTION TUBE FLOW ANALYSIS ENGINEERING EVALUATION UNIT
PERCENT OF TOTAL FLOW

S/N	Average Area 4 Flow		Average End Flow		Average Body Flow		S/N	Average Area 4 Flow		Average End Flow		Average Body Flow	
	High Flow	Low Flow	High Flow	Low Flow	High Flow	Low Flow		High Flow	Low Flow	High Flow	Low Flow	High Flow	Low Flow
1147	43.7	51.1	61.0	64.0	39.0	36.0	1171	43.4	57.0	60.7	65.8	39.3	34.2
1148	48.9	53.5	58.5	63.4	41.5	36.6	1172	42.9	46.6	59.3	61.6	40.7	38.4
1149	45.8	49.1	58.8	64.2	41.2	35.8	1173	40.0	45.2	60.2	66.8	36.7	33.2
1150	45.4	45.6	58.0	64.7	43.2	35.3	1175	40.1	47.3	59.3	65.0	40.7	35.0
1151	43.2	46.8	59.5	66.5	40.6	33.4	1176	41.5	53.0	57.5	66.2	42.5	33.8
1152	46.8	50.5	58.4	62.3	41.7	37.7	1186	45.0	50.5	61.0	62.5	39.0	37.5
1153	44.9	48.7	58.5	62.8	41.4	37.4	1187	38.5	48.0	61.0	64.0	39.0	36.0
1154	44.8	48.5	58.6	62.6	41.4	37.4	1188	40.5	57.0	64.0	67.0	36.0	33.0
1155	43.3	49.9	60.3	65.3	39.7	34.7	1189	43.0	45.0	62.0	65.5	38.0	34.5
1156	40.4	49.4	59.0	64.0	41.0	36.0	1190	42.5	54.5	56.5	62.0	43.5	38.0
1157	42.7	48.0	56.4	64.0	43.6	36.0	1192	42.0	52.5	60.0	63.0	40.0	37.0
1159	46.6	50.6	59.2	62.3	40.7	37.7	1193	49.5	52.5	60.5	65.5	39.5	34.5
1160	45.6	53.2	60.0	66.1	40.0	33.9	1194	44.0	50.0	58.0	62.0	42.0	38.0
1161	40.5	45.3	58.0	61.9	42.0	38.1	1196	45.5	51.5	58.5	62.0	41.5	38.0
1162	44.3	53.4	60.0	64.8	40.0	35.2	1198	48.0	54.5	61.0	67.0	39.0	33.0
1163	44.8	47.7	58.6	65.3	41.2	34.7	1199	44.5	47.0	59.0	64.0	41.0	36.0
1165	42.4	51.9	61.0	66.6	38.9	33.4	1200	45.5	49.5	59.0	65.0	41.0	35.0
1166	41.3	43.3	58.0	62.2	42.0	37.8	1201	43.0	51.5	59.5	64.0	40.5	36.0
1167	40.3	45.0	59.0	62.8	41.0	37.2	1202	45.0	49.5	59.0	68.0	41.0	38.0
1170	49.8	51.6	57.5	63.8	42.6	36.2	1203	45.5	51.0	59.5	66.0	40.5	34.0

TABLE XV

PRIOR MISSION DUTY CYCLE

ENGINEERING EVALUATION UNIT

Pulse No.	Propellant Pressure (psia)	On-Time (Seconds)	Off-Time (Minutes)	Pulse No.	Propellant Pressure (psia)	On-Time (Seconds)	Off-Time (Minutes)
1	278 ±4	123.5 ±.1	45 ±5	24	213 ±4	6.1 ±.1	-
2	268 ±4	17.3 ±.1	-	25	209 ±4	45.6 ±.1	45 ±5
3	265 ±4	40.3 ±.1	45 ±5	26	209 ±4	6.2 ±.1	-
4	265 ±4	5.5 ±.1	-	27	205 ±4	46.0 ±.1	45 ±5
5	259 ±4	40.8 ±.1	45 ±5	28	205 ±4	6.3 ±.1	-
6	259 ±4	5.6 ±.1	-	29	202 ±4	46.3 ±.1	45 ±5
7	253 ±4	41.3 ±.1	45 ±5	30	202 ±4	6.3 ±.1	-
8	253 ±5	5.6 ±.1	-	31	198 ±3	46.8 ±.1	45 ±5
9	247 ±4	41.8 ±.1	45 ±5	32	198 ±3	6.4 ±.1	-
10	247 ±4	5.7 ±.1	-	33	195 ±3	47.4 ±.1	45 ±5
11	242 ±4	42.3 ±.1	45 ±5	34	195 ±3	6.4 ±.1	-
12	242 ±4	5.7 ±.1	-	35	192 ±3	47.6 ±.1	45 ±5
13	237 ±4	42.8 ±.1	45 ±5	36	192 ±3	6.5 ±.1	-
14	237 ±4	5.8 ±.1	-	37	189 ±3	48.0 ±.1	45 ±5
15	231 ±4	43.3 ±.1	45 ±5	38	189 ±3	6.5 ±.1	-
16	231 ±4	5.9 ±.1	-	39	185 ±3	48.5 ±.1	45 ±5
17	226 ±4	43.8 ±.1	45 ±5	40	185 ±3	6.6 ±.1	-
18	226 ±4	6.0 ±.1	-	41	182 ±3	48.9 ±.1	45 ±5
19	222 ±4	44.2 ±.1	45 ±5	42	182 ±3	6.7 ±.1	-
20	222 ±4	6.0 ±.1	-	43	179 ±3	49.3 ±.1	45 ±5
21	217 ±4	44.7 ±.1	45 ±5	44	179 ±3	6.7 ±.1	-
22	217 ±4	6.1 ±.1	-	45	176 ±3	49.8 ±.1	45 ±5
23	213 ±4	45.2 ±.1	45 ±5	46	176 ±3	6.8 ±.1	-

TABLE XV (Cont.)

PRIOR MISSION DUTY CYCLE

ENGINEERING EVALUATION UNIT

Pulse No.	Propellant Pressure (psia)	On-Time (Seconds)	Off-Time (Minutes)	Pulse No.	Propellant Pressure (psia)	On-Time (Seconds)	Off-Time (Minutes)
47	173 ±3	50.3 ±.1	45 ±5	71	144 ±3	55.2 ±.1	45 ±5
48	173 ±3	6.8 ±.1	-	72	144 ±3	7.5 ±.1	-
49	170 ±3	50.7 ±.1	45 ±5	73	142 ±3	55.4 ±.1	45 ±5
50	170 ±3	6.9 ±.1	-	74	142 ±3	7.7 ±.1	-
51	168 ±3	50.9 ±.1	45 ±5	75	140 ±3	56.1 ±.1	45 ±5
52	168 ±3	6.9 ±.1	-	76	140 ±3	7.8 ±.1	-
53	166 ±3	51.2 ±.1	45 ±5	77	138 ±3	56.8 ±.1	45 ±5
54	166 ±3	7.0 ±.1	-	78	138 ±3	7.9 ±.1	-
55	163 ±3	51.8 ±.1	45 ±5	79	137 ±3	57.2 ±.1	45 ±5
56	163 ±3	7.0 ±.1	-	80	137 ±3	8.0 ±.1	-
57	160 ±3	52.3 ±.1	45 ±5	81	135 ±3	58.0 ±.1	45 ±5
58	160 ±3	7.1 ±.1	-	82	135 ±3	8.1 ±.1	-
59	158 ±3	52.6 ±.1	45 ±5	83	133 ±3	58.9 ±.1	45 ±5
60	158 ±3	7.2 ±.1	-	84	133 ±3	8.2 ±.1	-
61	155 ±3	53.1 ±.1	45 ±5	85	131 ±3	59.6 ±.1	45 ±5
62	155 ±3	7.2 ±.1	-	86	131 ±3	8.3 ±.1	-
63	153 ±3	53.5 ±.1	45 ±5	87	130 ±3	60.0 ±.1	45 ±5
64	153 ±3	7.3 ±.1	-	88	130 ±3	8.4 ±.1	-
65	151 ±3	53.9 ±.1	45 ±5	89	128 ±3	61.0 ±.1	45 ±5
66	151 ±3	7.3 ±.1	-	90	128 ±3	8.5 ±.1	-
67	149 ±3	54.2 ±.1	45 ±5	91	127 ±3	61.4 ±.1	45 ±5
68	149 ±3	7.4 ±.1	-	92	127 ±3	8.6 ±.1	-
69	146 ±3	54.8 ±.1	45 ±5	93	126 ±3	1200.0 ±.1	-
70	146 ±3	7.5 ±.1	-		Blowdown to 100±3 (Ref.)		

The test results obtained on the EEU TCA are presented on Figures 49 , 50 , 51 . The acceptance test produced normal performance characteristics relative to prior units of the same design. The initial catalyst bed ΔP at 20 seconds into the first run was 22.9 psia which is in the mid-range of all previous units subjected to the same test. Figure 49 presents the specific impulse and thrust characteristics obtained for acceptance and mission testing at the 20-second point into each ambient temperature start firing. Both parameters decreased nearly linearly as a function of decaying pressure with thrust decaying from 240 lbs to 158 lbs as specific impulse decayed from 237 seconds to 231 seconds. There was no indication of washout tendency throughout the mission.

Figure 50 shows the propellant flow and associated catalyst bed pressure drop characteristics. The latter characteristic was low in relation to prior unit characteristics through mission testing confirming the prior observation that pair firings tend to reduce buildup rate in catalyst bed pressure drop.

Figure 51 presents manifold metal and upstream catalyst bed temperature adjacent to the manifold face. The characteristics indicated are lower in magnitude than most other units following the lower ΔP characteristics observed for this unit. The apparent relationship between these measurements and ΔP is consistent in theory which assumes that lower ΔP results from the movement of the reaction zone downstream, further away from the manifold.

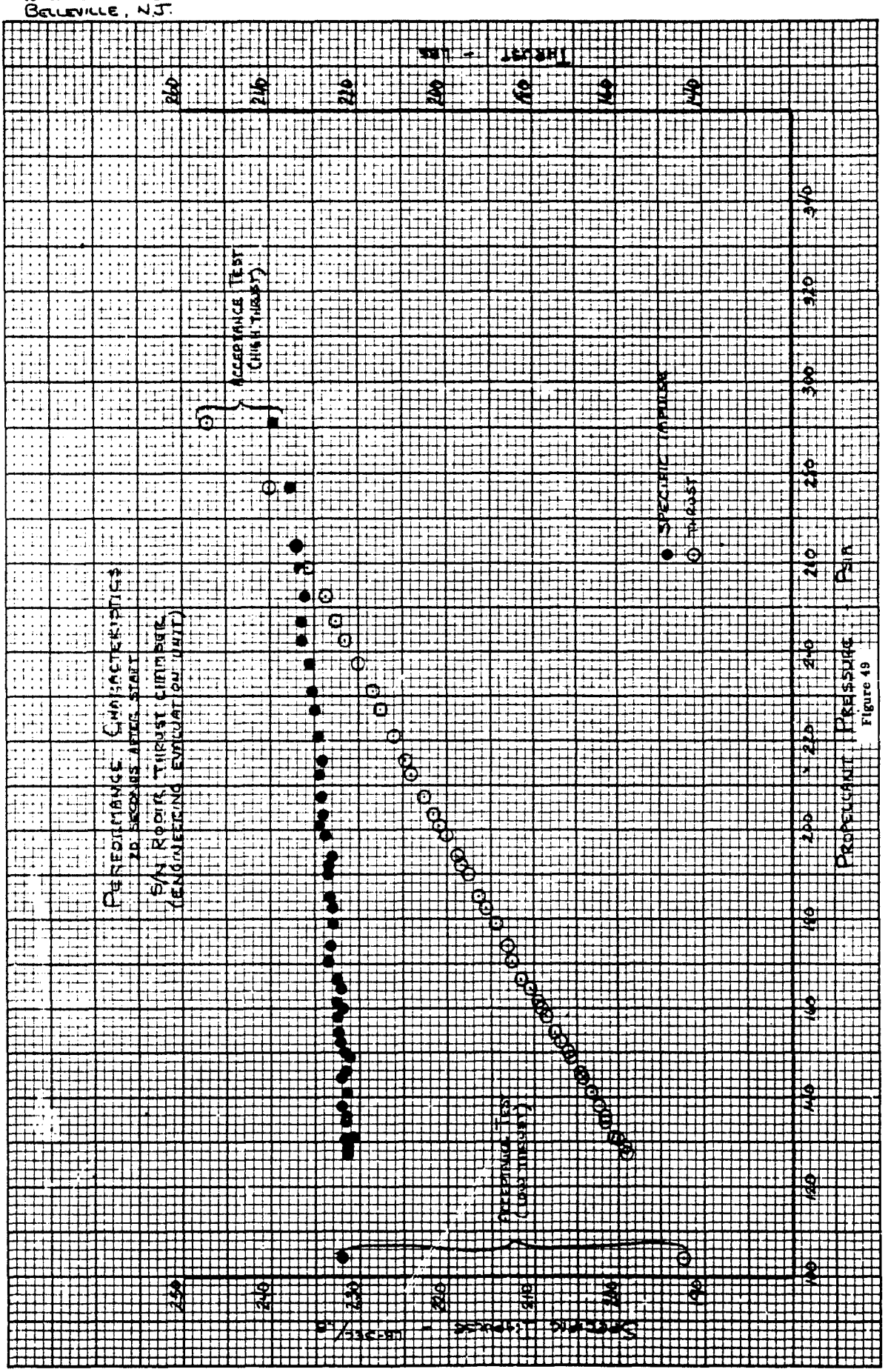
WALTER KIDDE & CO
BELLEVILLE, N.J.
PERFORMANCE CHARACTERISTICS
10 SECONDS AFTER START
E/N ROOM TEMPERATURE
(ENGINEERING EVALUATION UNIT)
ACCEPTANCE TEST
(HIGH THRUST)
SPECIFIC IMPULSE
THRUST
PROPELLANT PRESSURE
PSIA
ACCEPTANCE TEST
(LOW THRUST)

Figure 49

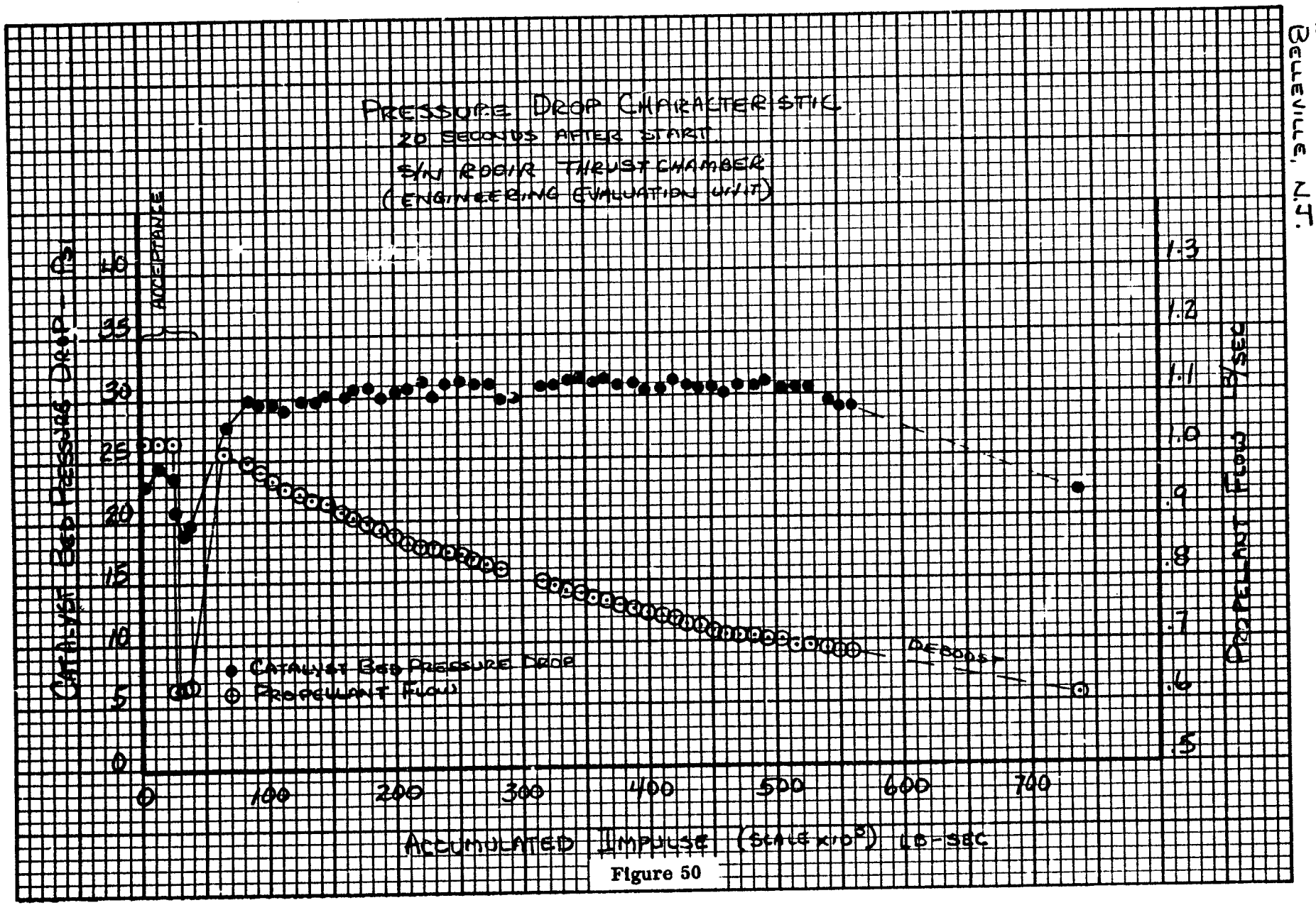
PRESSURE DROP CHARACTERISTIC
20 SECONDS AFTER START
S/N R0010 THRUST CHAMBER
(ENGINEERING EVALUATION UNIT)
WALTER KIDDE & CO
BELLEVILLE, N.J.
CATALYST BED PRESSURE DROP - PSI
ACCEPTANCE
CATALYST BED PRESSURE DROP
PROPELLANT FLOW
DECREASE
THRUST - LBS
SPECIFIC IMPULSE - LB-SEC/LB
ACCUMULATED IMPULSE (SCALE X10³) LB-SEC
0
5
10
15
20
25
30
35
40
100
200
300
400
500
600
700
.5
.6
.7
.8
.9
1.0
1.1
1.2
1.3

Figure 50

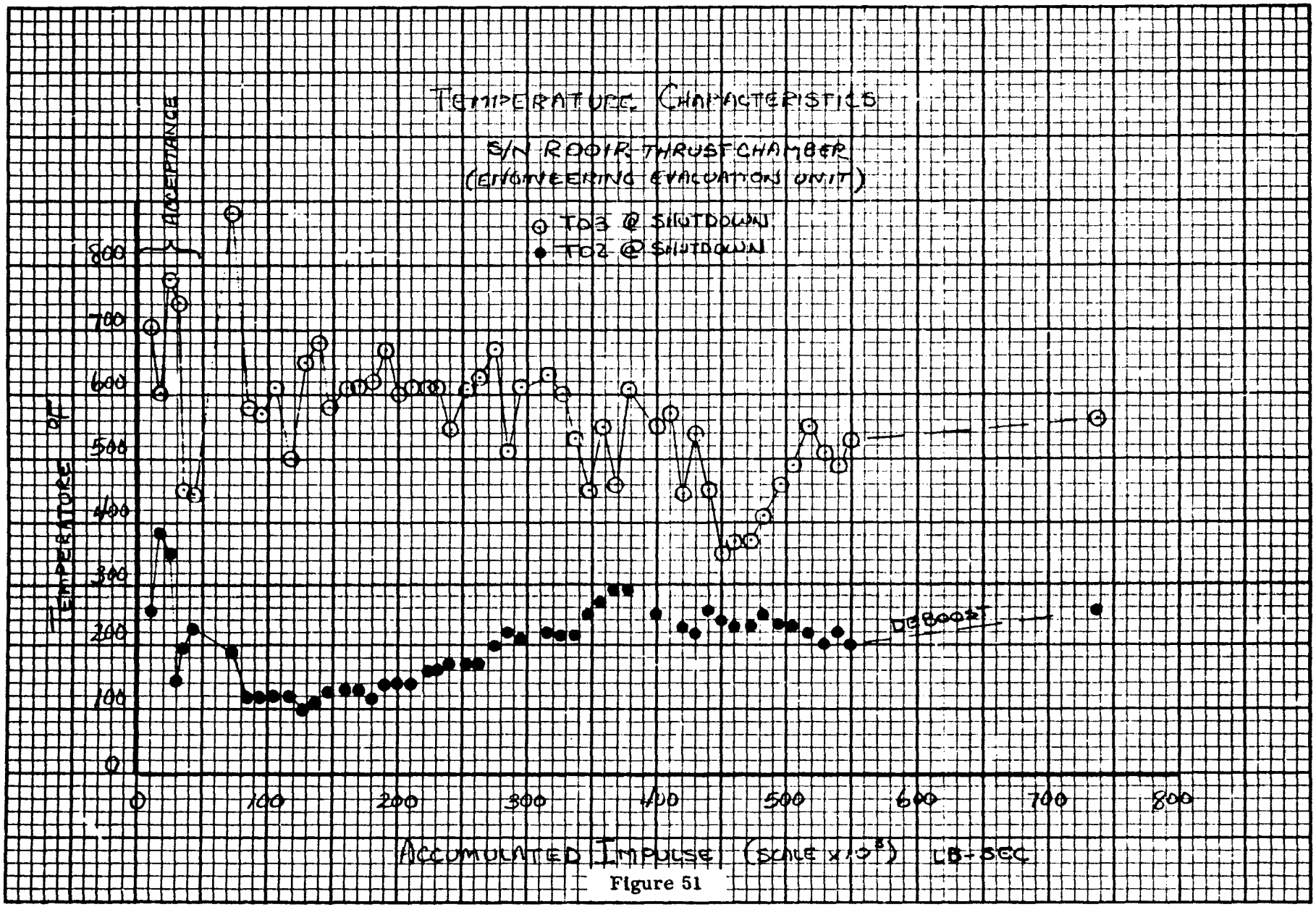
TEMPERATURE CHARACTERISTICS
S/N R001P THRUST CHAMBER
(CONVERGING EVACUATION UNIT)
TO3 @ SHUTDOWN
TO2 @ SHUTDOWN
ACCEPTANCE
TEMPERATURE °F
800
700
600
500
400
300
200
100
0
0
100
200
300
400
500
600
700
800
ACCUMULATED IMPULSE (SCALE x 10⁸) LB-SEC

Figure 51

APPENDIX IV

PRAT BUILD DATA AND PRIOR PERFORMANCE

Manifold flow data for the PRAT unit is presented on Figure 52, the Manifold Flow Calibration Sheet. This sheet gives individual injection point flow point data as well as a total flow measured independently at each of two flow levels. All four total flows, those measured directly and the sum of the individual flows at each flow level must fall within prescribed limits for the manifold to pass acceptance test. This requirement is in addition to individual injection point flow requirements on Figure 52. Relative injection point location is presented in Figure 42.

Individual distribution tube flow data is presented on Table XVI, listed in element serial number order. Included are average area 4 flow, average end flow (area 3 plus area 4) and average body flow (area 1 plus area 2). The number in each location is the average of two flow measurements taken at that condition. The ship-set average area 4 flow at low flow for the PRAT unit was $49.7\frac{\pi}{10}$.

The PRAT unit was subjected to a standard acceptance test including eight firings, two from ambient temperature; five were at 290 psia propellant pressure (250 lbs thrust) and three were at 105 psia propellant pressure (150 lbs thrust). Total accumulated impulse was 43,588 lb-sec in 227.6 seconds of accumulated run time.

The mission duty cycle conducted included an initial pair firing of 30,000 and 4000 lb-sec with 45 minutes off-time between firings. This pair was followed by 22 single firings of 21,500 lb-sec with each firing starting with ambient temperature of 70 - 90°F hardware. Cooldown time between firings was approximately two hours. The final firing was of 1200 seconds duration from an ambient temperature start.

A listing of the mission accomplished is presented on Table XVII. The initial propellant pressure was 301 psia and was allowed to decay throughout the mission, ending up at 110 psia at the end of the 1200 second firing. Propellant temperature throughout the mission was 100 ±5°F. A total of 25 firings were accomplished, including 25 ambient temperature starts. Total impulse accumulated was 687,425 lb-sec in an accumulated run time of 3773 seconds.

MANIFOLD FLOW CALIBRATION SHEET
FIGURE 3

P/N 894998 S/N 016 DATE 5/4/71

SINGLE POINT FLOW-HIGH
INLET PRESSURE 42.0 PSIG TIME 60.04 SEC.

INJECTOR	1	2	3	4	5	6	7	8	9	10	11	12	13	14	15	16	17	18	19	20	21	22	23	24
GROSS	1.260	1.761	1.757	1.752	1.754	1.737	1.779	1.760	1.842	1.745	1.730	1.766	1.789	1.805	1.787	1.792	1.860	1.790	1.813	1.971	1.700	1.730	1.800	1.792
TARE	.196	.194	.194	.202	.204	.208	.206	.198	.204	.200	.204	.200	.200	.200	.200	.194	.196	.200	.208	.203	.194	.202	.194	.196
NET-LBS.	1.064	1.567	1.563	1.540	1.550	1.529	1.573	1.562	1.638	1.545	1.526	1.566	1.589	1.605	1.587	1.598	1.664	1.590	1.605	1.768	1.506	1.528	1.606	1.596
RATIO NET/Avg	.68	.99	.99	.98	.99	.97	1.00	.99	1.04	.98	.97	.99	1.01	1.02	1.01	1.02	1.06	1.01	1.06	1.13	.96	.97	1.02	1.02
RATIO LIMITS	85 / 85	109 / 89	109 / 89	109 / 89	109 / 89	109 / 89	109 / 89	111 / 91	112 / 92	111 / 91	112 / 92	111 / 91	112 / 92	111 / 91	112 / 92	111 / 91	112 / 92	111 / 91	112 / 92	113 / 93	106 / 86	106 / 86	113 / 93	106 / 86

INJECTOR	25	26	27	28	29	30	31	32	33	34	35	36	37
GROSS	1.728	1.884	1.739	1.726	1.927	1.807	1.728	1.836	1.718	1.727	1.794	1.886	1.780
TARE	.196	.204	.196	.204	.208	.198	.194	.200	.200	.200	.196	.206	.200
NET-LBS.	1.532	1.680	1.543	1.522	1.719	1.609	1.534	1.636	1.518	1.527	1.598	1.680	1.580
RATIO NET/Avg	.97	1.01	.98	.97	1.09	1.02	.97	1.04	.97	.97	1.02	1.07	1.01
RATIO LIMITS	106 / 86	113 / 93	106 / 86	106 / 86	113 / 93	106 / 86	106 / 86	113 / 93	106 / 86	106 / 86	113 / 93	106 / 86	106 / 86

TOTAL FLOW (NET) LBS	÷ TIME SEC.	= FLOW RATE LBS/SEC.	TOTAL FLOW (NET) LBS.	÷37 = AVG. FLOW (NET)
58.033	÷ 60.04	= .9608 *	58.033	÷37 = 1.568

TOTAL FLOW INLET PRESSURE 42.0 PSIG TIME 60.0 SEC.
GROSS 57.25
TARE 1.45
NET 55.8 LBS.
RATE .930 LBS/SEC.*

SINGLE POINT FLOW-LOW
INLET PRESSURE 14.6 PSIG TIME 90.0 SEC.

INJECTOR	1	2	3	4	5	6	7	8	9	10	11	12	13	14	15	16	17	18	19	20	21	22	23	24
GROSS	1.118	1.532	1.542	1.522	1.528	1.519	1.551	1.536	1.602	1.532	1.506	1.532	1.552	1.572	1.556	1.571	1.623	1.571	1.584	1.674	1.478	1.492	1.562	1.580
TARE	.196	.194	.194	.202	.204	.208	.206	.198	.204	.200	.204	.200	.200	.200	.200	.194	.196	.200	.208	.203	.194	.202	.194	.196
NET-LBS.	.922	1.338	1.348	1.320	1.324	1.311	1.345	1.338	1.398	1.332	1.302	1.332	1.352	1.372	1.356	1.377	1.427	1.371	1.376	1.471	1.284	1.290	1.368	1.384
RATIO NET/Avg	.69	1.00	1.02	.99	.99	.98	1.01	1.00	1.05	1.00	.98	1.00	1.01	1.03	1.01	1.03	1.07	1.03	1.03	1.03	.96	.96	1.02	1.02
RATIO LIMITS	85 / 85	109 / 89	109 / 89	109 / 89	109 / 89	109 / 89	109 / 89	113 / 93	116 / 96	113 / 93	113 / 93	113 / 93	113 / 93	113 / 93	113 / 93	113 / 93	113 / 93	113 / 93	113 / 93	113 / 93	106 / 86	106 / 86	113 / 93	106 / 86

INJECTOR	25	26	27	28	29	30	31	32	33	34	35	36	37
GROSS	1.540	1.544	1.502	1.494	1.573	1.573	1.516	1.607	1.493	1.501	1.582	1.486	1.557
TARE	.196	.204	.196	.204	.208	.194	.194	.200	.200	.200	.196	.206	.200
NET-LBS.	1.294	1.340	1.306	1.290	1.365	1.379	1.321	1.407	1.293	1.301	1.386	1.280	1.357
RATIO NET/Avg.	.97	1.00	.98	.97	1.04	1.03	.99	1.05	.97	.97	1.04	.96	1.01
RATIO LIMITS	106 / 86	116 / 96	106 / 86	106 / 86	116 / 96	106 / 86	106 / 86	116 / 96	106 / 86	106 / 86	116 / 96	106 / 86	106 / 86

TOTAL FLOW (NET) LBS.	÷ TIME SEC.	= FLOW RATE LBS./SEC.	TOTAL FLOW (NET) LBS.	÷37 = AVG. FLOW (NET)
49.257	÷ 90.0	= .547 *	49.257	÷37 = 1.33

TOTAL FLOW INLET PRESSURE 14 PSIG TIME 92.06 SEC.
GROSS 51.289
TARE 2.030
NET 49.159 LBS
RATE .535 LBS./SEC.*

ORIGINAL SIGNED BY

TEST CONDUCTOR M. ALNS
WK INSPECTOR J. SOLDA
LMSC QA REP W. DOLL
ACCEPTABLE ✓ UNACCEPTABLE

* PLOT ON GRAPH - (PAGE 10.)

DISTRIBUTION TUBE FLOW ANALYSIS
PRODUCTION RELIABILITY ASSESSMENT UNIT
PERCENT OF TOTAL FLOW

S/N	Average Area 4 Flow		Average End Flow		Average Body Flow		S/N	Average Area 4 Flow		Average End Flow		Average Body Flow	
	High Flow	Low Flow	High Flow	Low Flow	High Flow	Low Flow		High Flow	Low Flow	High Flow	Low Flow	High Flow	Low Flow
1201	43.0	51.5	59.5	64.0	40.5	36.0	1226	43.5	51.0	63.0	64.5	37.0	35.5
1203	45.5	51.0	59.5	66.0	40.5	34.0	1227	43.0	47.0	61.5	65.5	38.5	34.5
1204	43.0	49.0	60.5	64.0	39.5	36.0	1228	41.5	50.5	58.5	62.0	41.5	38.0
1205	45.5	48.5	59.5	66.5	40.5	33.5	1230	44.0	53.0	61.0	69.0	39.0	31.0
1206	43.5	48.0	59.5	62.5	40.5	37.5	1231	44.5	47.5	62.0	62.0	38.0	38.0
1207	46.5	50.0	60.0	63.0	40.4	37.0	1237	38.2	47.0	65.5	66.2	34.5	33.8
1208	43.0	52.5	58.0	63.0	42.0	37.0	1240	43.5	45.5	63.0	64.0	37.0	36.0
1209	44.5	50.0	58.5	65.5	41.5	34.5	1242	43.0	45.5	58.0	62.5	42.0	37.5
1210	50.0	58.0	60.0	69.5	40.0	30.5	1243	39.0	46.0	60.5	66.0	39.5	34.0
1211	45.0	55.0	60.5	66.5	39.5	33.5	1247	38.5	51.0	60.5	63.0	39.5	37.0
1212	44.0	49.0	60.0	66.0	40.0	34.0	1249	40.0	48.5	62.0	68.5	38.0	31.5
1213	46.0	45.5	59.0	64.0	41.0	36.0	1250	41.0	46.5	63.0	63.5	37.0	36.5
1214	45.5	48.5	59.0	66.0	41.0	34.0	1251	47.5	53.5	67.5	67.0	32.5	33.0
1219	42.0	46.0	60.5	66.0	39.5	34.0	1252	49.0	50.5	59.5	62.0	40.5	38.0
1220	38.5	46.5	62.5	62.5	37.5	37.5	1254	46.0	55.5	60.5	65.5	39.5	34.5
1221	43.5	54.0	61.5	62.5	38.5	37.5	1255	44.5	51.5	59.0	63.5	41.0	36.5
1222	42.0	45.0	62.5	64.5	37.5	35.5	1258	48.0	46.5	61.0	64.0	39.0	36.0
1223	49.0	53.5	58.0	62.5	42.0	38.5							
1224	43.0	47.5	60.5	63.0	39.5	37.0							
1225	45.5	48.0	60.0	62.0	40.0	38.0							

TABLE XVI

TABLE XVII

PRIOR MISSION DUTY CYCLE - PRAT UNIT

Pulse No.	Propellant Pressure (psia)	On-Time (Seconds)	Off-Time (Minutes)	Pulse No.	Propellant Pressure (psia)	On-Time (Seconds)	Off-Time (Minutes)
1	301±4	120.5±.1	45±5	14	182±3	112.1±.1	-
2	291±4	16.5±.1	-	15	176±3	113.9±.1	-
3	283±4	89.4±.1	-	16	171±3	113.9±.1	-
4	270±4	91.5±.1	-	17	166±3	117.5±.1	-
5	258±4	93.6±.1	-	18	161±3	119.3±.1	-
6	245±4	96.1±.1	-	19	156±3	121.2±.1	-
7	235±4	98.2±.1	-	20	151±3	123.3±.1	-
8	225±4	100.5±.1	-	21	147±3	125.0±.1	-
9	216±4	102.6±.1	-	22	143±3	126.9±.1	-
10	208±4	104.7±.1	-	23	139±3	128.7±.1	-
11	200±4	106.7±.1	-	24	135±3	130.6±.1	-
12	194±3	108.5±.1	-	25	133±3	1200.0±.1	-
13	188±3	110.3±.1	-				

The final 1200 second firing accumulated 178,600 lb-sec total impulse while using 754 lbs of propellant. This resulted in a total life accumulation of 4001 seconds of operation while accumulating 731,013 lb-sec total impulse and using 3101 lbs of propellant. Based upon these figures, the integrated specific impulse over the lifetime was 236 seconds.

The PRAT TCA successfully completed the production reliability assessment test, thereby verifying the integrity of the second production lot. The actual test results obtained on the PRAT TCA are presented on Figures 53, 54 and 55. The acceptance test produced normal performance characteristics relative to prior units of the same design. The initial catalyst bed ΔP at 20 seconds into the first run was 20.2 psia which is in the mid-range of all previous units subjected to the same test. Figure 53 presents the specific impulse and thrust characteristics obtained for acceptance and mission testing at the 20 second point into each ambient temperature start firing. Both parameters decrease nearly linearly as a function of decaying pressure with thrust decaying from 252 lbs. to 180 lbs. as specific impulse decayed from 239 seconds to 232 seconds, until the point of venturi decavitation was reached

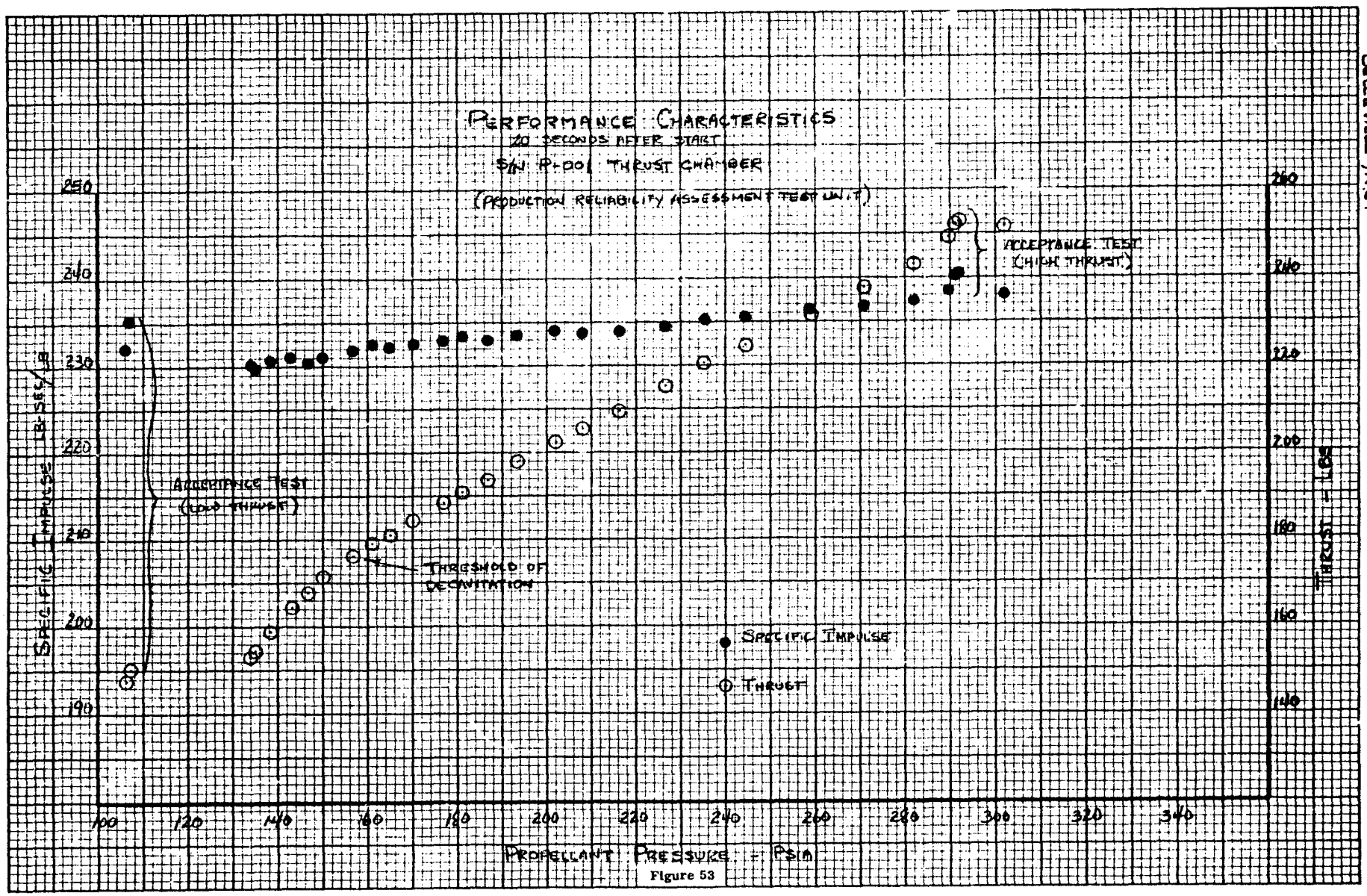
PERFORMANCE CHARACTERISTICS
20 SECONDS AFTER START
S/N P-001 THRUST CHAMBER
(PRODUCTION RELIABILITY ASSESSMENT TEST UNIT)
ACCEPTANCE TEST (HIGH THRUST)
ACCEPTANCE TEST (LOW THRUST)
THRESHOLD OF CAVITATION
SPECIFIC IMPULSE
THRUST
SPECIFIC IMPULSE - LB-SEC/LB
THRUST - LBS
PROPELLANT PRESSURE - PSIA
250
240
230
220
210
200
190
260
240
220
200
180
160
140
100
120
140
160
180
200
220
240
260
280
300
320
340
WALTER KIDDE & CO
BELLEVILLE, N.J.

Figure 53

at which point the flow characteristic changed producing a thrust droop and corresponding small fall-off in specific impulse. Decaviation is caused by an increase in upstream catalyst bed pressure beyond the recovery capability of the cavitating venturi. When this happens, the flow is no longer independent of the downstream pressure drops with resultant dropoff in flow.

The increase in catalyst bed pressure drop is presented on Figure 54. This plot shows a rapidly increasing pressure drop characteristic in spite of decreasing flow which attains a level just under 50 psi near the end of mission life. This is an increase of nearly 30 psi as compared to an increase of about 10 psi over the mission duty cycle conducted on the EEU. The difference is attributed to the cumulative duty cycle effect.

Figure 55 presents the manifold metal temperature and the upstream catalyst bed temperature characteristic over the PRAT mission. The primary significance of these characteristics is the apparent influence of catalyst bed pressure drop increase on these temperatures. The increased pressure drop is indicative of a more upstream position of the reaction zone with attendant increase in the catalyst bed temperature at the manifold face.

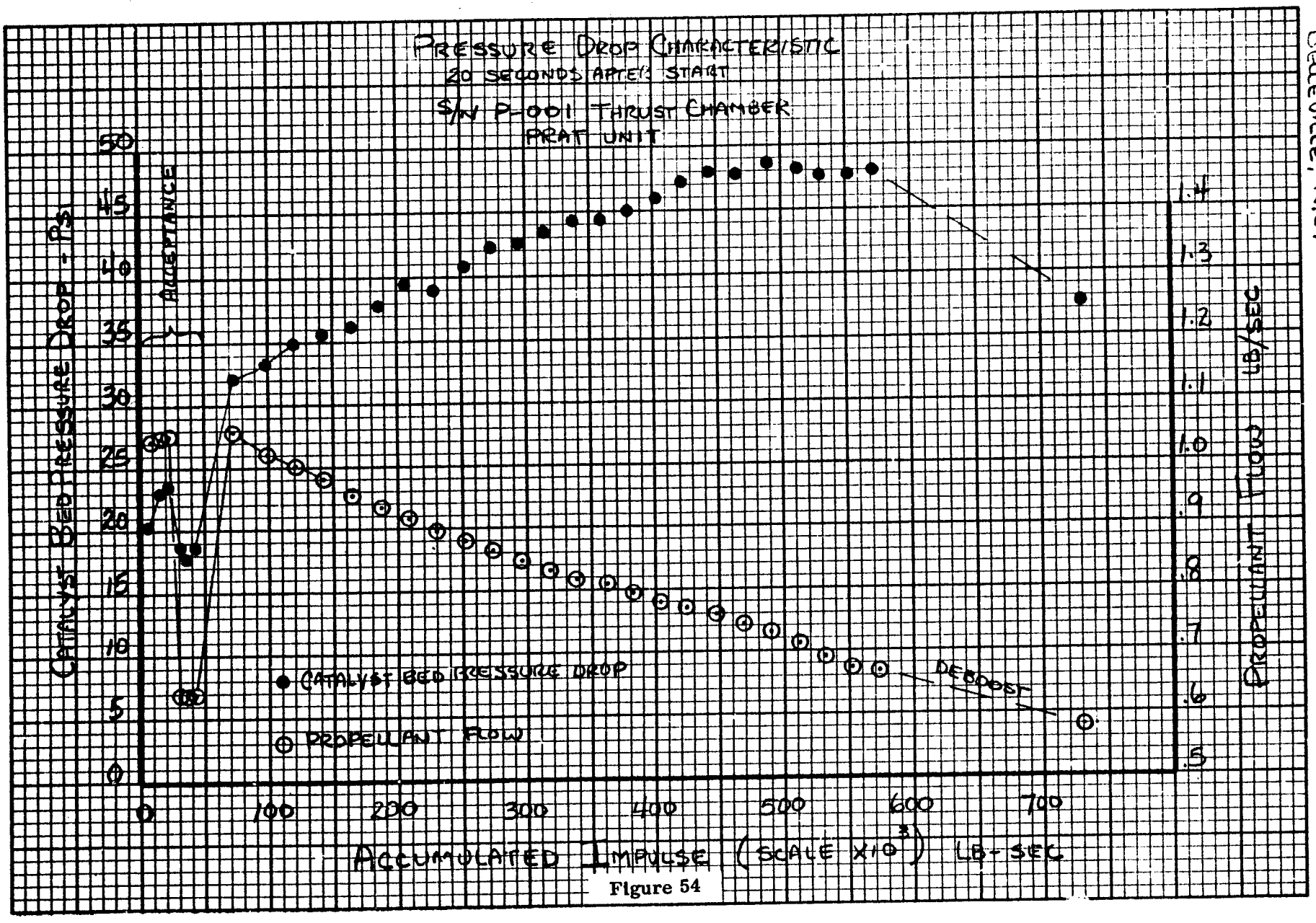
PRESSURE DROP CHARACTERISTIC
20 SECONDS AFTER START
S/N P-001 THRUST CHAMBER
PRAT UNIT
WALTER KIDDE & CO
BELLEVILLE, N.J.
CATALYST BED PRESSURE DROP - P.S.I.
ACCEPTANCE
PROPELLANT FLOW LB/SEC
CATALYST BED PRESSURE DROP
PROPELLANT FLOW
DEBOOST
ACCUMULATED IMPULSE (SCALE X10³) LB-SEC.
0
5
10
15
20
25
30
35
40
45
50
100
200
300
400
500
600
700
.5
.6
.7
.8
.9
1.0
1.1
1.2
1.3
1.4

Figure 54

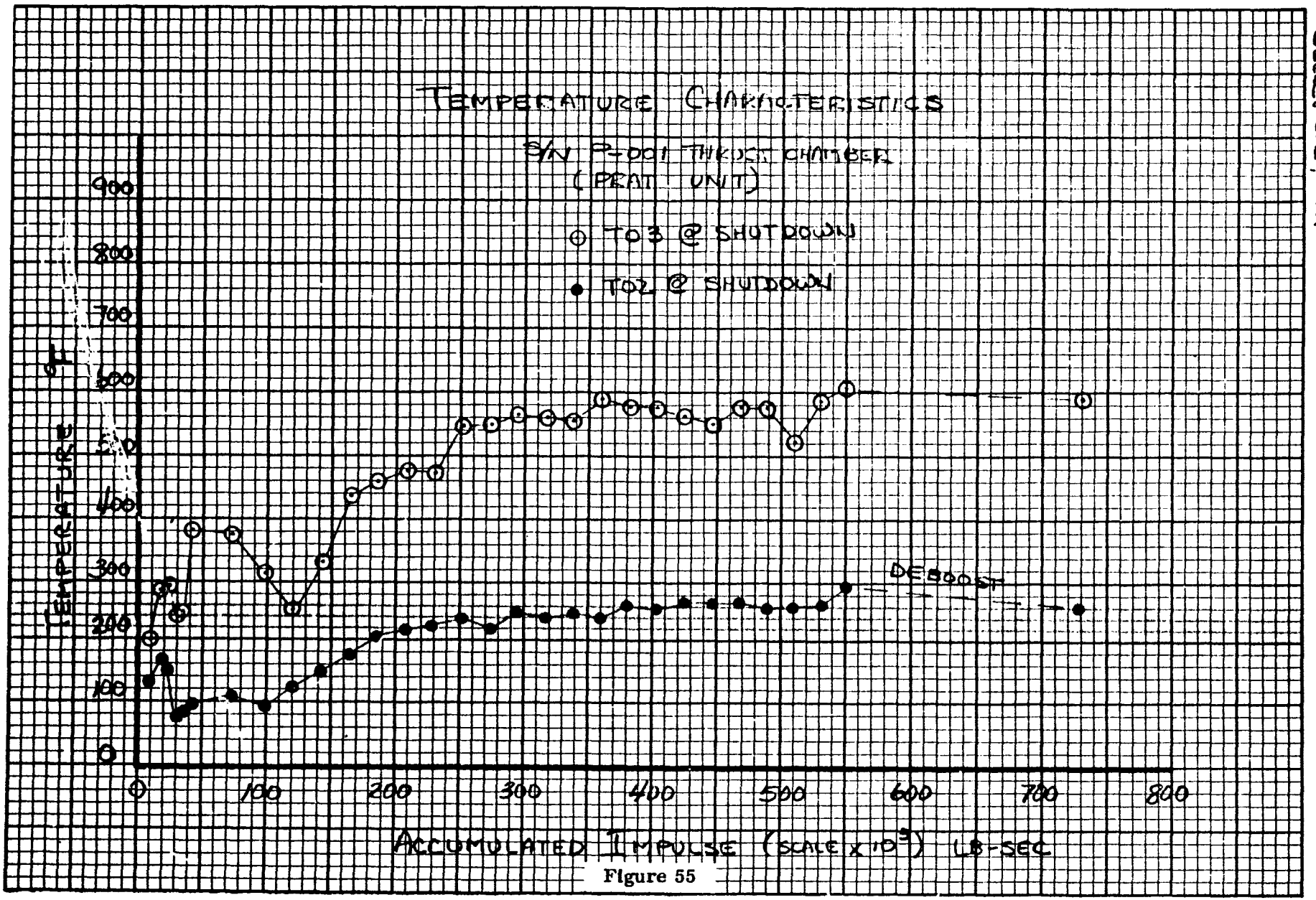

Figure 55

APPENDIX V

QUAD-VALVE DESCRIPTION

The quad-valve contains four independent solenoid operated elements manifolded together in a single body as shown in Figure 56. The total flow is passed through two parallel branches with each branch comprised of two valve elements in series. The use of two flow paths in parallel offers redundant protection against failure to open; the use of two valving elements in series offers redundant protection against failure to close. This configuration satisfies the requirement that a single failure should not prevent the TCA from operating. The design features of the quad-valve are presented in the following list:

Balanced force design - minimizes power requirements and produces a better force margin

Direct acting design - provides simplicity and attendant higher reliability

Welded flow path - hermetic seal eliminates potential seal leak points

Floating teflon seat - minimizes seat impact to improve life and reliability

Isolated coil design - allow selection of best magnetic materials

Redundant sealing - single bellows failure will not cause valve failure or even loss of operation.

The basic operation is best revealed by a detailed examination of one of the valving elements Figure 57. A conical metallic seat is machined as an integral part of the valve body. This seat is sealed by a spring-loaded conical teflon poppet. Energization of the solenoid causes the armature to lift, pulling the central stem and raising the poppet off the seat. The valve is hydraulically balanced for both upstream and downstream pressure by two stainless steel bellows.

The stem connects the poppet with the armature which is located outside the propellant area. An extension on the stem actuates a switch which serves as a position indicator for the valve.

The valve seat of the primary valve will also serve as a relief valve for fluid pressure rises between the valve seats in each leg. This feature prevents accidental firing of the motor.

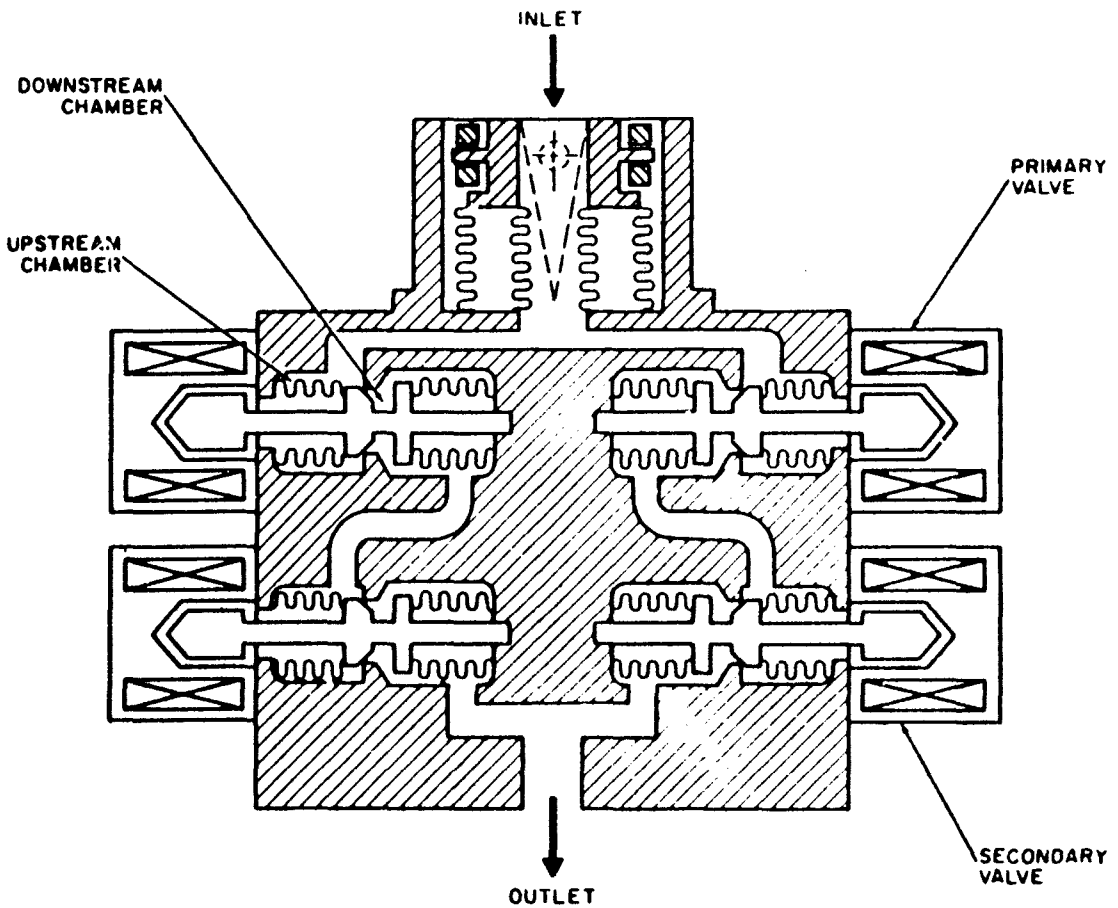

Figure 56 . SCHEMATIC OF QUAD-VALVE PACKAGE

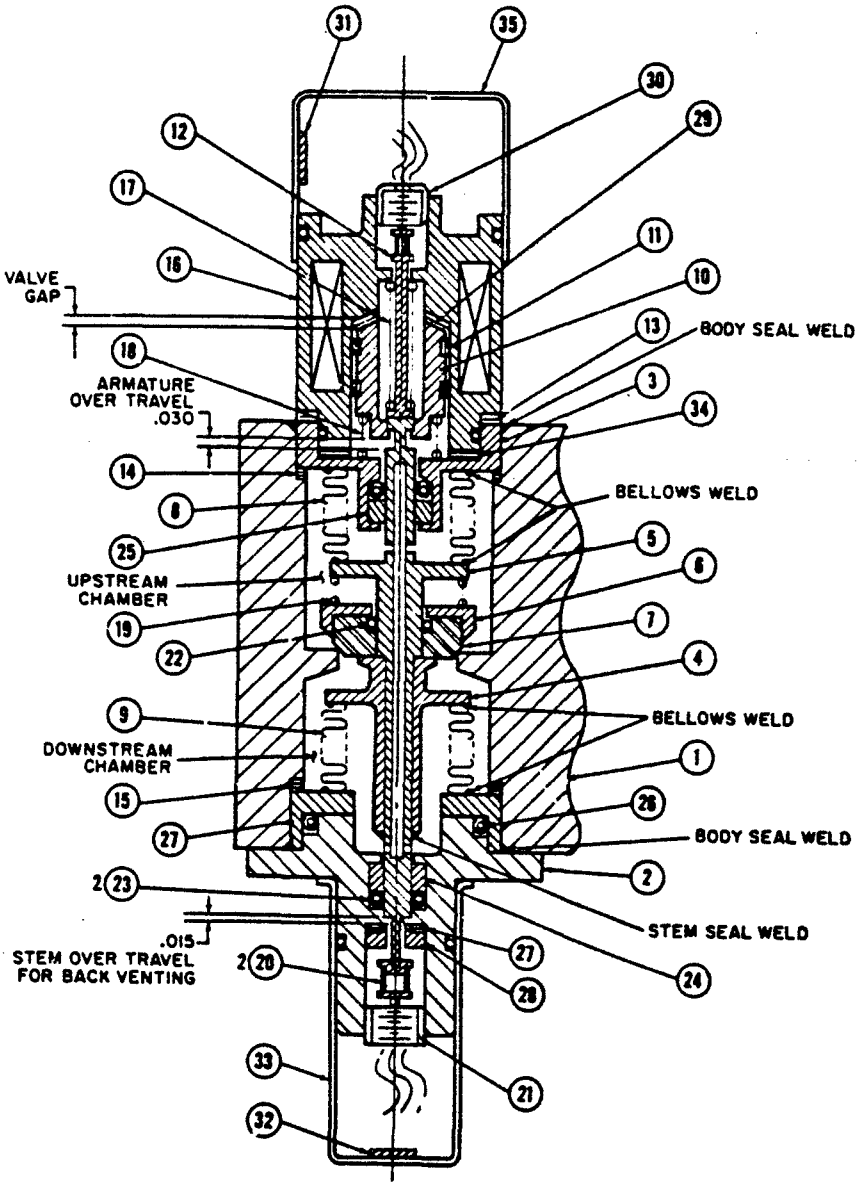

Figure 57 QUAD VALVE ELEMENT SCHEMATIC

It may also be noted that the internal cavities of the bellows at each end of the stem are interconnected by the hole in the center stem. If either bellows should develop a leak, the internal pressures will equalize so that force balances are maintained and the valve is still operable in a secondary mode. The omniseals on the stem are used to provide shaft sealing in this backup mode.

APPENDIX VI

CATALYST BED PRESSURE DROP NORMALIZATION TECHNIQUE

At least two reasonably accurate and useful techniques have been used to normalize and evaluate catalyst bed pressure drop data. Both techniques are based upon a combination of theoretical considerations and empirical results, and neither can be considered to be exact normalizations.

Method "A" of bed pressure drop evaluation is to plot the normalized pressure drop K_L versus the number of ambient starts.

$$K_L = \frac{\Delta P}{(\dot{W})^{.75}}$$

Where:

K_L = normalized bed pressure drop

ΔP = bed pressure drop (THB-THA) in PSI at 20 seconds into the firing.

$\dot{W}$ = propellant flow rate lb/sec.

Method "B" of bed pressure drop normalization is to plot R_c versus the number of ambient starts.

Where:

R_c = bed pressure drop parameter

P_c = chamber pressure (PSIA)

ΔP = bed pressure drop (THB-THA) in PSI at 20 seconds into the firing.

$K = \frac{\Delta P}{P_c}$

R = an empirical function of K by which ΔP is adjusted to the ΔP which would exist if the decomposition gas temperature were 1850° F.

Based upon Walter Kidde and Company engineering judgement, Method B more consistently correlates with actual test results. As a consequence, Kidde analysis of data is based upon Method B normalization. The derivation of this method is present in the following pages.

Catalyst bed pressure drop is a function of at least three prime factors:

a. Time into a particular firing.

b. Propellant flow rate.

c. The number of accumulated ambient starts.

To evaluate the effects of other variables such as design changes or duty cycle variations, it is necessary first to establish a normalization technique to eliminate the effects of the prime factors in the evaluations.

A description of the derivation of the catalyst bed pressure drop normalization technique follows. The derivation is not completely rigorous physically or mathematically, being basically a rationale for the best use of available information in evaluating bed pressure drop characteristics.

Turbulent flow of a fluid through a restriction follows the Bernoulli equation:

$$\Delta P = K_1 \quad \rho \frac{V^2}{2g} \qquad (1)$$

where

ΔP = pressure drop through the restriction

ρ = density of the fluid

V = velocity of the fluid

g = gravitational constant

K_1 = restriction resistance coefficient

Now:

$$V = \frac{\dot{\omega}}{A\rho} \tag{2}$$

where

$\dot{\omega}$ = flowrate

A = area normal to flow

$V_1\rho$ = as before

Substituting equation (2) into equation (1):

$$\Delta P = K_1 \frac{\dot{\omega}^2}{2g\rho A^2} \tag{3}$$

Since the flowrates of liquid hydrazine and gaseous decomposition products are the same but the density of liquid hydrazine is several orders of magnitude larger than that of the gases, the liquid pressure drop in the bed is negligible compared to that of the gas and will be ignored.

Gas flow through the sonic throat is:

$$= \frac{A_t P g}{C^*} \tag{4}$$

where

A_t = throat area normal to flow

P = chamber pressure

C* = characteristic gas velocity

$\dot{\omega}_1$,g = as before

Substituting equation (4) into equation (3):

$$\Delta P = K_1 \frac{A_t^2 P^2 g}{2\rho C^{*2} A^2} \tag{5}$$

Assuming the chamber pressure and temperature are representative of bed conditions:

$$\rho = \frac{P}{RT} \tag{6}$$

where

R = decomposition gas constant

T = chamber gas temperature

ρ, P as before

Substituting equation (6) into equation (5)

$$\Delta P = \frac{K_1 A_t^2 P^2 g RT}{2 C^{*2} A^2 P} \tag{7}$$

Grouping constants and rearranging equation (7):

$$\frac{\Delta P}{P} = K_2 \tag{8}$$

where

K_2 = bed resistance factor

ΔP, P as before

Bed resistance K_2 is approximately directly proportional to the length of the bed flow path and inversely proportional to the diameter of the particles according to various authors.

$$K_2 = K_3 \left(L/D\right) \tag{9}$$

where

K_3 = configuration constant

L = length of gas flow path in bed

D = pressure drop related mean particle diameter

K_2 = bed resistance factor

If the gas flow length of the bed and the mean particle diameter were constant during the life of the bed and for all operating conditions, it would be expected then that the K_2 bed resistance factor would be constant and no change in $\Delta P/P$ would be observable. However, this is not the case as $\Delta P/P$ actually decreases with time during a single firing, and $\Delta P/P$ actually builds up in value with accumulated firings when compared at the same time into each firing.

Sample analyses of used catalyst have consistently shown that the mean particle size has decreased from that of the original packing. This general trend is recognized as being the prime cause of the buildup in $\Delta P/P$ with life as the K_2 bed resistance would increase with decreasing particle diameter as shown by equation (9).

A consistently observable phenomenon is that $\Delta P/P$ decreases with time during a firing, and then, after shutdown and restarting, retraces nearly the same $\Delta P/P$ transient during the next firing.

Since the particle diameters cannot physically be undergoing, during a firing, nearly repeatable alterations from firing-to-firing of a nature to explain the transients, it is recognized from equation (9) that the prime cause of the transient ΔP decline during a firing is movement of the gas-generating decomposition zone downstream in the bed with time during a firing such that the bed gas flow length L is continuously shortened during a firing. In summary then, the $\Delta P/P$ buildup during life is essentially caused by the decreasing catalyst mean particle diameter D, while the $\Delta P/P$ transient decay during a single firing is caused by continuous downstream movement of the decomposition zone so that gas flow length L decreases during the firing.

In comparing life effects on bed pressure drop of factors such as the number of cold starts and duty cycles, it is evident that the life-dependent ΔP parameter should be the basis for comparisons. Based upon the foregoing analysis of ΔP effects, the meaningful life-dependent ΔP parameter is the "mean particle diameter" D. Since the diameter cannot physically be measured during sustained operations, another method is sought. It is apparent that $\Delta P/P$ cannot be used at any random time into a firing since L decays continuously and its value is unknown at a random time, and therefore a $\Delta P/P$ based on random time values would not serve as a direct measure of the particle diameter D. Comparing $\Delta P/P$ at a fixed time into the firing, such as 20 seconds from start, does not necessarily result in the same gas flow bed length L for all firings. However, if L could be elir inated, or made constant, as a factor in the $\Delta P/P$ equation (9), then a singular measure of D would be given by $\Delta P/P$. The normalization technique used eliminates L as a factor in the equation.

The bed gas flow length L is eliminated from consideration by comparing $\Delta P/P$ values at a constant value of chamber gas temperature (TCH). The rationale for this contention is as follows: In a given design configuration with a particular mean particle diameter D and with a particular throughput, the fraction dissociation of ammonia products increases as the bed length increases. Now, if the bed length is chosen to correspond to a particular fraction dissociation of ammonia corresponding to a particular value of TCH, then all engines of this configuration and mean particle size will have the same gas flow bed length with the same throughput. For the same configuration and throughput, a reduction in mean particle diameter D would necessitate a reduction in bed length L to maintain the same TCH. It follows then, that for a fixed configuration, TCH and throughput, L depends only on D. Now, from equation (9) it is evident that $\Delta P/P$ depends only on L and D. Consequently, since L depends only on D for TCH and throughput constant, it follows then that $\Delta P/P$ depends only on D for constant TCH and throughput. Therefore, any differences between $\Delta P/P$ values measured at the same TCH and throughput must be the result of either particle size D differences or configuration differences. For the same configuration then, any $\Delta P/P$ changes, with TCH and throughput held constant, would be a measure of particle size D changes, or mathematically:

$$R = f(D) \qquad (10)$$

where:

f = a function of ( )

$R = \frac{\Delta P}{P}$ with TCH and throughput at particular values.

D, ΔP, P as before.

Equation (10) shows that the resistance R at a particular throughput is a function only of mean particle diameter D, which is the desired life-dependent parameter to be used for evaluating life oriented pressure drop characteristics and bed condition. Therefore comparisons of R at a selected TCH value is the most direct evaluation of the bed condition in terms of its mean particle size D. The value of TCH selected is 1850°F which encompasses practially all data as an upper limit.

Since the nature of the various types of firings precludes measuring pressure drop at the same TCH for all firings, a correlation of the pressure drop, in terms of $\Delta P/P$, existing at 20 seconds into the firing to that which would exist at a constant 1850°F TCH was established from test results and used to adjust 20 second $\Delta P/P$ to the $\Delta P/P$ which would exist at 1850°F TCH which is the definition of R. This correlation is described by Table XVIII and in the normalization equation (12).

TABLE XVIII

CONVERSION FROM K TO R

K	R	K	R	K	R
.280	.280	.640	.479	.980	.596
.300	.298	.660	.487	1.000	.602
.320	.316	.680	.495	1.020	.609
.340	.332	.700	.501	1.040	.616
.360	.343	.720	.508	1.060	.622
.380	.354	.740	.515	1.080	.628
.400	.365	.760	.522	1.100	.634
.420	.377	.780	.529	1.120	.640
.440	.388	.800	.536	1.140	.645
.460	.400	.820	.543	1.160	.650
.480	.411	.840	.550	1.180	.655
.500	.421	.860	.557	1.200	.660
.520	.430	.880	.563	1.220	.665
.540	.439	.900	.570	1.240	.670
.560	.447	.920	.577	1.260	.675
.580	.455	.940	.584	1.280	.680
.600	.463	.960	.590	1.300	.685
.620	.471			1.400	.710

$$K = \left(\frac{\Delta P \text{ Bed}}{P_c}\right) 20 \text{ sec}$$

P_c = Chamber Pressure

T_c = Chamber Temperature

R = Corresponding, Normalized

$$\left(\frac{\Delta P \text{ Bed}}{P_c}\right) \text{ for } T_c = 1850^\circ F$$

The apparent effect of throughput, which so far has been considered as being constant, on the normalized pressure drop resistance R, was empirically established by comparing R values at high and low acceptance test and mission flowrate values at approximately the same point early in life. This throughput effect is accounted for by multiplying the R values by throughput raised to the .3 power or its equivalent $P,^{.3}$ as is apparent from equation (4):

$$R_c = R P^{.3} \tag{11}$$

Multiplying and dividing equation (11) by $\Delta P/P$ at 20 seconds into the firing, the overall normalization equation becomes:

$$R_c = \frac{\Delta P_{20}}{(P)^{.7}} \times \frac{R}{K} \tag{12}$$

where:

R_c = bed pressure drop parameter

P = chamber pressure (PSIA)

ΔP_{20} = bed pressure drop (THB-THA) in PSI at 20 seconds into the firing

$K = \frac{\Delta P_{20}}{P_c}$

R = an empirical function of K by which ΔP_{20} is adjusted to the ΔP which would exist if the decomposition gas temperature were 1850°F (Table

From the nature of the derivation in terms of isolating the "mean particle diameter" D as a parameter measured by the throughput and chamber temperature normalized pressure drop, it is evident that R_c is theoretically a singular measure of the mean particle diameters of the gas flow path for a given design configuration. Although it is not maintained that this concept is in reality completely valid, viewing the pressure drop results accordingly is useful in comprehending the nature of the pressure drop life buildup characteristics and duty cycle effects. Definite correlation of R_c resistance as a function of the number of ambient starts have been developed and the results of these tests are evaluated in this manner.

Security Classification

DOCUMENT CONTROL DATA - R&D

(Security classification of title, body of abstract and indexing annotation must be entered when the overall report is classified)

1. ORIGINATING ACTIVITY (Corporate author) Walter Kidde & Company, Inc. 675 Main St., Belleville, N. J. 07109	2a. REPORT SECURITY CLASSIFICATION Unclassified 2b. GROUP – –

3. REPORT TITLE

300-LB(f) MONOPROPELLANT HYDRAZINE THRUSTER LIFE EVALUATION

4. DESCRIPTIVE NOTES (Type of report and inclusive dates)

Final Report

5. AUTHOR(S) (Last name, first name, initial)

Hall, Gary M.
Layendecker, Thomas P.

6. REPORT DATE	7a. TOTAL NO. OF PAGES	7b. NO. OF REFS
Mar 1973	147	–

8a. CONTRACT OR GRANT NO.	9a. ORIGINATOR'S REPORT NUMBER(S)
FO4611-72-C-0027 b. PROJECT NO. 62100023058117 c. d.	9b. OTHER REPORT NO(S) (Any other numbers that may be assigned this report) –

10. AVAILABILITY/LIMITATION NOTICES

11. SUPPLEMENTARY NOTES	12. SPONSORING MILITARY ACTIVITY
–	Air Force Rocket Propulsion Laboratory Edwards AFB, California 93523

13. ABSTRACT

There was a primary need to demonstrate the extended life capability of a nominal 300-lb(f) monopropellant hydrazine thruster beyond qualification limits. In addition, there were secondary needs to attain end of life performance characteristics; first to verify a catalyst bed pressure drop buildup theory of performance degradation, and second to test a causal theory for the occurrence of "washout" performance degradation. The program documented herein takes three steps toward the fulfillment of these needs by conducting life tests on three thrust chambers, two which already had specified mission life accumulated and one which was refurbished to the "as new" condition. All three units tested demonstrated extended life capability, but each provided performance characteristics which reflected the particular type of duty cycle conducted. The unit which produced high catalyst bed pressure drop also produced higher than usual in-run manifold temperature. The other two units produced low catalyst bed pressure drop buildup and consequently attained a longer unencumbered life characteristic. Based upon these results, it is concluded that extended life capability is

DD FORM 1 JAN 64 1473

Unclassified
Security Classification

Continuation of DD 1473

demonstrated and the secondary need to verify catalyst bed pressure drop buildup theory was accomplished. However, "washout" performance characteristics were never accomplished preventing the accumulation of convincing data to support the causal theory. Recommendations based upon these findings include investigation and elimination of variability in sensitive build parameters, life testing to verify elimination of variability as well as obtain end of life data, and the determination of safe in-run and shutdown manifold temperature on high catalyst bed pressure drop units.

Security Classification

14. KEY WORDS	LINK A		LINK B		LINK C	
	ROLE	WT	ROLE	WT	ROLE	WT

INSTRUCTIONS

1. **ORIGINATING ACTIVITY:** Enter the name and address of the contractor, subcontractor, grantee, Department of Defense activity or other organization *(corporate author)* issuing the report.

2a. **REPORT SECURITY CLASSIFICATION:** Enter the overall security classification of the report. Indicate whether "Restricted Data" is included. Marking is to be in accordance with appropriate security regulations.

2b. **GROUP:** Automatic downgrading is specified in DoD Directive 5200.10 and Armed Forces Industrial Manual. Enter the group number. Also, when applicable, show that optional markings have been used for Group 3 and Group 4 as authorized.

3. **REPORT TITLE:** Enter the complete report title in all capital letters. Titles in all cases should be unclassified. If a meaningful title cannot be selected without classification, show title classification in all capitals in parenthesis immediately following the title.

4. **DESCRIPTIVE NOTES:** If appropriate, enter the type of report, e.g., interim, progress, summary, annual, or final. Give the inclusive dates when a specific reporting period is covered.

5. **AUTHOR(S):** Enter the name(s) of author(s) as shown on or in the report. Enter last name, first name, middle initial. If military, show rank and branch of service. The name of the principal author is an absolute minimum requirement.

6. **REPORT DATE:** Enter the date of the report as day, month, year, or month, year. If more than one date appears on the report, use date of publication.

7a. **TOTAL NUMBER OF PAGES:** The total page count should follow normal pagination procedures, i.e., enter the number of pages containing information.

7b. **NUMBER OF REFERENCES:** Enter the total number of references cited in the report.

8a. **CONTRACT OR GRANT NUMBER:** If appropriate, enter the applicable number of the contract or grant under which the report was written.

8b, 8c, & 8d. **PROJECT NUMBER:** Enter the appropriate military department identification, such as project number, subproject number, system numbers, task number, etc.

9a. **ORIGINATOR'S REPORT NUMBER(S):** Enter the official report number by which the document will be identified and controlled by the originating activity. This number must be unique to this report.

9b. **OTHER REPORT NUMBER(S):** If the report has been assigned any other report numbers *(either by the originator or by the sponsor)*, also enter this number(s).

10. **AVAILABILITY/LIMITATION NOTICES:** Enter any limitations on further dissemination of the report, other than those imposed by security classification, using standard statements such as:

(1) "Qualified requesters may obtain copies of this report from DDC."

(2) "Foreign announcement and dissemination of this report by DDC is not authorized."

(3) "U. S. Government agencies may obtain copies of this report directly from DDC. Other qualified DDC users shall request through _____."

(4) "U. S. military agencies may obtain copies of this report directly from DDC. Other qualified users shall request through _____."

(5) "All distribution of this report is controlled. Qualified DDC users shall request through _____."

If the report has been furnished to the Office of Technical Services, Department of Commerce, for sale to the public, indicate this fact and enter the price, if known.

11. **SUPPLEMENTARY NOTES:** Use for additional explanatory notes.

12. **SPONSORING MILITARY ACTIVITY:** Enter the name of the departmental project office or laboratory sponsoring *(paying for)* the research and development. Include address.

13. **ABSTRACT:** Enter an abstract giving a brief and factual summary of the document indicative of the report, even though it may also appear elsewhere in the body of the technical report. If additional space is required, a continuation sheet shall be attached.

It is highly desirable that the abstract of classified reports be unclassified. Each paragraph of the abstract shall end with an indication of the military security classification of the information in the paragraph, represented as *(TS)*, *(S)*, *(C)*, or *(U)*.

There is no limitation on the length of the abstract. However, the suggested length is from 150 to 225 words.

14. **KEY WORDS:** Key words are technically meaningful terms or short phrases that characterize a report and may be used as index entries for cataloging the report. Key words must be selected so that no security classification is required. Identifiers, such as equipment model designation, trade name, military project code name, geographic location, may be used as key words but will be followed by an indication of technical context. The assignment of links, rules, and weights is optional.

Security Classification